

University of Windsor

Scholarship at UWindor

Electronic Theses and Dissertations

Theses, Dissertations, and Major Papers

2008

Effect of block face shell geometry and grouting on the compressive strength of concrete block masonry

Laura Duncan
University of Windsor

Follow this and additional works at: <https://scholar.uwindsor.ca/etd>

Recommended Citation

Duncan, Laura, "Effect of block face shell geometry and grouting on the compressive strength of concrete block masonry" (2008). *Electronic Theses and Dissertations*. 8099.
<https://scholar.uwindsor.ca/etd/8099>

This online database contains the full-text of PhD dissertations and Masters' theses of University of Windsor students from 1954 forward. These documents are made available for personal study and research purposes only, in accordance with the Canadian Copyright Act and the Creative Commons license—CC BY-NC-ND (Attribution, Non-Commercial, No Derivative Works). Under this license, works must always be attributed to the copyright holder (original author), cannot be used for any commercial purposes, and may not be altered. Any other use would require the permission of the copyright holder. Students may inquire about withdrawing their dissertation and/or thesis from this database. For additional inquiries, please contact the repository administrator via email (scholarship@uwindsor.ca) or by telephone at 519-253-3000ext. 3208.

**EFFECT OF BLOCK FACE SHELL GEOMETRY AND GROUTING ON THE
COMPRESSIVE STRENGTH OF CONCRETE BLOCK MASONRY**

by
Laura J. Duncan

A Thesis
Submitted to the Faculty of Graduate Studies
through Civil and Environmental Engineering
in Partial Fulfillment of the Requirements for
the Degree of Master of Applied Science at the
University of Windsor

Windsor, Ontario, Canada
2008
© 2008 Laura Duncan



Library and
Archives Canada

Bibliothèque et
Archives Canada

Published Heritage
Branch

Direction du
Patrimoine de l'édition

395 Wellington Street
Ottawa ON K1A 0N4
Canada

395, rue Wellington
Ottawa ON K1A 0N4
Canada

Your file Votre référence
ISBN: 978-0-494-47089-3
Our file Notre référence
ISBN: 978-0-494-47089-3

NOTICE:

The author has granted a non-exclusive license allowing Library and Archives Canada to reproduce, publish, archive, preserve, conserve, communicate to the public by telecommunication or on the Internet, loan, distribute and sell theses worldwide, for commercial or non-commercial purposes, in microform, paper, electronic and/or any other formats.

The author retains copyright ownership and moral rights in this thesis. Neither the thesis nor substantial extracts from it may be printed or otherwise reproduced without the author's permission.

AVIS:

L'auteur a accordé une licence non exclusive permettant à la Bibliothèque et Archives Canada de reproduire, publier, archiver, sauvegarder, conserver, transmettre au public par télécommunication ou par l'Internet, prêter, distribuer et vendre des thèses partout dans le monde, à des fins commerciales ou autres, sur support microforme, papier, électronique et/ou autres formats.

L'auteur conserve la propriété du droit d'auteur et des droits moraux qui protègent cette thèse. Ni la thèse ni des extraits substantiels de celle-ci ne doivent être imprimés ou autrement reproduits sans son autorisation.

In compliance with the Canadian Privacy Act some supporting forms may have been removed from this thesis.

Conformément à la loi canadienne sur la protection de la vie privée, quelques formulaires secondaires ont été enlevés de cette thèse.

While these forms may be included in the document page count, their removal does not represent any loss of content from the thesis.

Bien que ces formulaires aient inclus dans la pagination, il n'y aura aucun contenu manquant.

■ ■ ■
Canada

DECLARATION OF PREVIOUS PUBLICATION

This thesis includes figures and tables from 1 original paper that has been previously published in a peer reviewed conference proceedings, as follows:

Duncan, L.J.; Das, S.; Chidiac, S.E. (2008) Strength of Concrete Masonry Prisms Composed of Various Units, *2nd Canadian Conference on Effective Design of Structures*, 20–23 May 2008, Hamilton, Ontario, Canada.

Chapter 3 – Figure 3.5, Figure 3.15, Figure 3.24, Figure 3.25, and Table 3.7

Chapter 4 – Table 4.3, Table 4.4, and Table 4.5

Chapter 5 – Figure 5.1 and Figure 5.3

I certify that I have obtained a written permission from the copyright owner(s) to include the above published material(s) in my thesis. I certify that the above material describes work completed during my registration as graduate student at the University of Windsor.

I declare that, to the best of my knowledge, my thesis does not infringe upon anyone's copyright nor violate any proprietary rights and that any ideas, techniques, quotations, or any other material from the work of other people included in my thesis, published or otherwise, are fully acknowledged in accordance with the standard referencing practices. Furthermore, to the extent that I have included copyrighted material that surpasses the bounds of fair dealing within the meaning of the Canada Copyright Act, I certify that I have obtained a written permission from the copyright owner(s) to include such material(s) in my thesis.

I declare that this is a true copy of my thesis, including any final revisions, as approved by my thesis committee and the Graduate Studies office, and that this thesis has not been submitted for a higher degree to any other University of Institution.

ABSTRACT

Canadian and American standards provide the compressive strength of concrete masonry assemblage as dependant on compressive strength of blocks, mortar type, and percentage of grout. It is common in construction to sporadically place non-standard units in masonry walls. Moreover, grout can have many different mix proportions causing a difference in compressive strength, stiffness, and grout-unit bond strength.

This research studied the effect of block geometry and the combination of two different block geometries on ungrouted prism strength. As well, this study focused on the effects of grout strength, grout stiffness, and grout-block bond strength on the compressive strength of grouted masonry prisms.

This study showed that block geometry affected prism compressive strength when the prism was comprised of one type of block. This was untrue for prisms with two different geometries. Grout strength and stiffness were found to affect prism strength. Bond strength was found to only affect the stiffness and not the strength of the grouted masonry prisms.

DEDICATION

For all of you who inspired me
Showed the way and let me see
The obstacles I must defeat
And all the things I can complete

ACKNOWLEDGEMENTS

This project was undertaken under the supervision of Dr. S. Das and Dr. S. E. Chidiac. I am deeply thankful for their kindness, patience, endless assistance, constructive observations, continuous support, and encouragement throughout my studies. They devoted time, resources, and extensive efforts to provide all necessary materials and research facilities for this work.

My appreciation also goes out to the committee members: Dr. N. Zamani-Kashani and Dr. M. K. S. Madugula for their beneficial suggestions which helped to improve this thesis.

Heartfelt thanks go out to all technical staff: Lucien Pop, Patrick Seguin, Matthew St. Louis, Andrew Jenner, and William Middleton of the University of Windsor, and Bernard Nieuwenhuis, Maurice Forget, and Dave Perrett of McMaster University who assisted with building and designing equipment, specimen construction and testing, and all other laboratory work.

Special appreciation goes to McMaster University Centre for Effective Design of Structures, Canadian Concrete Masonry Producers Association, and the Canada Masonry Centre for donating materials and funding needed for this project.

Finally, I would like to thank my entire family and all of my friends, especially Kristen Ross, Jessica Maruncic, Meiling Chen, Daniel Grenier, Michael Ferguson, Zachary Djokich, and my brother Richard Duncan, without whom I would have not gotten this far.

TABLE OF CONTENTS

DECLARATION OF PREVIOUS PUBLICATION	iii
ABSTRACT	iv
DEDICATION	v
ACKNOWLEDGEMENTS	vi
LIST OF TABLES	xi
LIST OF FIGURES	xiii
1. INTRODUCTION.....	1
1.1 General	1
1.2 Objective and Scope.....	3
1.3 Methodology	4
1.4 Organization of Thesis	4
1.5 Notation.....	5
2. LITERATURE REVIEW.....	8
2.1 Introduction	8
2.2 Masonry Units.....	8
2.2.1 Physical Properties	9
2.2.2 Compressive Strength	12
2.3 Mortar.....	14
2.3.1 Compressive Strength	15
2.3.2 Mortar-Block Interaction.....	16
2.3.3 Mortar Bedding Type.....	16
2.4 Grout.....	17
2.4.1 Compressive Strength and Elastic Modulus.....	18
2.5 Prisms	19
2.5.1 Construction and Curing	20
2.5.2 Compressive Strength	20

2.5.3 Modulus of Elasticity	23
2.6 Codes and Standards	24
2.7 Summary	26
3. EXPERIMENTAL PROGRAM	27
3.1 Introduction	27
3.2 Block Units.....	28
3.2.1 Dimensions.....	28
3.2.2 Water Content, Density, and Absorption	28
3.2.3 Compressive Strength	32
3.3 Mortar.....	35
3.3.1 Flow.....	35
3.3.2 Compressive Strength	36
3.4 Grout.....	37
3.4.1 Spread.....	39
3.4.2 Compressive Strength and Modulus of Elasticity	40
3.5 Prism.....	43
3.5.1 Construction	43
3.5.1.1 Geometrical Prism Construction	44
3.5.1.2 Grouted Prism Construction.....	46
3.5.2 Capping	48
3.5.3 Instrumentation and Setup.....	49
3.6 Summary	53
4. MATERIAL PROPERTIES.....	54
4.1 Introduction	54
4.2 Test Results	57
4.2.1 Block Properties	57
4.2.1.1 Compressive Strength	57
4.2.1.2 Density and Initial Rate of Absorption	58
4.2.2 Mortar Properties.....	60

4.2.3 Grout Properties	62
4.3 Analysis and Discussion.....	64
4.3.1 Block	64
4.3.2 Mortar.....	65
4.3.3 Grout.....	65
5. GEOMETRICAL PRISM RESULTS AND ANALYSIS	67
5.1 Introduction.....	67
5.1.1 Background	67
5.1.2 Outline of Investigation.....	71
5.2 Experimental Test Results.....	72
5.2.1 Failure Modes.....	72
5.2.2 Compressive Strength	75
5.2.3 Stress-Strain Characteristics.....	78
5.3 Multi-Linear Regression Analysis	81
5.3.1 Regression Model 1.....	81
5.3.2 Regression Model 2.....	90
5.4 Comparison of Models.....	96
6. GROUTED PRISM RESULTS AND ANALYSIS	100
6.1 Introduction.....	100
6.1.1 Background	100
6.1.2 Outline of Investigation.....	101
6.2 Experimental Test Results.....	101
6.2.1 Failure Modes.....	101
6.2.2 Compressive Strength	104
6.2.3 Stress-Strain Characteristics.....	106
6.3 Multi-Linear Regression Analysis	108
6.3.1 Regression Model.....	108
6.3.2 Elastic Modulus Estimation	114

7. CONCLUSIONS AND RECOMMENDATIONS.....	117
7.1 General	117
7.2 Conclusions	121
7.3 Recommendations	122
REFERENCES.....	123
APPENDIX A	126
APPENDIX B	130
APPENDIX C	133
Vita Auctoris	137

LIST OF TABLES

Table 2.1: CSA S304.1-04 (2004) Table 4	25
Table 2.2: ACI 530.1-05 (2005) Table 2	25
Table 3.1: Unit dimensions	28
Table 3.2: Standard block values	31
Table 3.3: Lintel block values.....	32
Table 3.4: Knock-out block values	32
Table 3.5: Block compressive strength.....	34
Table 3.6: Grout mix proportions	38
Table 3.7: Geometrical prism types	45
Table 3.8: Grouted prism types.....	47
Table 4.1: Critical regions for testing $\mu = \mu_0$ (Johnson, 2005)	55
Table 4.2: Critical regions for testing $\mu - \mu_0 = \delta$ (Johnson, 2005)	56
Table 4.3: Block compressive strength results (MPa)	58
Table 4.4: Block density (kg/m^3)	59
Table 4.5: Block IRA ($\text{kg/m}^2/\text{min}$)	59
Table 4.6: Mortar compressive strength	61
Table 4.7: Grout strength and stiffness	63
Table 5.1: Geometrical prism results	76
Table 5.2: Analysis of variance for model 1	87
Table 5.3: 95% confidence intervals for model 1 coefficients	88
Table 5.4: Analysis of variance for E_m	89
Table 5.5: Analysis of variance for model 2.....	93
Table 5.6: 95% confidence intervals for model 2 coefficients	94
Table 5.7: Analysis of variance for E_m	96

Table 6.1: Grouted prism results.....	105
Table 6.2: Analysis of variance for grouted regression model	113
Table 6.3: 95% confidence intervals for coefficients	114
Table 6.4: Grouted prism modulus of elasticity.....	115
Table 6.5: Analysis of variance for grouted E_m	115

LIST OF FIGURES

Figure 2.1: Standard concrete masonry block (stretcher)	10
Figure 2.2: Standard concrete masonry block (splitter)	10
Figure 2.3: Lintel concrete masonry block	11
Figure 2.4: Knock-out concrete masonry block	11
Figure 2.5: Joint reinforcement.....	22
Figure 3.1: Fully submerged weight test setup	29
Figure 3.2: Initial rate of absorption test.....	30
Figure 3.3: Unit capping	33
Figure 3.4: Unit test setup.....	34
Figure 3.5: Failed standard block.....	34
Figure 3.6: Flow test table	36
Figure 3.7: Brass caliper	36
Figure 3.8: Mortar cube testing.....	37
Figure 3.9: Grout mixing process	39
Figure 3.10: Grout spread test.....	40
Figure 3.11: Coring grout cylinders.....	41
Figure 3.12: Grout cylinders	41
Figure 3.13: Linear potentiometer (S13FLP-12A-10K)	42
Figure 3.14: Failed grout cylinders.....	42
Figure 3.15: Capped prism specimen (S)	44
Figure 3.16: Prism Type L: side view.....	45
Figure 3.17: Prism Type K: side view	45
Figure 3.18: Prism Type SL: side view	46
Figure 3.19: Prism Type SK: side view	46

Figure 3.20: Grouting prism specimens.....	48
Figure 3.21: Capped prisms curing: side view.....	49
Figure 3.22: Load cell sketch.....	50
Figure 3.23: Wheatstone's bridge diagram.....	50
Figure 3.24: Test setup.....	52
Figure 3.25: Linear potentiometers on prism specimen.....	52
Figure 5.1: Standard prism crack pattern.....	73
Figure 5.2: Web failure of standard prism.....	73
Figure 5.3: Lintel prism crack pattern.....	74
Figure 5.4: Knock-out prism crack pattern.....	75
Figure 5.5: Cross section through the core of S, L, and SL prisms.....	77
Figure 5.6: Stress versus strain relationship.....	79
Figure 5.7: Schematic of the LPs locations.....	79
Figure 5.8: Residuals versus f'_m	83
Figure 5.9: Residuals versus f'_{block}	83
Figure 5.10: Residuals versus f'_{mortar}	84
Figure 5.11: Residuals versus $A_{faceshell}$	84
Figure 5.12: Residuals versus $f'_{block}{}^2$	85
Figure 5.13: Residuals versus $f'_{mortar}{}^2$	85
Figure 5.14: Residuals versus $f'_{mortar}{}^3$	86
Figure 5.15: Residuals versus ρ	86
Figure 5.16: Predicted versus measured values for model 1.....	87
Figure 5.17: Predicted versus measured values for E_m for model 1.....	90
Figure 5.18: Residuals versus f'_m	91
Figure 5.19: Residuals versus f'_{block}	92
Figure 5.20: Residuals versus f'_{mortar}	92

1. INTRODUCTION

1.1. GENERAL

Unreinforced concrete masonry is composed of concrete blocks and mortar. Concrete blocks are available in a wide variety of strength, shape, and size for various construction purposes. Mortar type is classified by strength and provides uniform bearing between units, and bonds these units in a system to create a composite system. During masonry construction, it is currently common practice to place non-standard concrete units sporadically in walls. This is done to use up all materials, and reduce material costs since blocks are ordered in skids of 75. This creates an excess of non-standard units if fewer than 75 or a multiple of 75 is needed. The effect of using non-standard units in standard masonry construction is currently unknown.

Fine and coarse grout can be used as infill in cores or walls or columns, or between withes of walls. It is important for the grout to have a high slump to ensure high flow and slump flow to fill all voids. For design purposes, standards CSA S304.1-04 (2004) and ACI 530.1-05 (2005) specify masonry compressive strength, f'_m , as dependent on block strength, mortar type, and amount of grout. Grout strength, grout stiffness, and grout-unit bond strength is not considered.

Drysdale and Hamid (1982) reported that prism strength increases with increasing unit compressive strength; however this relationship is not linear. Ramamurthy et al. (2000) studied the effect of various block-mortar strength ratios, block geometries, mortar bedding, block height to thickness (h/t) ratio, and mortar joint thickness on the

compressive strength of hollow concrete prisms. Three types of concrete blocks were used in the investigation: three-core conventional, two-core conventional and core-aligned blocks which had two cores. The prisms comprised of the three-core block, which were face-shell bedded and face-shell capped, had vertical splitting of the web shells at a lower stress level than a full-bedded prism, and an efficiency factor which ranged between 0.68 and 0.42. Prisms constructed using the conventional two-core block had full mortar bedding and lower efficiency factors between 0.55 and 0.78. Prisms comprised of the core-aligned blocks were also fully mortar bedded, behaved similar to solid masonry, and had a maximum efficiency factor. The compressive strength of the masonry prisms was considered to be dependent on block strength, mortar strength, and type of block geometry. Type of block geometry was taken as the ratio of bedded area of the web to the total area of the web. These results do not reveal the effect of constructing walls using standard and non-standard concrete units on the strength and stiffness of masonry walls.

Hedstrom and Hogan (1990) studied the effect of grout properties on the compressive strength of grouted concrete masonry prisms. It was suggested that as the aggregate to cement ratio increases, the compressive strength of the prism decreases, although this relationship becomes less pronounced as the ratio increases. This correlation between aggregate to cement ratio and prism compressive strength was determined to be different for fine and coarse grout; however the relationship remains the same. These results suggested that the stiffness of the grout, which is a function of aggregate to cement ratio, influences the compressive strength of grouted concrete masonry prisms.

1.2. OBJECTIVE AND SCOPE

This research project was a combination of two investigations. The first investigation was undertaken to determine the effect of block geometry on the compressive strength and stiffness of concrete masonry prisms. Standard, lintel, and knock-out blocks were used in different combinations to produce five prism types. A minimum of five prism specimens of each type were tested in order to obtain an accurate representation of the compressive strength and elastic modulus of the prisms. Two prism sets were constructed using a combination of standard and lintel and standard and knock-out blocks in order to investigate the effect of including one non-standard unit in a prism, while the remaining three prism sets were constructed solely of standard, lintel, and knock-out units.

The second investigation was undertaken to determine the effect of grout compressive strength and stiffness, and grout-unit bond on the compressive strength of grouted concrete masonry. Three sets of masonry prisms were grouted using a different grout mix. These were used to study the effect of the grout properties on the compressive strength. Another set of prisms had the cores of the blocks painted with a high gloss acrylic paint, and the cores were oiled prior to grouting to prevent bonding between the grout and units. This prevented the paste from the grout from transferring and thus creating a bond. One of the three grout mixes previously discussed were used in this prism set. A minimum of five prisms for each set were tested.

1.3. METHODOLOGY

In order to determine the effect of geometrical shape on the compressive strength of concrete masonry prisms, standard stretcher block and two types of non-standard block types were chosen to be used in the investigation. Five prisms were built using each unit type in a running bond, four courses high, and one block in both length and width. As well, in order to determine the effect of mixing unit types, two additional prism sets were constructed using three courses of standard block and one course of each non-standard block.

Three grout mixes were prepared to produce a variety of strength and stiffness. These three grout mixes were each cast in five prisms constructed of standard stretcher units. Another five prisms have the cores painted with a high gloss acrylic paint in order to prevent bonding between the grout and the units. The effects of mixing standard and non-standard block types on the compressive strength and stiffness of the prisms were studied using statistics in order to determine the confidence level. The results are also compared to the methods postulated by current standards.

1.4. ORGANIZATION OF THESIS

The materials in this thesis are organized as follows: Chapter 2 contains a detailed review of previous research which pertains to these studies. Detailed descriptions of all test procedures are discussed in Chapter 3. Chapter 4 provides the results from individual tests conducted on the constituents of the masonry prisms. The results of the prism tests and the statistical analysis completed on these results for each investigation are discussed in

Chapters 5 and 6. Chapter 7 contains a summary of results, overall conclusions, and recommendations based on this investigation.

1.5. NOTATION

A summary of the symbols is listed below for convenience of the reader, even though each symbol used in this thesis is described where it first appears.

A	initial block weight
$A_{\text{faceshell}}$	block face shell area
A_{net}	block net area
A_{total}	total prism compressive area
B	fully submerged block weight
b_i	variable coefficient
C	saturated surface dry block weight
c	constant
CI	confidence interval
COV	coefficient of variance
D	oven (bone) dry block weight
df	degrees of freedom
E	absorption block weight
e	residual error value
E_g	grout modulus of elasticity
E_m	masonry prism modulus of elasticity

F_o	calculated f-value
$F_{v1:v2:\alpha}$	critical f-value
f_{block}^c	block compressive strength
f_{grout}^c	grout compressive strength
f_{mortar}^c	mortar compressive strength
f_m^c	masonry prism compressive strength
$f_{m(\text{Equation 5.16})}^c$	ungROUTED prism compressive strength
H_o	null hypothesis
H_1	alternative hypothesis
I	high stiffness grout prism set
IRA	initial rate of absorption
K	knock-out prism set
L	lintel prism set
N	normal grout prism set
n	number of samples
P	painted (no bond) prism set
P_i	applied load
P_{ultimate}	ultimate applied load
R	high strength grout prism set
R^2	coefficient of determination
r	number of variables used in multi-linear regression analysis
S	standard prism set
s	standard deviation

SL	standard plus lintel prism set
SK	standard plus knock-out prism set
SS _E	error sum of squares
SS _R	residual sum of squares
SS _T	total sum of squares
t	calculated t-value
t _α	critical t-value
w	water content
x _i	independent variable
y	dependent variable
\tilde{y}	model values for dependant variable y
α	100% - CI
δ	constant
ε	strain
μ	calculated mean
μ _o	assumed mean
ρ	density
σ _i	compressive strength
σ _{ultimate}	ultimate compressive strength
v ₁	number of parameters
v ₂	n - v ₁

2. LITERATURE REVIEW

2.1 INTRODUCTION

In order to properly appreciate the way in which grouted concrete masonry assemblages perform, it is important to understand the properties of each constituent (concrete block, mortar, and grout), as well as their effects on concrete masonry when integrated. During the process of obtaining information on concrete masonry structures, it is imperative to define specific testing procedures in order to achieve useful information, from which principles can be determined and used in the design process. This chapter presents a review of the above mentioned aspects of concrete masonry construction which was observed in previous studies.

2.2 MASONRY UNITS

Concrete masonry units are available in many shapes, sizes, and strength intended for various uses in masonry construction. The standard block, which comes in two different shapes is most frequently used. Other commonly used blocks include open-end units, double open-end units, lintel units, and knock-out units, as well as many others. Although the effect of geometrical shape on masonry compressive strength has not been extensively studied, shape and size has been shown to have some effect on the compressive strength of masonry (Ganzerli et al., 2003 and Thomas and Mujumdar, 2003). The influence of mortar and grout properties on the properties of masonry assemblages has been investigated through several laboratory tests (Colville and Wolde-Tinsae, 1990, Hedstrom and Hogan, 1990, Isaacs, 1975, Khalifa and Magzoub, 1994, and Self, 1975).

2.2.1 Physical Properties

Standard hollow concrete blocks with 390 x 190 x 190 mm in dimensions, are the most common and are available in two types: (i) stretcher block and (ii) splitter block. The stretcher block (Figure 2.1) has two tapered cores and recesses on both ends (otherwise known as frogged ends). The splitter unit (Figure 2.2) also has two tapered cores, however only one end is frogged while the other is flat. These units also have two central webs so that each half has two webs once the block has been split.

Pallets containing standard blocks typically contain both stretcher and splitter units, however only stretcher units are commonly used for determining the properties. Although splitter units are used in standard construction practice for end or half blocks in a running bond, the standard stretcher unit is considered the typical and is the controlling state for strength.

Lintel (Figure 2.3) and knock-out (Figure 2.4) units have the same dimensions as standard hollow blocks; however their geometries are quite different. Lintel units have a consistent cross section in the shape of a “U” throughout the length of the block, where the inner sides of the face shells are tapered and the base of the unit is solid. Knock-out units contain two cores (similar to standard units); have flat ends, and webs which are separated from the face shells for all except the bottom section of the unit so that the web can be easily detached.

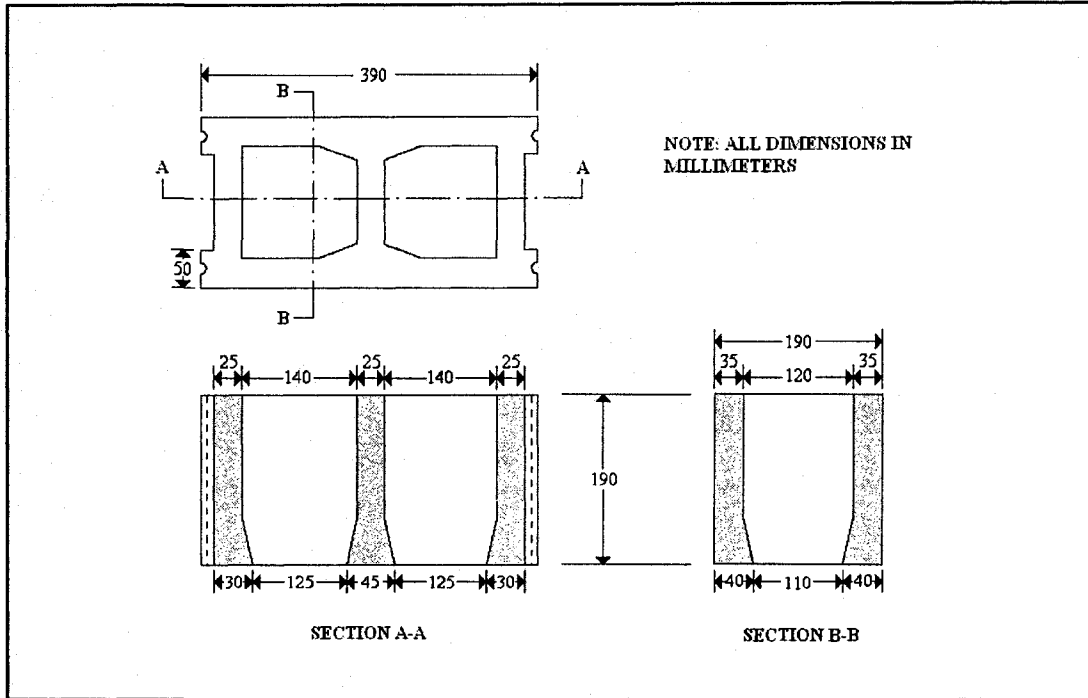


Figure 2.1: Standard concrete masonry block (stretcher)

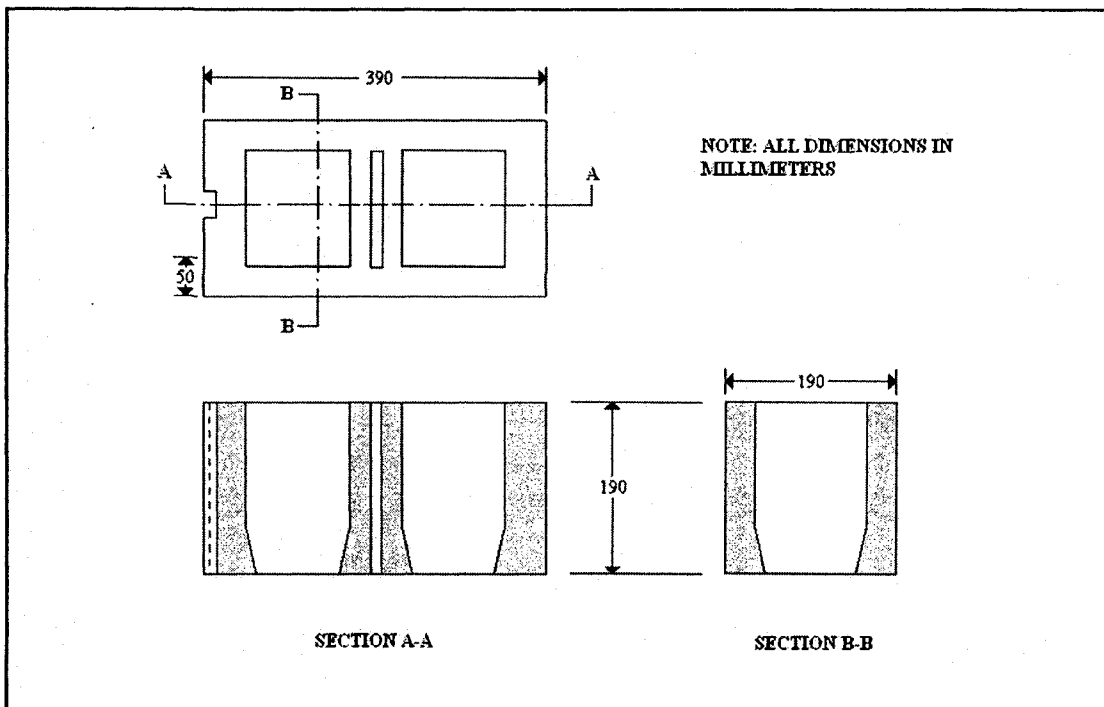


Figure 2.2: Standard concrete masonry block (splitter)

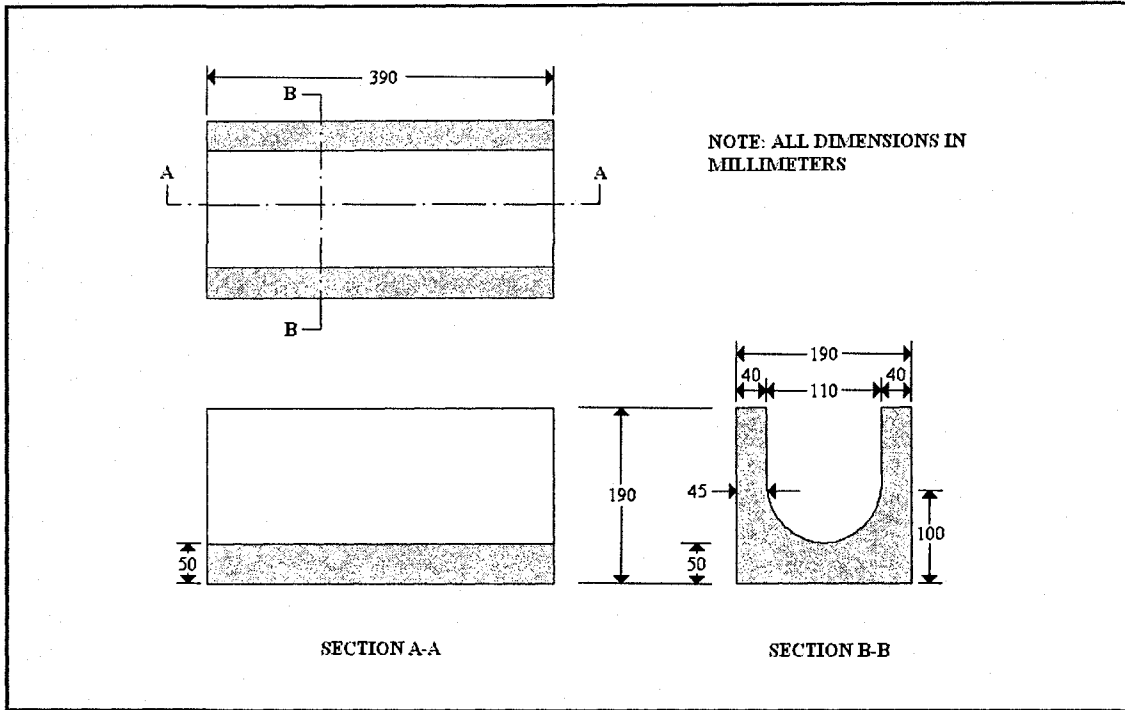


Figure 2.3: Lintel concrete masonry block

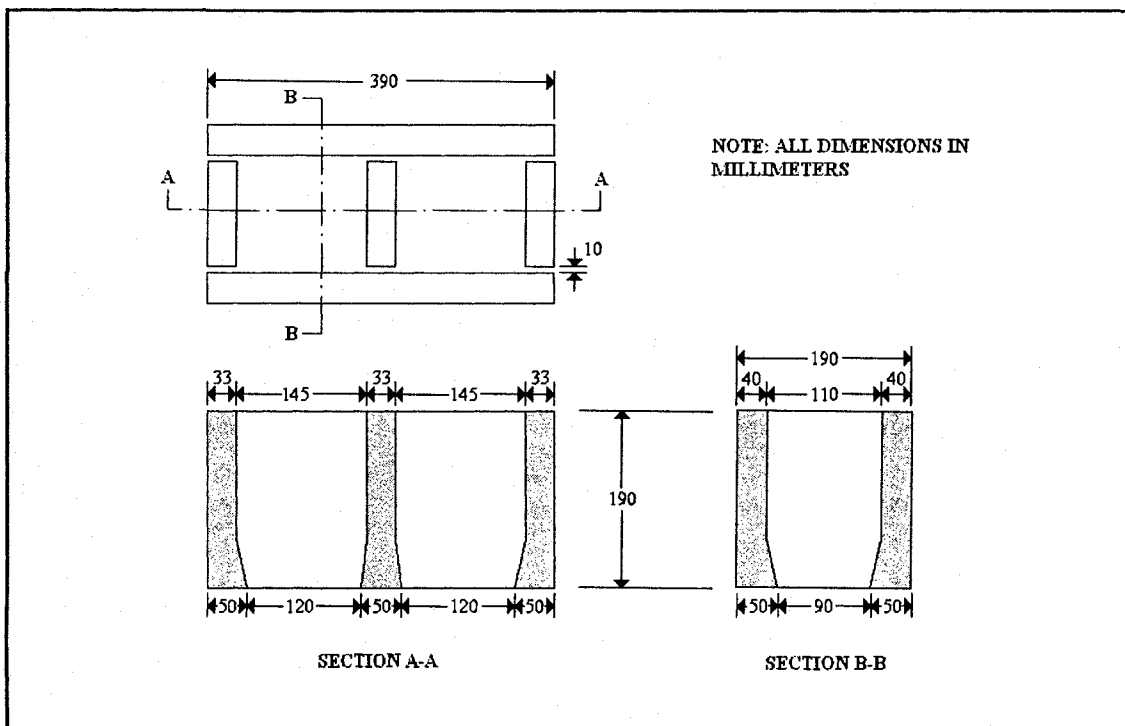


Figure 2.4: Knock-Out concrete masonry block

2.2.2 Compressive Strength

Concrete masonry block units come in various shapes and the size (dimensions) of these shapes may vary depending on the unit. Regardless of shape and size, all units are produced with an equivalent unit compressive strength, f'_{block} . CSA A165-04 (2004) and ASTM C140-05a (2005) provide the test methods used in determining the compressive strength of concrete masonry units.

Ganzerli et al. (2003) studied the use of coupons for determining the compressive strength of full size units. Specifically, they studied the proper dimension and location of the coupons, and the relationship between coupon and unit strength for various shapes of units. It was found that coupons with a height to thickness ratio of 3:1 and length to thickness ratio of either 4:1 or 5:1 provided the best correlation between coupon compressive strength and full size unit compressive strength. It was also noted that the height to thickness and length to thickness ratios of 2:1 and 4:1 suggested by ASTM C140-01 (2001) were indicated as appropriate ratios. Ganzerli et al. (2003) also found that coupons cut from the top, middle, and bottom of the face shell gave different results. They attributed this to the varying compaction levels during manufacture. No suggestion as to the most representative location for cutting coupons was given. Varying compaction levels was also implied as being responsible for an inconsistency in the relationship between coupon and full size unit compressive strength with respect to unit shape.

Thomas and Mujundar (2003) also investigated the use of coupons for determining the compressive strength of full size concrete masonry units. They found that full size units

were preferable for estimating block compressive strength, followed by half length units, and finally coupons. Testing showed that coupons should still be produced according to ASTM C140-01 (2001) with length to height to thickness ratios of 4:2:1. Half length and coupons had compressive strengths with coefficients of variation of 7.5% and 10%, respectively. The test results for the compressive strength of full size units had a coefficient of variation of 5%.

The block producers have the ability to produce concrete masonry blocks with different strengths. In general, as the compressive strength of a masonry unit increases, so does the prism strength (Drysdale and Hamid, 1982). The ratio of tensile strength to compressive strength provides a better indication of the effect. This is because tension is created on the block webs in ungrouted concrete masonry when compressive force is applied on prisms. Although Drysdale and Hamid (1982) suggested that a more accurate estimation of prism compressive strength may be determined with this method, it was also stated that it is possible that the process may not be economical due to increased testing costs.

Surface roughness, face shell and web tapering, moisture content, and initial rate of absorption may also affect the properties of concrete masonry units. Drysdale and Hamid (1982) and Khalifa and Magzoub (1994) have investigated these factors, and their findings are discussed.

Drysdale and Hamid (1982) suggested that there is not a significant impact on the strength of masonry unit due to the surface roughness, since units with smooth surfaces continue to

produce the frictional resistance to confine lateral expansion of mortar. Since mortar and capping materials bond easily to concrete surfaces that are smooth or have been cut with a saw, this suggestion is reasonable.

Colville and Wolde-Tinsae (1990) have determined that face shell and web tapering can lead to a reduction in unit compressive strength due to change in cross-sectional area throughout the prism height. This difference found to be insignificant for ungrouted masonry, where there is only face shell bedding, as tapering of the face shell is minimal. Web tapering may restrict grout flow, creating voids in grouted concrete masonry, thus reduces the ultimate compressive strength of the assemblage.

The unit compressive strength of concrete masonry is reduced for units with higher water contents; however they produce more consistent results. This could be due to lower water absorption from mortar to the unit, resulting in weaker bond strength. However, higher initial rates of absorption (IRAs) of concrete masonry blocks produce stronger mortar-bond strengths, which in turn increase the compressive strength of the masonry system. O'Leary (1996) however found that block moisture content and initial rate of absorption (IRA) were not considered to be major factors that affect prism compressive strength.

2.3 MORTAR

Mortar has a significant role in the construction of concrete masonry structures. Its primary function is to bond concrete masonry blocks together, although it also fills cracks and crevices while providing a uniform bedding surface. The thickness of the mortar joint

is preferably 10 mm. However, it was found that joint width does not produce a significant change in prism strength for a variation of 6 mm ($\frac{1}{4}$ in) to 16 mm ($\frac{5}{8}$ in).

When preparing mortar for concrete masonry construction, it is important to be able to maintain the consistency in properties of the mortar from batch to batch. Mixing mortar by the 'Proportion Method' ensures the ability to obtain mortar with similar properties, such as compressive strength, workability, and water content.

2.3.1 Compressive Strength

Specimens used in determining the compressive strength of mortar are 50 mm cubes. They are prepared and cured in accordance with CSA A179-04 (2004b) in order to obtain consistent results. Cubes are loaded in a compressive testing machine until failure occurs, to obtain the ultimate strength of the mortar. Minimum allowable compressive strengths of Type S and Type N mortar at 7 and 28 days are provided in Table 6 of CSA A179-04 (2004b).

The compressive and flexural strength of mortar was investigated by Thomas and Mujumdar (2003). It was found that decreasing the amount of Portland cement used in the mix will significantly decrease the compressive strength of the mortar and the flexural bond strength. An increase in mortar aggregate ratio (less cement to sand volume) has also been shown to decrease the masonry strength (Farney et al., 2005).

2.3.2 Mortar-Block Interaction

While mortar has its own physical properties, the interaction between the block and mortar is of interest. According to Khalifa and Magzoub (1994), reduction in the block-mortar strength ratio reduces the lateral tensile stresses which develop due to the deformational incompatibility when compressed normal to the bed face. This indicates that a mortar strength close to that of the unit strength will provide the highest prism strength.

Although Farney et al. (2005) suggest that the effect of water content is negligible when determining mortar quality, it is important to maintain an appropriate amount of water when mortar is applied to the block face in order to produce a proper bond. Mortar with low water content combined with a unit having a high initial rate of absorption can produce separation between the mortar and unit. This may be caused when too much water is removed from the mortar. In contrast, too much water in mortar may result in units floating on the mortar bed, which also results in a poor mortar-unit bond.

2.3.3 Mortar Bedding Type

Different types of masonry systems require different forms of mortar bedding. Two common types of bedding include face shell bedding and full mortar bedding. Khalifa and Magzoub (1994) performed studies and found a number of differences between the two types of mortar bedding. Face shell bedding creates deep beam action on the web creating additional bending effects and cracking at relatively lower loads than full bedding. Face shell bedded prisms experience a highly non-uniform stress-strain distribution, with

maximum tensile stress in the web of the block. The full mortar bedded prisms have a uniform stress-strain distribution and maximum tensile stress occurs in the mortar.

Self (1975) indicated that prism bedding type is not required to be the same as the wall in question, since the overall prism strength is determined by dividing the ultimate load by the net bedded area.

2.4 GROUT

Although grout is not always utilized in concrete masonry construction, it is an effective tool for increasing the overall strength of a system by creating a connection between masonry blocks and reinforcement. To ensure proper placement of grout in masonry assemblages, it must flow well in order to fill all the required areas. Other factors such as aggregate size and modulus of elasticity are also important considerations when determining the effects of grout on the compressive strength of concrete masonry structures. A thorough knowledge of each constituent is essential to the analytical process.

It is important to maintain consistency when preparing and testing any type of material, therefore standard test methods and specifications are recommended in CSA A179-04 (2004b). Consistent mix proportions, aggregate types, and procedures assist in obtaining a quality product, while testing for 7 and 28 day strengths verifies that all measures were followed correctly.

2.4.1 Compressive Strength and Elastic Modulus

Grout compressive strength can be determined in several ways. Cubical or cylindrical grout specimens can be moulded or cored out of a grouted block cell. The block unit will absorb some water from the grout, similar to what occurs when concrete masonry is grouted during construction in the field. Moulded cylinders retain water which could have been lost during the curing process. Thus, it was found that on the average, moulded specimen can have a 9.7% higher compressive strength than cored specimens from the same grout (Hedstrom and Hogan, 1990). It is typical for cut specimen to be considered the more accurate assessment when testing grout.

The deformation of grout specimen is recorded to obtain the average Elastic Modulus during compressive strength tests. Since the grouted area of masonry assemblage can be as high as 50% of the total area (S304.1-04, 2004d), the way in which grout acts while under compressive loads has an impact on the properties of grouted concrete masonry assemblages.

Cylinders typically have a 2:1 length to diameter ratio and are capped with sulphur in accordance with CSA Test Method A23.2-9C (2004c). An alignment device is used in conjunction with capping plates to ensure the specimen is perpendicular and a minimum of three repeat tests are performed to obtain a suitable range of data.

Grout improves the capacity of the block unit in compression by providing lateral support to walls and reducing slenderness. If there is a large deformational incompatibility

between the block and grout, the two components will act separately, and prism compressive strength can be significantly reduced. Large lateral expansion due to grout flexibility may lead to premature failure of the block's shell.

Hedstrom and Hogan (1990) found that stress-strain measurements of grout are linear over the loading range. Establishing the Modulus of Elasticity between 0.05 and 0.33 of the grout strength, provides an approximation of E_g as

$$E_g = 500f'_{grout} \quad (2.1)$$

2.5 PRISMS

Tests on full scale masonry systems can be impractical due to labour expenses, time consumption, and large spatial requirements. In order to perform research economically, smaller specimen need to be tested, whose behaviour should correspond to that of the larger system. Prisms which are 3, 4 or 5 units in height tend to have a good correlation to their corresponding wall segments, which have reduced platen end restraint and provide a minimum of two mortar beds for analyzing deformation (Maurenbrecher, 1978; and Wong and Drysdale, 1985). Khalifa and Magzoub (1994) found that as wall height increases the compressive strength decreases due to slenderness effects. Prisms of 4 units in height are generally utilized, due to a lower coefficient of variation, without greatly effecting slenderness or reducing strength (Maurenbrecher, 1978).

2.5.1 Construction and Curing

In order to obtain similar results to what would be consistent to field construction, it is important to have a mason build the specimen in the same manner as on the construction site. This pertains to plumbness, mortar bedding, and block placement among others. Bedding pattern is very important since stack bonded prisms result in higher compressive strengths than running bond prisms. Stack bonded prisms do not account for the behaviour differences with running bond prisms (Khalifa and Magzoub, 1994). The results of testing cannot be applied if prisms are not built in the same fashion as their corresponding wall segments.

The curing process begins after prisms are built. The way in which prisms are cured can have a large effect on their compressive and tensile strengths, since water absorption and grout shrinkage can be partly controlled. Commonly, prisms are cured either in air with a relative humidity of 30% to 70%, or initially under polythene with a relative humidity of more than 90% (Maurenbrecher, 1978). Prism compressive strength can be up to 10% less when cured under polythene in the shade compared to prisms cured uncovered and exposed to the sun (Maurenbrecher, 1980).

2.5.2 Compressive Strength

Tests on full-scale concrete masonry walls can be very extensive, and may provide many restraints that can hinder the process. Storage of large specimen until the common 28 day testing time can be difficult. Thus, the possibility of testing specimen on a smaller scale is very appealing, and has commonly been considered. Long et al. (2005) found prisms

constructed of half-scale units produce similar results to those constructed of full size units. This type of modeling is not currently used; however it may soon be, due to the reduced storage area and potential smaller material and labour costs.

It is important to minimize the possibility of an eccentric loading when testing concrete masonry prisms in compression. This can be accomplished by using pinned ends as opposed to flat ends, although the majority of testing is completed using flat end connections (Maurenbrecher, 1978). The compressive strength will be reduced and deformation will not occur evenly, consequently altering the stress-strain relationship, if a prism is not loaded concentrically.

Prisms which are not level when loaded can create eccentric loading cases due to an angle of the applied load. Prisms are capped to produce level specimens to reduce this effect. It is important that the capping material used is stronger than that of the concrete masonry prism, so that failure does not occur in the capping material. As with unit testing, the prism capping process can be simplified by using fiberboard; however there is a reduction in the compressive strength of the prism (Maurenbrecher, 1985 and 1980).

It is important to keep a constant loading rate up to failure when loading concrete masonry prisms, so that results can be approximated to a constant strain rate, which gives lower strength results than a constant load rate, making this procedure more conservative (Maurenbrecher, 1978). Stress-strain curves which are obtained from tests commonly contain no plastic loading range, indicating a brittle behavior. At low loads, lateral strains

vary from tension to compression. However, at high loads lateral strains are tensile, and thus become very large while approaching the failure load as vertical cracking occurs.

In some cases, joint reinforcement, as shown in Figure 2.5, is used to increase the compressive strength. When joint reinforcement is used, stresses are increased, and failure mode may change to shear instead of splitting. Joint reinforcement can also restrict flow through the cores when grout is involved. Combined with web un-alignment, which can also create higher stresses due to improper filling of cores, it is possible that the compressive strength of concrete masonry can be greatly diminished (Khalifa and Magzoub, 1994).

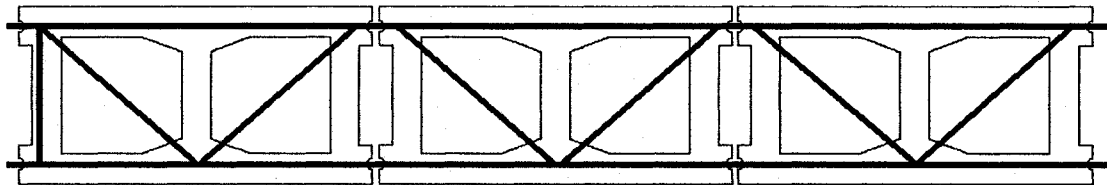


Figure 2.5 Joint reinforcement

A study by Ramamurthy et al. (2000) investigated the effect of unit geometry on prism compressive strength. Three cell units, standard two cell units, and web aligned two cell units were used. The study indicated a strong correlation between prism compressive strength (f'_m) and block strength (f'_{block}), mortar strength (f'_{mortar}) and ratio of bedded web area to total web area (r). The prisms comprised of the web aligned two cell units were found to be the most efficient during testing. It was also stated that the three cell units were the least efficient during testing.

2.5.3 Modulus of Elasticity

When evaluating the properties of concrete masonry assemblage, one of the most important properties is the modulus of elasticity. Although there are many ways to determine the elastic modulus, the most appropriate for design purposes is the chord modulus from 5% to 33% or 5% to 50% of the masonry compressive strength, and can be directly related to the prism strength by a single coefficient (Colville and Wolde-Tinsae, 1993). It was found that the elastic modulus of concrete masonry (E_m) increases primarily until 28 days of age. The increase then becomes insignificant.

It has been suggested that the modulus of elasticity of the masonry system (E_m) should not be computed based solely on the compressive strength of masonry (f'_m) but on the elastic moduli of the components (Ameny et al., 1983). For grouted masonry, this would include the elastic moduli of the unit, grout, and mortar, which may become very complex, and may not be a reasonable suggestion. CSA S304.1-04 (2004d) states that E_m for both ungrouted and grouted masonry may be taken as follows:

$$E_m = 850f'_m \quad (2.2)$$

According to Colville and Wolde-Tinsae (1993), a more accurate approach can be used to re-evaluate the current equation for evaluating E_m , and altering the equation from the traditional American value of $E_m = 1000f'_m$ to the following equation:

$$E_m = 667f'_m \quad (2.3)$$

Although this would be more economical, it is less conservative than the Canadian value. Equations 2.4 and 2.5 are the recommended relationships between masonry compressive strength and elastic modulus by ACI 530.1-05 (2005) and the UBC (2007), respectively.

$$E_m = 900 f'_m \quad (2.4)$$

$$E_m = 750 f'_m \quad (2.5)$$

These relationships are more conservative than the relationship suggested by Colville and Wolde-Tinsae (1993).

2.6 CODES AND STANDARDS

Current Canadian and American standards provide an estimation of concrete masonry strength (f'_m) based on the masonry components. Table 4 in CSA 304.1-04 (2004d) bases the compressive strength (f'_m) normal to the bed joint as a function of unit compressive strength, mortar type, and amount of grout (Table 2.1). It does not consider unit tensile strength, unit geometry, unit stiffness, grout strength, grout stiffness, or the bond between grout and units.

Table 2.1 CSA S304.1-04 (2004) Table 4

Specified compressive strength of unit (average net)	Type S mortar		Type N mortar	
	Hollow	Solid ¹ or grouted	Hollow	Solid ¹ or grouted
40 or more	22	17	14	10.5
30	17.5	13.5	12	9
20	13	10	10	7.5
15	9.8	7.5	8	6
10	6.5	5	6	4.5

¹Linear interpolation is permitted.

²For semi-solid concrete block units, the effective cross sectional area shall be used in combination values with the f_m for solid units

Table 2 in ACI 530.1-05 (2005) indicates that the compressive strength of concrete masonry (f_m) is based on unit strength and mortar type only (Table 2.2). Clause 1.4B states that for grouted masonry, the grout must either conform to ASTM C476 (2002) or have a compressive strength equal to or greater than f_m , but not less than 2000 psi (13.79 MPa).

Table 2.2 ACI 530.1-05 (2005) Table 2

Net area compressive strength of concrete masonry units, psi (MPa)		Net area compressive strength of masonry, psi ¹ (MPa)
Type M or S mortar	Type N mortar	
1250 (8.62)	1300 (8.96)	1000 (6.9)
1900 (13.10)	2150 (14.82)	1500 (10.34)
2800 (19.31)	3050 (21.03)	2000 (13.79)
3750 (25.86)	4050 (27.92)	2500 (17.24)
4800 (33.10)	5250 (36.20)	3000 (20.69)

¹ For units of less than 4 in. (102 mm) height, 85 percent of the values listed.

SUMMARY

The effects of unit and mortar properties on the compressive strength of concrete masonry prisms are important for the understanding of concrete masonry structures. However, the scope of this study is not to determine these effects. Tests completed to determine unit and mortar properties provide a verification of consistency. Concrete block size has been investigated in previous studies, however geometrical shape has not.

Grouted concrete masonry has been examined in connection with the effect of grout compressive strength on the strength of masonry prisms. Currently CSA S304.1-04 (2004) provides an estimation of masonry strength with regards to unit strength, mortar type and amount of grout. ACI 530.1-05 (2005) supplies an approximate compressive strength of concrete masonry with respect to unit strength and mortar type only. Grout compressive strength and stiffness should be considered when determining the strength of concrete masonry prisms.

3 EXPERIMENTAL PROGRAM

3.1 INTRODUCTION

Physical and mechanical properties of each constituent of the masonry assemblage are essential for characterizing the mechanical properties of concrete masonry systems. This chapter discusses various elements of the concrete masonry assemblage and test procedures that were used to characterize the mechanical and physical properties. The University of Windsor testing facility was used for testing prism, mortar, and grout specimens, while the testing facility at McMaster University was used for the testing of unit specimens.

Three types of concrete masonry block were used for this study: (a) standard (stretcher) unit, (b) lintel unit, and (c) knock-out unit. Prism specimens were prepared and tested to determine i) the effect of three different unit shapes (geometry) on concrete masonry compressive strength and ii) effect of grout properties (strength and stiffness) on concrete masonry compressive strength. The prism specimens used to determine the effect of unit shape (geometry) on compressive strength were all ungrouted. Three block types as mentioned above and their combinations were used to determine the influence of geometric shape of concrete blocks on compressive strength of masonry construction. However, only standard (stretcher) block units were used to determine the effect of grout properties on the compressive strength of masonry assemblage. The following subsections describe the various tests used for determining the properties of block units, mortar, grout, and prisms.

3.2 BLOCK UNITS

Properties analyzed to characterize the block unit are: dimensions, water content, density, initial rate of absorption, and compressive strength. Test methods and results are presented next.

3.2.1 Dimensions

All of the blocks used in this study possess the standard nominal size of 200 mm (8 in) x 200 mm (8 in) x 400 mm (16 in). The dimensions of five blocks from each unit type were measured with a caliper accurate to 0.01 mm. The average values are given in Table 3.1. The results have a coefficient of variation is less than 10%, indicating conformity to the standard requirement in CSA A165-04 (2004a). A more detailed evaluation of block dimensions is given in Tables A3-A5 in Appendix A.

Table 3.1 Unit dimensions

Block Type	Width (mm)	Height (mm)	Length (mm)	Face-shell Thickness (mm)	Web Thickness (mm)
Standard	194.2 ± 0.4	193.0 ± 1.0	395.8 ± 0.8	33.12 ± 0.1	26.25 ± 0.2
Lintel	192.4 ± 0.5	192.8 ± 1.3	395.4 ± 1.1	40.29 ± 0.2	N/A
Knock-out	194.2 ± 0.4	191.6 ± 0.5	396.8 ± 0.4	39.16 ± 0.1	35.74 ± 0.1

3.2.2 Water Content, Density, and Absorption

The water content, density, and initial rate of absorption of concrete masonry units were measured for quality control purposes. These three properties can affect the way that water transfers from mortar or grout to the unit during curing. Test procedures from CSA

A165-04 (2004a) and ASTM C140-05a (2005) were used for determining these properties and are described next.

In order to obtain the unit water content, the units previously measured for dimensions were initially weighed to obtain the first weight, *A*. Then, they were submerged in water for 24 hours until they became fully saturated. Each unit was then weighed while fully submerged in the water, *B*, by placing the unit on a 'shelf' resting on a scale (Figure 3.1).

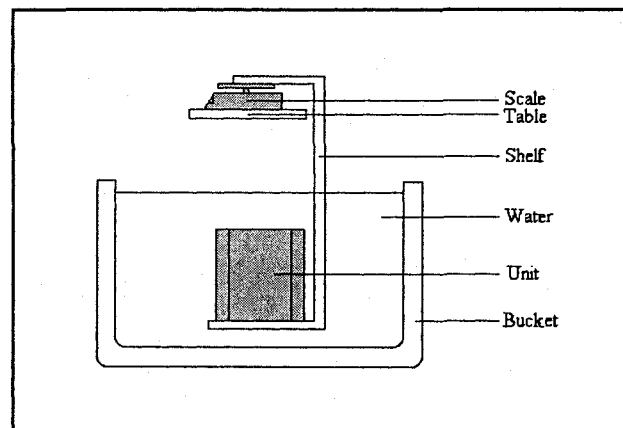


Figure 3.1 Fully submerged weight test setup

Subsequently, the blocks were removed from the water for one minute in room temperature to drip dry at the surface and the weight was again recorded, *C*. This value is called the saturated surface dry (SSD) weight. After drying all units for 48 hours, the oven dry (bone dry) weights were determined, *D*. Using these values, the water content at which the units were received and the density of each block were determined using the following relationships:

$$\text{Water Content (\%)} = \frac{A-D}{C-D} \times 100 \quad (3.1)$$

$$\text{Density (kg/m}^3\text{)} = \frac{D}{C-B} \times 1000 \quad (3.2)$$

Initial rate of absorption (*IRA*) for each unit type was then determined by submerging the bottom 1 mm of each bone dry unit in water (Figure 3.2) for one minute, followed by removing it out of the water, and then by weighing after the bottom is towel dried, *E*. The relationship used for determining the *IRA* is as follows.

$$\text{IRA (kg/m}^2\text{/min)} = \frac{E-D}{\text{Net Area (m}^2\text{)}} \quad (3.3)$$

Where,

$$\text{Net Area (m}^2\text{)} = \frac{\frac{C-D}{D} \times 10^3}{\text{height (m)}} \quad (3.4)$$

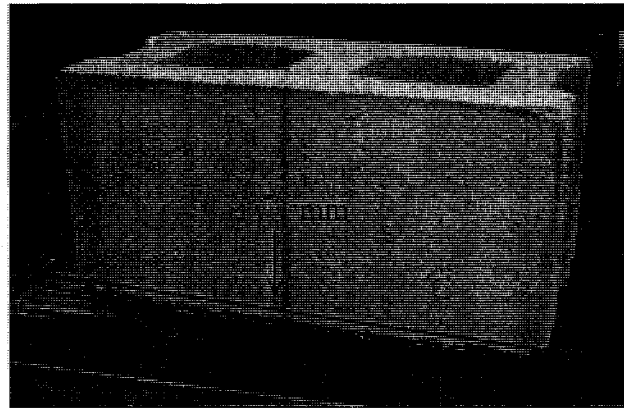


Figure 3.2 Initial rate of absorption test

All weights were determined at the McMaster University Structures Laboratory using a scale accurate to 0.001kg. The final values for water content, density, and *IRA* are

presented in Tables 3.2, 3.3, and 3.4 for standard units, lintel units, and knock-out block units, respectively. The coefficient of variation for the net area and density of the three block types were low (ranging from 0.36 to 0.59 for net area and 0.47 to 0.52 for density). The coefficients of variation for the water content were also low (ranging from 2.96 to 5.39), with the knock-out units having the least variation in the results. Therefore, the variations in measured of net area, density, and water content are acceptable as suggested in CSA A165-04 (2004a). The coefficient of variation of the initial rate of absorption findings for all three block types was very high. It is possible that more testing could provide amore accurate representation of the initial rate of absorption of each block.

Table 3.2 Standard block values

Block	Net Area (mm²)	Water Content (%)	Density (kg/m³)	IRA (kg/m²/min)
1	39729	5.65	2109	0.529
2	39361	5.16	2126	0.686
3	39591	5.52	2122	0.505
4	39906	5.57	2126	0.501
5	39381	4.98	2137	0.584
Mean	39594	5.38	2124	0.561
St. Dev	232	0.29	10.1	0.08
COV (%)	0.59	5.39	0.47	13.78

Table 3.3 Lintel block values

Block	Net Area (mm²)	Water Content (%)	Density (kg/m³)	IRA (kg/m²/min)
1	31869	8.64	1952	1.851
2	31758	9.14	1973	1.669
3	31741	9.66	1952	3.403
4	32173	9.38	1965	1.834
5	31751	9.27	1951	2.551
Mean	31858	9.22	1959	2.262
St. Dev	183	0.38	9.91	0.72
COV (%)	0.57	4.12	0.49	31.95

Table 3.4 Knock-out block values

Block	Net Area (mm²)	Water Content (%)	Density (kg/m³)	IRA (kg/m²/min)
1	44750	6.72	2056	1.408
2	44880	6.77	2049	1.604
3	44932	6.50	2063	1.424
4	45183	6.73	2057	1.350
5	44865	7.06	2035	2.296
Mean	44922	6.76	2052	1.616
St. Dev	160	0.20	10.7	0.39
COV (%)	0.36	2.96	0.52	24.22

3.2.3 Compressive Strength

The compressive strength of concrete masonry prisms is known to be affected by the compressive strength of the concrete unit. This is indicated by the design tables in CSA S304.1-04 (2004d) and ACI 530.1-05 (2005), which show masonry compressive strength is dependent on unit strength, mortar type, and percentage of grout (0 to 100%). The test method used in this study for determining the compressive strength of each type of masonry unit followed test methods CSA A165-04 (2004a) and ASTM C140-05a (2005).

It is important to cap the unit properly on both surfaces (top and bottom) to ensure it is leveled and has smooth loading surfaces (Figure 3.3) before the compressive strength is determined. A gypsum plaster compound (Hydro-Stone Gypsum Cement) was applied on a greased steel plate and the unit placed on top and leveled for capping. Top and bottom capping was left to cure for a minimum of 45 minutes before capping the other face of the unit. This was done to ensure the capping was hardened enough and thus, no uneven settlements on the capped surfaces would occur. Full bedded capping was used for unit compressive strength tests.

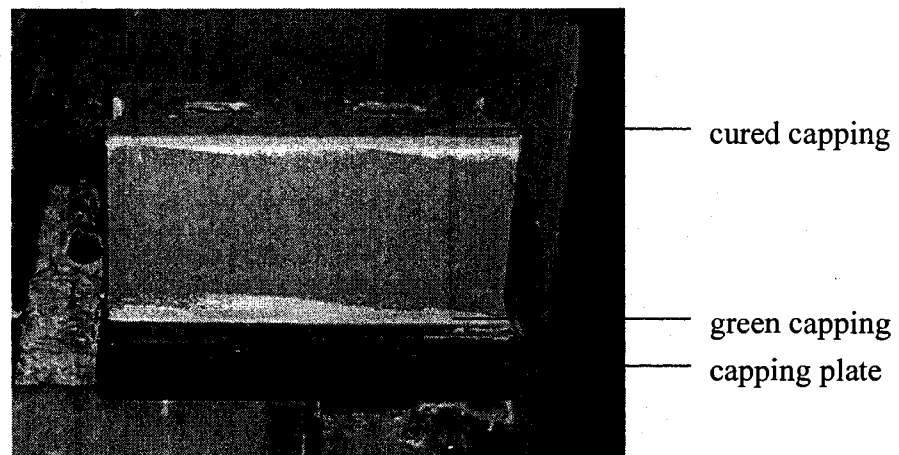


Figure 3.3 Unit capping

The compressive strengths of the units were determined using the prism test set-up of the McMaster University structures lab. Top and bottom bearing plates of 100 mm (4 in) thickness were used and the centre of the block was aligned with the centre of the loading jack using plumb-bobs to ensure concentric loading (Figure 3.4). Each unit was then loaded at a uniform rate until failure occurred (Figure 3.5).

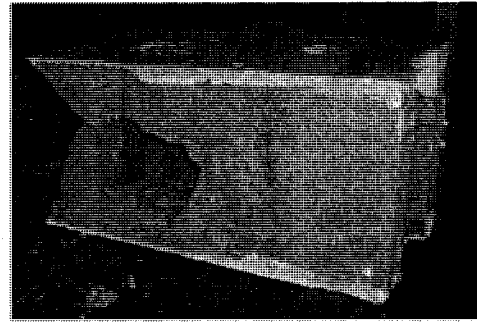
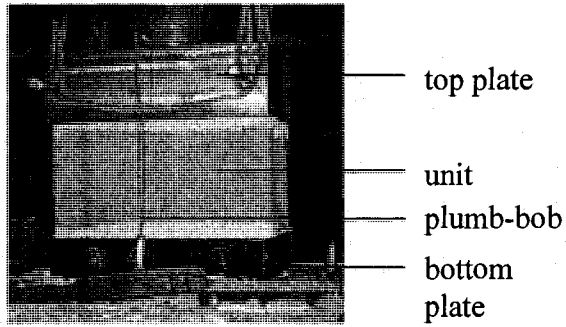


Figure 3.4 Unit test setup **Figure 3.5 Failed standard block (Duncan, 2008)**

The compressive strength was calculated by dividing the maximum load by the net compressive area (full bedded area) of the block (Equation 3.5). The average strength of each unit type can be found in Table 3.5.

$$f'_{block} = \frac{P_{ultimate}}{A_{net}} \quad (3.5)$$

Table 3.5 Block compressive strengths

Block	Standard			Lintel			Knock-Out		
	P_{max} (kN)	A (mm ²)	f'_{block} (MPa)	P_{max} (kN)	A (mm ²)	f'_{block} (MPa)	P_{max} (kN)	A (mm ²)	f'_{block} (MPa)
1	1420	39729	35.9	980	31869	30.8	1540	44750	34.3
2	1330	39361	33.6	1030	31758	32.3	1620	44880	36.1
3	1280	39591	32.3	920	31741	28.9	1615	44932	36.0
4	1330	39906	33.6	980	32173	30.8	1404	45183	31.3
5	1340	39381	33.8	850	31751	26.7	1424	44865	31.7
Mean	1340	39594	33.8	952	31858	29.9	1521	44922	33.8
St. Dev	50.5	232.0	1.3	69.1	183.3	2.2	102.6	160.4	2.3
COV (%)	3.8	0.6	3.8	7.3	0.6	7.3	6.7	0.4	6.7

The standard and knock-out blocks exhibited the same compressive strength statistically, whereas the lintel blocks are found to have a compressive strength that is 12% lower on

average. The lintel units which had the lowest compressive strength also had the highest coefficient of variance. All three unit types met the requirements for 5 tests according to CSA A165-04 (2004a). According to CSA A165-04 (2004a), an additional five units need to be tested if the coefficient of variation is larger than 10%.

3.3 MORTAR

Type S mortar was used for both the geometrical (ungrouted) and grouted test specimens. The mortar was prepared by mixing the materials (Portland Cement Type 10, Ivory Autoclaved Finishing Lime, masonry sand, and water) in a wheelbarrow with a hoe. After mixing, no additional water was added to maintain consistency among all mortar batches used for prism construction. The mortar mix that could not be used within an hour of mix was discarded. For a detailed description of mix proportions see Table A8 in Appendix A.

Two tests were performed on the mortar: i) flow test and ii) strength test. The flow test was conducted for quality purposes and completed as each mortar batch was being mixed. Mortar cube tests were also conducted to determine the compressive strength of mortar at 28 day and prism test day. The following subsections present test methods used to determine the properties of mortar.

3.3.1 Flow

The flow test was performed while mortar was being mixed to verify quality and texture properties. Mortar was placed with a tamping rod in a greased standard brass made flow cone with a 100 mm (4 in) diameter at the base, 50 mm (2 in) diameter at top, and 25mm

(1 in) high (See Figure 3.6). The cone was then removed, allowing the mortar to spread onto the standard flow table. The table was then cranked (lifted up and then dropped) 25 times before measuring the flow value. The optimal flow value recommended in CSA A179-04 (2004b) for mortar (between 100% and 115%) was maintained for all batches. If a batch of mortar had a very high flow, it was mixed for a few minutes in order to let some water evaporate until the recommended flow value was achieved. The diameter of mortar mix was measured using a standard brass caliper (Figure 3.7).



Figure 3.6 Flow test table

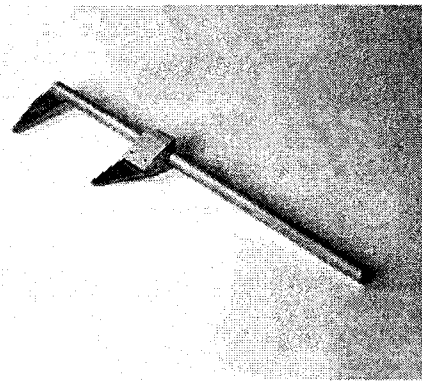


Figure 3.7 Brass caliper

3.3.2 Compressive Strength

In order to determine the compressive strength of the mortar, cube specimens were cast in greased 50 mm (2 in) standard mortar cube moulds. The mortar cubes were removed from the moulds 24 hours after casting, and left at room temperature to cure in air until testing. After 28 days, 3 mortar cubes from each batch were tested to obtain the 28 day strength. Three more cubes from same mortar batch were tested on the day of prism test to determine the compressive strength of the mortar at the day of prism tests. A 2000 MPa (300 ksi) capacity compression testing machine (Riehle) was used to test the mortar

specimen (Figure 3.8). Two steel plates were used to increase the height of the cube to prevent sticking of the machine at low heights.

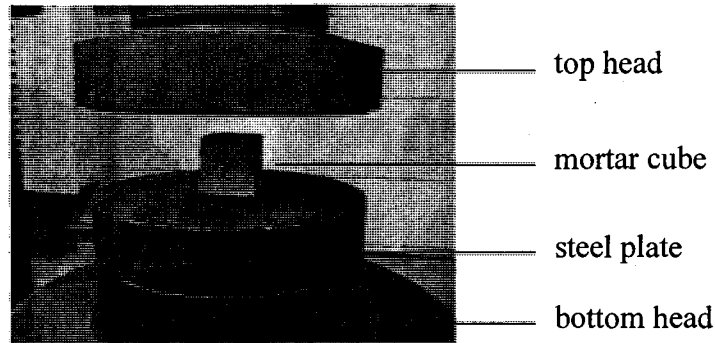


Figure 3.8 Mortar cube testing

3.4 GROUT

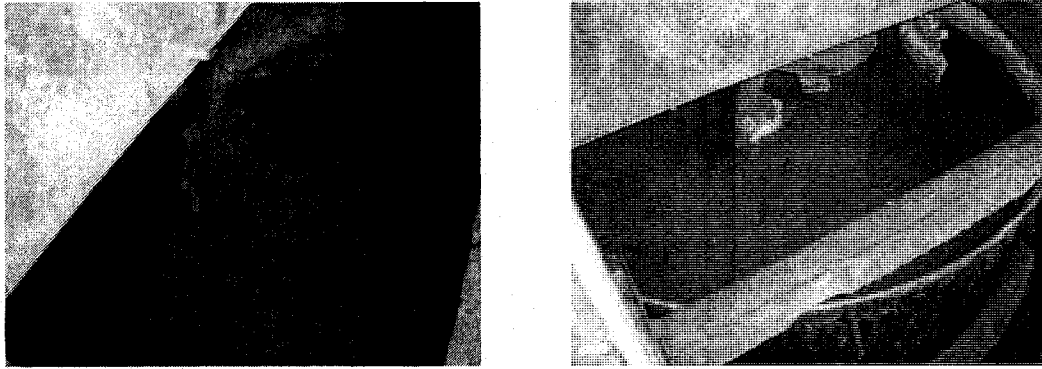
All grouted prism specimen were constructed using standard (stretcher) units only. In order to determine the effects of grout properties on the compressive strength and modulus of elasticity of grouted masonry prisms, three different types of grout were used in four sets of prisms (Table 3.6). Two of these three grout mixes were fine grout and thus, no coarse aggregate was used in this mix. These two mixes had the same proportions and were used in the N and P prism sets. The N prisms were built with standard blocks and showed a good bond between the block and grout. The P prisms were also constructed of standard blocks. The cores of the prisms were painted with a high gloss acrylic paint (Beauti-Tone) and oiled with form release prior to grouting to prevent a bond between the units and grout. The other two mixes were coarse grouts (R and I) where coarse aggregate was used. These mixes had different properties (strength and stiffness). A water reducer

(Master Builders Technologies, Glenium 3400NV) was used to obtain a high flow of the grout and to avoid use of excess water.

Table 3.6 Grout mix proportions

Materials	Grouted Prism Type			
	N (Normal)	R (Strength)	I (Stiffness)	P (Painted)
Cement (kg)	1.6	1.8	2.1	1.6
Sand (kg)	7.9	5.7	5.7	7.9
Lime (kg)	0.1	0	0	0.1
Pea Gravel (kg)	0	3.1	4.1	0
Water (kg)	1.4	1.1	1.6	1.4
Admixture	for flow	for flow	for flow	for flow

All grout batches were mixed in the same manner in order to maintain consistency. The dry ingredients for each mix, including variations of cement (Portland Type 10, St. Lawrence), sand (coarse), hydrated lime (Ivory Autoclaved Finishing Lime), and pea gravel, were placed in a concrete mixer (Eirich Machines Inc.) and mixed before slowly adding the total amount of water. The water reducing admixture (Glenium 3400NV, Master Builders Technologies) was then added in parts as recommended by the manufacturer until the grout had the optimum spread (discussed in subsection 3.4.1). The effect of including admixture can be seen in Figure 3.9.



(a) (b)
Figure 3.9 Grout mixing process (a) before admixture (b) after admixture

Two tests were performed on the grout specimens in order to ensure its quality and to determine the effects of grout properties. The spread of grout is a good indicator of how the grout will flow into the voids of the masonry specimen, while a compressive test provides the compressive strength of the cured grout. It is also important to determine the modulus of elasticity of the grout. The modulus of elasticity of grout was used to study its effect on the properties of grouted masonry prism specimens. The following subsections present test methods for various tests used to determine the properties of grout.

3.4.1 Spread

In order to ensure proper placement of grout in prism cores, quality control of grout is important to ensure that the grout can flow into all of the crevices and fill all of the voids. Quality control of grout was achieved by performing spread tests on each batch with the same standard flow table and cone used for mortar testing. The table and cone were both greased before the grout mix was placed into the cone with a tamping rod. The cone was removed and the grout was observed to ensure it spread uniformly to a value of 100% to 115% of the original base value, as recommended by CSA A179-04 (2004b). The spread

was measured in the same manner as the mortar flow. However, the table was not cranked for the grout flow test. Figure 3.10 shows a typical grout spread test.

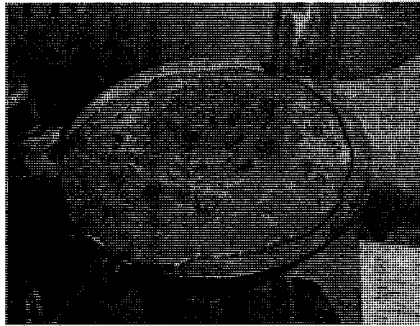


Figure 3.10 Grout spread test

3.4.2 Compressive Strength and Modulus of Elasticity

Cylindrical grout specimens were used to determine the compressive strength and modulus of elasticity of the cured grout, in accordance with CSA A23.3-3C (2004). The cores of single standard units were grouted and cured in air for six days. Grout cylinders of 50 mm (2 in) diameter were then drilled out of the grouted cores of the standard masonry units (Figure 3.11). A concrete drill with a diamond tip bit (Target Diamond Core Drill, model number DR-150) was used to core the cylindrical specimens from the blocks. Each cylinder was then trimmed to have a 2:1 height to diameter ratio, using a wet saw (General Electric, model number 5KC184BG81BU) with a diamond tipped blade.



Figure 3.11 Coring grout cylinders

Once the grout cylinders were surface dried for 24 hours after coring and cutting, cylinder dimensions were measured using a caliper accurate to 0.01 mm, and the cored specimens were capped in order to have a uniform surface for loading. A sulphur capping compound was used (Figure 3.12), as it is quick and simple for capping small cylinders. After heating, sulphur was placed on a greased capping plate and the cylinder was dipped in the semi-liquid sulphur and allowed to dry for 3-5 minutes. The process only takes 5 to 10 seconds for each cap. Excess capping material was then removed and each cylinder was then ready for tests.

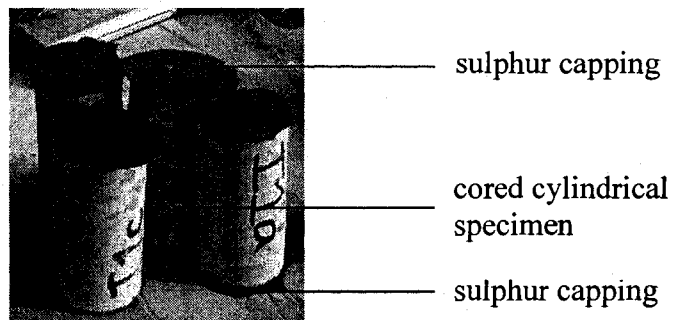


Figure 3.12 Grout cylinders

The cylinders were allowed to completely dry overnight, before they were tested to determine 7-day compressive strength. A calibrated 2000 MPa compression testing machine (Riehle) was used at a loading rate of 4.4 N/sec. A spring loaded linear potentiometer (LP) with a 12 mm (0.5 in) gauge length made by Techni Measure (model number S13FLP-12A-10K) with an accuracy of 3% was used to determine the deformation of the concrete over the full specimen length during loading (Figure 3.13). Test data were recorded at load increments of 4.5 kN (1000 lbs). The ultimate (maximum) load was recorded and loading continued until visible failure was observed (Figure 3.14).

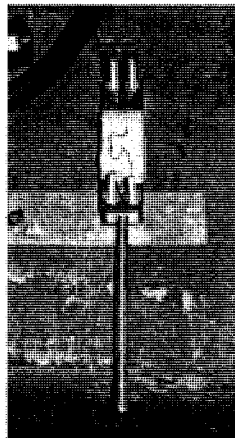


Figure 3.13 Linear potentiometer (S13FLP-12A-10K)



Figure 3.14 Failed grout cylinders

The modulus of elasticity of grout (E_g) was determined using the deformation data from the linear potentiometer during loading, taken over the full length of the core without capping. The specimens used for the prism test day compressive strength were cored, cut, measured and capped the same way and at the same time as the 7 day specimens. However, they were stored at room temperature until testing.

3.5 PRISM

Prism specimens are commonly used to simulate similar conditions in masonry assemblages while reducing space and cost requirements. It is important to prepare specimen that are as close to construction processes as possible and maintaining consistency throughout. Two half units were obtained by sawing a full unit in half. When cutting the knock-out blocks, the middle web was removed to ensure safety. All cuts were made with a large diamond blade (500 mm diameter) on a wet saw so that blocks were sawn in one direction, minimizing the chance of misalignment of cuts if a smaller blade was used instead.

The compressive strength (f'_m) and the Modulus of Elasticity (E_m) of the masonry specimens were determined by loading prism specimens in compression perpendicular to the bed joint. Cracking sounds and the mode of failure were observed and recorded during the tests. The following subsections present test methods for various tests used to determine the properties of prisms.

3.5.1 Construction

A certified mason from The Canadian Masonry Design Centre constructed all the prism specimens to maintain consistency and quality of the specimens. Mortar was mixed and used within an hour after water was added to the dry mortar mix. This prevented excess evaporation of water from the mortar before it was applied to the masonry prisms. No additional water was used to maintain consistency once the mortar batches were mixed. A level was used to ensure plane mortar joints, all of which were tooled to have a concave

joint. Both the geometrical and grouted prism specimens were four units high in a typical running bond pattern (See Figure 3.15). As shown, 2nd and top (4th) courses were comprised of two half units.

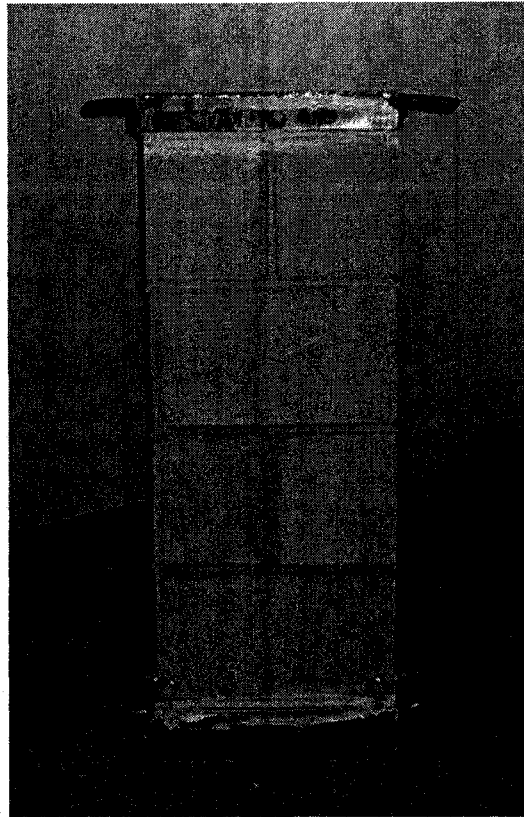


Figure 3.15 Capped prism specimen (S) (Duncan, 2008)

3.5.1.1 Geometrical Prism Construction

Five types of prisms were built to obtain a variety of construction practices (Table 3.7). Face shell bedding was used on all of the prisms to maintain consistency and practices similar to those on construction sites. The control specimens (Type S) were constructed of standard (stretcher) masonry units for all four courses where the bottom layer was a full unit and the top layer was comprised of two half units (Figure 3.15).

Table 3.7 Geometrical prism types (Duncan, 2008)

Prism Type	Block Types
Standard (S)	Standard
Lintel (L)	Lintel
Knock-out (K)	Knock-out
Standard plus lintel (SL)	3 standard, 1 full size lintel
Standard plus knock-out (SK)	3 standard, 1 full size knock-out

Prism types L and K were constructed of all four courses consisting of all lintel blocks and knock-out blocks, respectively (Figures 3.16 and 3.17). While cutting the knock-out blocks, the centre web was removed for safety precautions. Therefore, the half blocks in the knock-out prisms did not have the outer web (Figure 3.17).

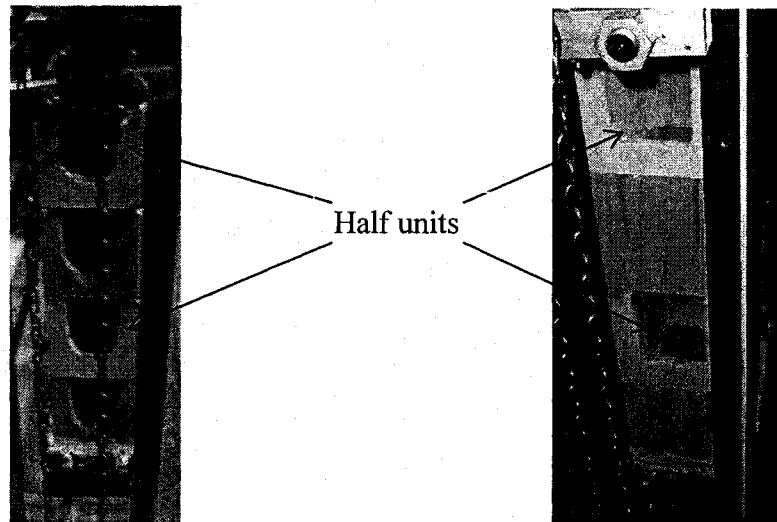


Figure 3.16 Prism Type L: side view

Figure 3.17 Prism Type K: side view

Prism types SL and SK were constructed of both standard and lintel blocks and standard and knock-out block, respectively. These specimens were constructed using half standard units for the 4th and 2nd layers. The bottom course was a full size standard unit. The 3rd course from the bottom of the prism was a full size lintel unit for SL prisms, and a full size knockout unit for SK prisms (see Figures 3.18 and 3.19, respectively).

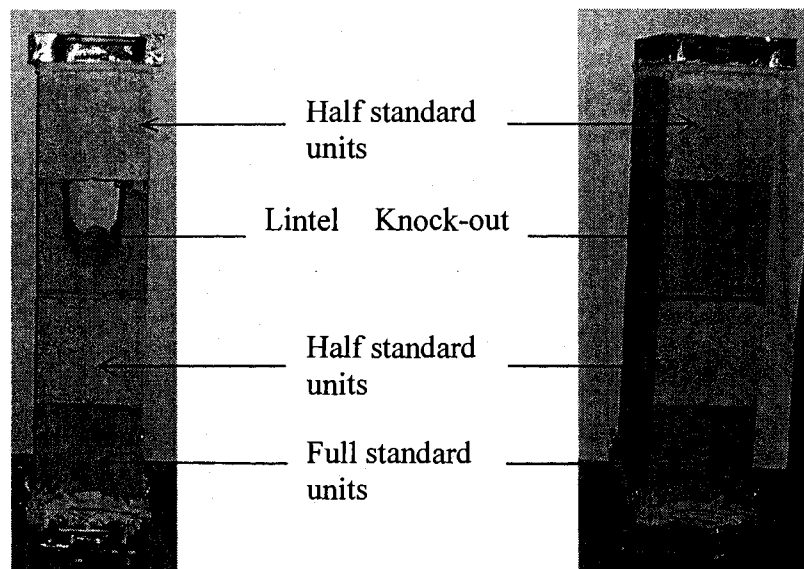


Figure 3.18 Prism Type SL: side view

Figure 3.19 Prism Type SK: side view

3.5.1.2 Grouted Prism Construction

All grouted prism specimens were constructed using standard (stretcher) units only (Type S). Four sets of five prism specimens were built (Table 3.8). For the purpose of this study, the first set (type N) was used as control specimens. Prism set R was grouted with Type R (strength) grout and used to determine the effect of grout strength on the compressive strength of masonry assemblage. The third set, prism set I, was grouted with Type I (stiffness) grout and used to study the effect grout stiffness on the compressive strength of

masonry construction. The final set, prism set P (painted), was used to determine the effect of bond strength between grout and masonry units on the compressive strength of masonry assemblage. This set had the cores of the blocks painted using a high gloss exterior paint (Beauti-Tone, Interior/Exterior Alkyd Enamel Gloss) in order to create a separation between the grout and blocks. A form releasing agent was applied on the painted core surfaces prior to grouting in order to prevent bonding of the grout and unit.

Table 3.8 Grouted prism types

Prism Set	Description
Normal (N)	Regular bond, normal strength and normal stiffness grout
Strength (R)	Regular bond, high strength and normal stiffness grout
Stiffness (I)	Regular bond, high stiffness and normal strength grout
Painted (P)	No bond, normal strength and normal stiffness grout

Due to core overlapping, the fissures on the sides of the prisms were closed using a weak mortar consisting of three parts sand to one part cement by volume. This ensured that the grout placed into the prism cores remained inside the core, and did not excrete out the sides.

Before grouting each specimen, each prism was cleaned using compressed air and then sealed at the base using a low-strength mortar to prevent excretion of any grout through the bottom. In order to ensure that set P had no bonding between units and grout a form release agent (Stone Manufacturing Ltd. Premium Low Odour Form Releases: Bronze)

was applied on top of the paint in the cores of the prism. The specimens from sets N, R, and S were lightly sprayed with water to optimize moisture transfer from the green grout to the units to aid in creating a good bond between the grout and prism.

Grout was placed into the prism cores in small equal amounts, varying each core, to maintain an even level within the specimen (Figure 3.20). Once the prisms were filled, a vibrator was inserted into each core and removed only once to ensure all areas of the cores were completely filled.

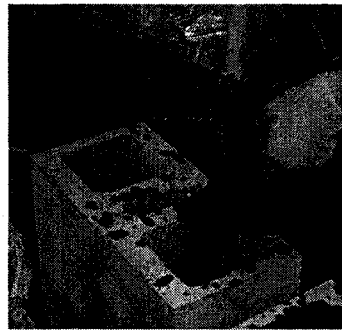


Figure 3.20 Grouting prism specimens

All prisms were covered with a tarp and kept in damp conditions using buckets of water under the tarp for the first twenty four hours in order to reduce cracking and separation of the grout from the unit. They were then exposed to normal room conditions for the continuation of the curing process.

3.5.2 Capping

It is important to have all prisms loaded uniformly. Thus, both top and bottom surfaces of each prism were capped using gypsum plaster (Gypsum Cement, Hydro-Stone). The top

and bottom capping plates were 50 mm (2 in) and 100 mm (4 in) thick, respectively and had an area equal to the area of the loading plates (200 mm x 400 mm). Prism specimens were lowered onto the bottom 100 mm thick capping plate (topped with green gypsum plaster) using an overhead crane. They were then leveled using a level and rubber mallet. The prism with its bottom cap was left to air cure for a minimum of forty five minutes before the top face capping was applied. Green gypsum plaster was placed on the top of the prism and the 50 mm top plate was lowered into place. The top plate was then leveled using a level and rubber mallet. After capping both surfaces the prisms were left for air curing over night before the strength test was carried out. Capped prisms can be seen in Figure 3.21.

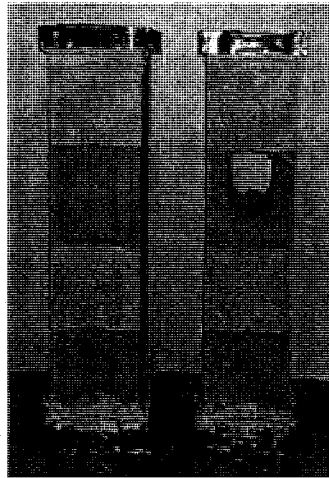


Figure 3.21 Capped prisms curing: side view

3.5.3 Instrumentation and Test Set-up

The compressive strength and modulus of elasticity of the prism specimens were determined by applying an axi-symmetric compressive load on the prism specimens. A

custom made donut shaped 3000 kN compression type load cell was used for acquiring the load data (see Figure 3.22). The load cell had eight strain gauges placed on the exterior face of the ring using the Wheatstone's bridge configuration (Figure 3.23). Four gauges were placed horizontally making up one full bridge and the other four were placed vertically to make the second complete bridge. These gauges were spaced equal distances apart, and alternating in direction (Figure 3.22). The load cell was calibrated before the first test and again after all the tests were completed using at 2000 kN (300 kip) compression testing machine.

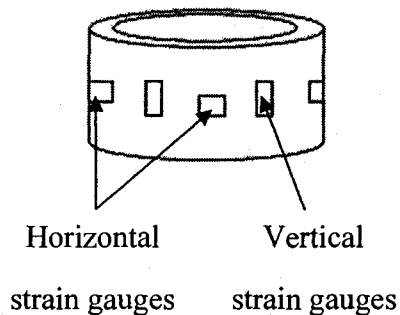


Figure 3.22 Load cell sketch

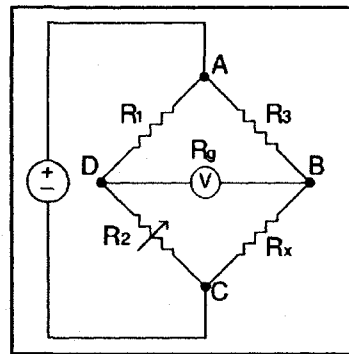


Figure 3.23 Wheatstone's bridge diagram

The load cell was attached to a 300 ton capacity double acting loading jack for applying the load on the specimen (see Figure 2.5). The compressive strength was then determined using the average compressive area of the prism. In the case of the geometrical (ungROUTED) sets of prisms, only the face shell (mortared area) area was considered. For the grouted prism specimens, the total prism area (face shell, webs, and cores) was considered. The compressive strengths of the geometrical and grouted prism sets were

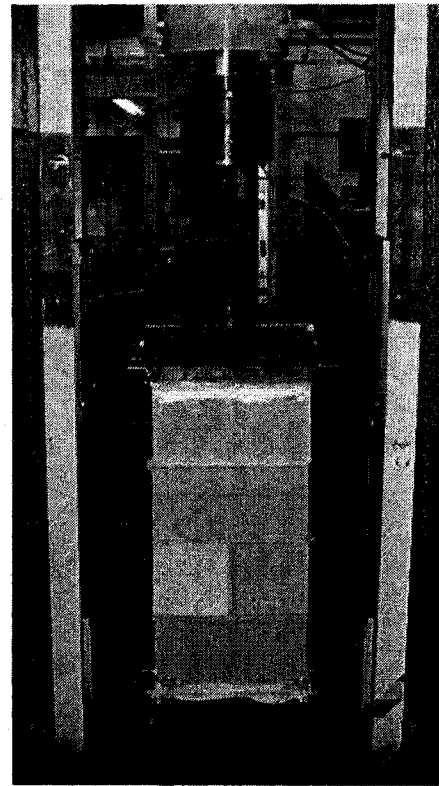
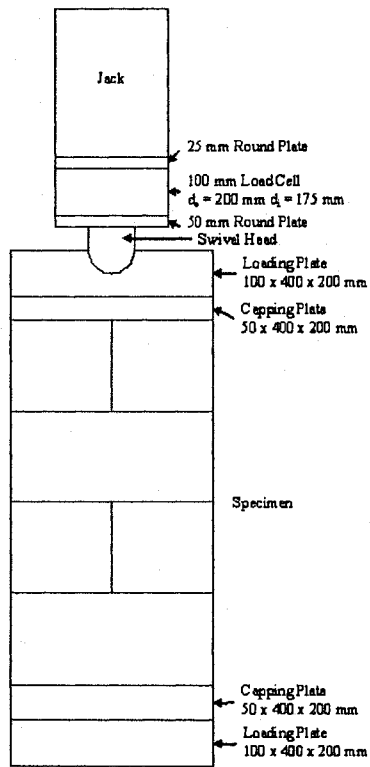
calculated using Equations 3.6 and 3.7, respectively, and are further discussed in chapters 5 and 6 respectively.

$$f'_m = \frac{P_{ultimate}}{A_{faceshell}} \quad (3.6)$$

$$f'_m = \frac{P_{ultimate}}{A_{total}} \quad (3.7)$$

A cylindrical swivel head was used between the load cell and the top loading plate to ensure application of an axi-symmetric axial vertical compressive load from the loading jack to a 100 mm (4 in) thick loading plate, which was placed on top of the prism (see Figure 3.24a). A 100 mm (4 in) bearing plate was also used at the base of the prism. This thickness was determined by calculating the distance from the platen edge to the corner of the specimen in accordance with ASTM C140-05a (2005). A photo of the prism test set-up is shown in Figure 3.24b.

The strain during loading was calculated from the deformation measurements through linear potentiometers (Techni Measure, S13FLP-12A-10K) as shown in Figure 3.26. The gauge length of strain measurement was 610 mm which covered three mortar joints. The strain data was used to calculate the stress values which occurred during loading. The modulus of elasticity was then determined from the stress-strain relationship and it is discussed in Chapters 5 and 6 for the geometrical and grouted prism sets, respectively.



(a) (b)
Figure 3.24 Test setup a) schematic b) photo (Duncan, 2008)

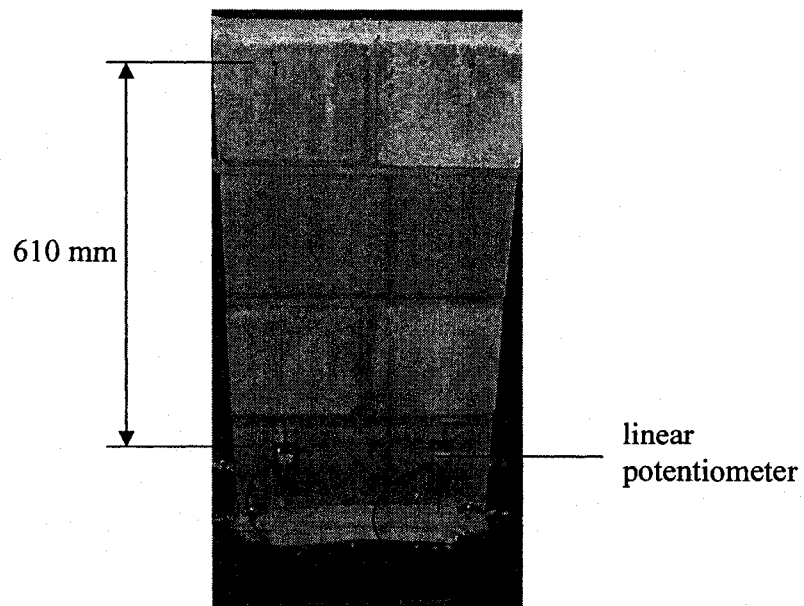


Figure 3.25 Linear potentiometers on prism specimen (Duncan, 2008)

3.6 SUMMARY

This chapter discussed tests method and test setup that were used in this study for determining various properties of materials and prism specimens. Consistency was maintained during preparation, construction, and testing of all constituents by following guidelines provided by the Canadian Standards Association and ASTM International. Tests were conducted at The University of Windsor and McMaster University. The following three chapters present and discuss test results obtained from this study.

4 MATERIAL PROPERTIES

4.1 INTRODUCTION

The properties of each constituent (block, mortar and grout) need to be determined. Only then can any conclusions be made of their effect on prism compressive strength. Each set of test data needs to be evaluated using the t-test method to determine if the data statistically represents the actual properties of the masonry components. This chapter discusses properties obtained from the tests of constituents of the masonry prism specimens used in this study. Compressive strength, density, and initial rate of absorption of units, compressive strength of mortar and grout, and stiffness of mortar and grout were determined and test results are presented in this chapter.

The two sample t-test is a statistical procedure used for evaluating whether the means of two groups are *statistically* different from each other (Johnson, 2005). A one sample t-test is used for verifying if the mean of one sample adequately represents the results. For a small sample with one mean, the t-test is used to determine if the calculated mean (μ) is acceptable within a specified confidence interval. In this test, the t-value is determined using equation 4.1, then compared to the critical t-value (t_α).

$$t = \frac{\mu - \mu_o}{S/\sqrt{n}} \quad (4.1)$$

Where μ is the actual sample mean,
 μ_o is the assumed mean,
 S is the standard deviation, and
 n is the sample number.

The critical t-value (t_α) is determined from a t-value table (Johnson, 2005). The table uses the specified confidence interval (CI) and the degrees of freedom for determining t_α . The degree of freedom is the number of opportunities for change and is defined as one less than the sample number. Typically the confidence interval is taken as either 95% or 99%. Depending on the alternative hypothesis, the “null hypothesis” ($\mu = \mu_0$) must be rejected based on the comparison of t and t_α . Table 4.1 produces the conditions of the t-test. If the null hypothesis ($\mu = \mu_0$) is not rejected then the calculated mean is acceptable within the specified CI. In Table 4.1 μ is the measured mean, μ_0 is the assumed (predicted) mean, t is the test t-value, and t_α ($t_{\alpha/2}$) is the critical t-value. If the “null hypothesis” is rejected this results in a non-representative mean.

Table 4.1 Critical regions for testing $\mu = \mu_0$ (Johnson, 2005)

Alternative hypothesis	Reject null hypothesis if:
$\mu < \mu_0$	$t < -t_\alpha$
$\mu > \mu_0$	$t > t_\alpha$
$\mu \neq \mu_0$	$t < -t_{\alpha/2}$ or $t > t_{\alpha/2}$

A two sample t-test is also used to determine whether or not the two sets of data are related. Each set of data has an actual mean (μ_1 and μ_2) and variance (σ_1^2 and σ_2^2). The “null hypothesis” (Equation 4.2) in this case assumes the difference of two means (μ_1 and μ_2) remains constant (δ) (Johnson, 2005). It is tested on the basis of independent sample sizes, n_1 and n_2 , respectively.

$$\mu_1 - \mu_2 = \delta \tag{4.2}$$

The critical t-value (t_α or $t_{\alpha/2}$) is determined based on a CI and degrees of freedom. The t-value for a two sample mean is calculated using equations 4.3 and 4.4.

$$t = \frac{\mu_1 - \mu_2 - \delta}{S_p \sqrt{\frac{1}{n_1} + \frac{1}{n_2}}} \quad (4.3)$$

Where μ_1 is the mean of set 1,

μ_2 is the mean of set 2,

δ is a constant,

n_1 is the number of data in set 1,

n_2 is the number of data in set 2, and

S_p^2 is the pooled sum of squares of sets 1 and 2, defined as

$$S_p^2 = \frac{(n_1 - 1)S_1^2 + (n_2 - 1)S_2^2}{n_1 + n_2 - 2} \quad (4.4)$$

Where S_1 is the standard deviation of set 1, and

S_2 is the standard deviation of set 2

As with the 1-sample t-test with one mean, the rejection of the “null hypothesis” is determined based on the comparison of t and t_α . The correct evaluation depends on the respective alternative hypothesis used (Table 4.2). If the “null hypothesis” is not rejected, the difference between the two sample means is constant. This indicates that the two samples are statistically related (Johnson, 2005).

Table 4.2 Critical regions for testing $\mu_1 - \mu_2 = \delta$ (Johnson, 2005)

Alternative hypothesis	Reject null hypothesis if
$\mu_1 - \mu_2 < \delta$	$t < -t_\alpha$
$\mu_1 - \mu_2 > \delta$	$t > t_\alpha$
$\mu_1 - \mu_2 \neq \delta$	$t < -t_{\alpha/2}$ or $t > t_{\alpha/2}$

For this study, a CI of 95% was chosen. The “null hypotheses” used in this study are: (i) $\mu = \mu_0$ for a single sample data set and (ii) $\mu_1 - \mu_2 = \delta$ for a two sample data set; where δ was taken as zero (thus the null hypothesis states that the two means are statistically equal). The alternative hypotheses used for this study are (i) $\mu \neq \mu_0$ and (ii) $\mu_1 - \mu_2 \neq \delta$, respectively. The “null hypothesis” is rejected if the calculated t-value for a two sample test is either less than $-t_{\alpha/2}$, or greater than $t_{\alpha/2}$.

4.2 TEST RESULTS

The test results of the properties of the constituents were first examined before analysis was undertaken. The following sections provide the results obtained from block tests, mortar tests, and grout tests.

4.2.1 Block Properties

For the purpose of this study, the compressive strength, density, and initial rate of absorption of each unit type were investigated.

4.2.1.1 Compressive Strength

Three different units: (i) standard (stretcher) unit, (ii) knock-out unit, and (iii) lintel unit were used in this study. Five units for each block type were used to determine the compressive strength. The test data for the units are presented in Table 4.3. The coefficient of variation for the standard, lintel, and knock-out units are 4%, 7%, and 6% respectively. These results indicate that the variation among block types is consistent.

The detailed values for area, ultimate load, and strength are shown in Tables A3-A5 in Appendix A.

Table 4.3 Block compressive strength results (MPa) (Duncan, 2008)

Test Number	Standard Unit	Lintel Unit	Knock-out Unit
1	35.9	30.8	34.3
2	33.6	32.3	36.1
3	32.3	28.9	36.0
4	33.6	30.8	31.3
5	33.8	26.7	31.7
Mean	33.8	29.9	33.8
St. Deviation	1.27	2.17	2.28
COV (%)	4	7	6

The proportioned block compressive strength for prism types SL and SK were taken as the weighted average (three parts standard block strength and one part lintel or knock-out block strength). Therefore the block strength for the SL type prisms was taken as 31.1 MPa. Since the block strength of the S and K blocks was the same, the block strength for the SK prisms remained at 33.8 MPa.

4.2.1.2 Density and Initial Rate of Absorption

The density and IRA of the three block types were determined by testing 5 units for each block type and calculating using Equations 3.2 and 3.3. The results including the mean and COV for the block density are given in Table 4.4. The results show that the three block types have little variation in their densities given that the COV is less than 1%.

The IRA results, given in Table 4.5, show higher coefficients of variation, with the lintel and knock-out blocks having significantly higher values. The mean IRA for the standard units, lintel units, and knock-out units were 0.53 kg/m²/min, 2.26 kg/m²/min, and 1.62 kg/m²/min, respectively. The IRA results indicate that the bond strength between block and mortar for the three block types can be different. The block density was taken as the weighted average for the SL and SK prisms in the same manner as block strength previously discussed in section 4.2.1.1.

Table 4.4 Block density (kg/m³) (Duncan, 2008)

Test Number	Standard Unit	Lintel Unit	Knock-out Unit
1	2109	1952	2056
2	2126	1973	2049
3	2122	1952	2063
4	2126	1965	2057
5	2137	1951	2035
Mean	2124	1959	2052
St. Deviation	10	10	11
COV (%)	0.5	0.5	0.5

Table 4.5 Block IRA (kg/m²/min) (Duncan, 2008)

Test Number	Standard Unit	Lintel Unit	Knock-out Unit
1	0.529	1.851	1.408
2	0.686	1.669	1.604
3	0.505	3.403	1.424
4	0.501	1.834	1.350
5	0.584	2.551	2.296
Mean	0.561	2.262	1.616
St. Deviation	0.08	0.72	0.39
COV (%)	14	32	24

4.2.2 Mortar Properties

Six 50 mm (2 in) mortar cubes were cast from each batch of mortar produced during construction of the prism specimens. Three cubes from each mortar batch were used to determine 28 day strength to verify if the average strength met the strength requirement of CSA A179-04 (2004). The other three cubes were tested on the day of prism tests. The results of the mortar tests are given in Table 4.6. The results show that there a 15% increase in the mortar compressive strength between 28 day and prism test day. This indicates that the mortar continued to hydrate and increase its strength. Tables A1 and A2 in Appendix A have detailed descriptions of all prisms and their corresponding mortar batches.

The two sample t-test (with a 95% CI) indicated that the test day strength for mortar batch one was statistically comparable with batches 2, 3, 5, 10 and 11, using the t-test. Batch 2 was statistically comparable with batches 1, 3, and 5 through 11. The compressive strength of batch 3 was found to be statistically comparable with batches 1, 2, 4, and 5. Batch 5 was statistically comparable with batches 1, 2, 3, 7, and 11. The compressive strength of batch 6 was found to be statistically comparable with batches 2, 3, and 8-10, while batch 8 was comparable with batches 2, 6, 9 and 10. Since each batch had different means and standard deviations, when the strength of one batch was found to be statistically comparable with two other batches, this did not mean that those two batches statistically comparable, as can be seen. Table B2 in Appendix B gives a detailed summary of the mortar t-tests.

Table 4.6 Mortar compressive strength

Batch	28 day strength (MPa)	28 day average (MPa)	Standard deviation	COV (%)	Test day strength (MPa)	Test day average (MPa)	Standard deviation	COV (%)
1	19.31	19.94	1.6	8	20.86	22.29	1.4	6
	21.72				22.41			
	18.79				23.61			
2	19.65	19.13	0.8	4	21.72	22.41	3.2	14
	19.48				19.65			
	18.27				25.86			
3	19.13	20.22	1.5	7	21.20	22.06	0.9	4
	19.65				22.93			
	21.89				22.06			
4	18.79	17.06	2.7	16	14.97	15.37	1.0	7
	18.44				14.58			
	13.96				16.55			
5	15.00	15.86	0.8	5	21.72	20.57	1.6	8
	16.03				21.20			
	16.55				18.79			
6	18.10	18.85	0.7	3	26.63	24.53	2.1	9
	19.31				24.56			
	19.13				22.41			
7	14.65	15.51	1.1	7	18.27	18.21	0.2	1
	15.17				18.36			
	16.72				18.01			
8	23.44	22.93	0.6	3	27.15	27.29	1.9	7
	23.10				29.30			
	22.24				25.42			
9	19.82	21.49	1.5	7	25.77	25.65	0.4	2
	22.58				26.03			
	22.06				25.17			
10	19.99	20.40	0.4	2	24.05	24.19	0.7	3
	20.68				24.91			
	20.51				23.61			
11	19.48	19.88	0.4	2	20.17	19.99	0.6	3
	20.34				20.51			
	19.82				19.31			
Mean	19.21	19.21			22.05	22.05		
St. Dev	2.4				3.5			
COV (%)	13				16			

4.2.3 Grout Properties

When a prism is fully grouted, the area of grout is a significant portion of the overall compressive area of the prism. Therefore, it is important to understand how the grout contributes to the compressive strength of the prism. The strength and stiffness of the grout was determined in accordance with the test procedures described in CSA A179-04 (2004).

Three types of grout were used in this study to determine the effect of grout properties and the effect of bond between grout and unit on the compressive strength of the masonry assemblages. The first grout type, called "Normal" was used in the normal (N) and painted (P) prism sets. The other two types of grout are called "Strength" used in prism set R and "Stiffness" type, used in prism set I. These two grout types were used to determine the effects of changing the strength and stiffness of grout on the compressive strength of the prisms. The 7 day strength and stiffness of each grout type were determined using 5 cylindrical specimens for each grout mix. The dimensions of the cylindrical specimen were 50 mm in diameter with a height to diameter ratio of 2:1. The mean strength of each grout type was compared to the minimal 7 day strength specifications given in CSA A179-04 (2004). Another 5 grout specimens for each grout mix were tested on the day of prism tests. These values are shown in Table 4.7.

Table 4.7 Grout strength and stiffness

Type	7 Day	7 Day	Test Day	No. of Days	Test Day
	f_g (MPa)	E_g (GPa)	f_g (MPa)		E_g (GPa)
N	10.9	11.7	17.0	28.0	8.7
St. Dev	2.8	6.7	2.0		2.3
COV (%)	26	57	12		27
R	30.8	16.6	30.7	33.0	13.5
St. Dev	3.0	3.1	2.5		2.6
COV (%)	10	19	8		20
I	25.3	12.4	27.5	34.0	15.0
St. Dev	2.9	4	3.1		2.2
COV (%)	12	33	11		15
P	19.8	5.8	21.2	28.0	8.0
St. Dev	1.8	1.6	3.0		1.1
COV (%)	9	28	14		13

Grout sets N and P sets provided different compressive strengths even though the same mix was used. Their elastic modulus, however, is relatively comparable at test day. Both the compressive strength and stiffness of type R and I grouts were not much different, even though the mix proportions were different. The 7 day strength and stiffness were not representative of the properties at test day. No consistent trend could be determined and there is no rational explanation for this. The detailed test data are shown in Table A6 of Appendix A and the t-test data is shown in Table B3 of Appendix B.

4.3 ANALYSIS AND DISCUSSION

The following sub-sections present the results of the t-tests performed on the block, mortar, and grout specimens. All statistical analyses were undertaken using Minitab 15 Statistical Software (Minitab Inc., 2008). A discussion on the test results is also presented.

4.3.1 Block

The block compressive strength is used for quality control and to estimate the compressive strength of a masonry assemblage (CSA S304.1-04, 2004). The compressive strength found from the tests is considered as an accurate representation of the unit property. The 1-sample t-test was undertaken using commercially available software, Minitab 15 Statistical Software (Minitab Inc., 2008). The test data indicates that the compressive strength of the standard, lintel, and knock-out units can be taken as 35 MPa, 30 MPa and 35 MPa, respectively, with a 95% confidence interval. The 2-sample t-test shows that the compressive strengths of the standard and knock-out units are statistically the same. This implies that the comparison of the strength of the prisms made of standard units only, knock-out units only, and a mixture of standard and knock-out units will not be influenced by the unit strength.

The average IRA and density of each unit type were also evaluated using the 1-sample t-test. The IRA for the standard, lintel, and knock-out units were found to be statistically different with values estimated at 0.6, 2.3 and 1.6 kg/m²/min respectively (Tables 3.2 through 3.4). The same results were obtained for their respective densities, which can be taken as 2125, 1950, and 2050 kg/m³ (Tables 3.2 through 3.4). These results suggest that

the amount of water absorbed from the mortar during construction and curing will vary for each unit type. Therefore, this can potentially result in different bond strengths.

4.3.2 Mortar

Each mortar batch had a sample size of 3 for each test day resulting in a low number of degrees of freedom. However, the 1-sample t-test data showed that the average values of strengths are statistically acceptable with a confidence interval of 95%. As well, the overall average mortar strength of 22 MPa was also proven to be statistically correct for all mortar mixes combined.

4.3.3 Grout

Using the 1-sample t-test with a confidence interval of 95%, the average test-day compressive strengths found were: 17 MPa (N), 28 MPa (R), 28 MPa (I), and 21 MPa (P). As discussed in section 4.2.3, the N and P grouts exhibited different compressive strengths even though the mix proportions were the same. The 2-sample t-test using the N and P grout types proved that they are, however statistically comparable with a CI of 95%. The R and I grout mixes, although comprised of varied mix proportions, showed the same compressive strength and were also statistically comparable according to the 2-sample t-test.

The stiffness (modulus of elasticity, E_g) of each grout type was determined from the stress-strain curve produced during loading of the specimens. The average modulus of elasticity for each grout type was determined to be an accurate representation of the

physical property by means of the 1-sample t-test. Types N and P were proven to have the same modulus of elasticity statistically (8 GPa), while R and I had the same modulus of elasticity statistically (13.5 GPa).

5 GEOMETRICAL PRISM RESULTS AND ANALYSIS

5.1 INTRODUCTION

As with the constituents of the masonry assemblages, the properties of each prism type must be investigated to ensure that the numerical results properly represent the actual properties of the masonry specimens. The effect of the properties of masonry assemblage components on the prism properties must then be determined. This chapter discusses the results obtained from the geometrical prism sets.

The compressive strength and stiffness data obtained from each prism set in the geometrical group was analyzed using the t-test to ensure that the experimental results are able to statistically represent the properties of the masonry specimens. After these results are verified, multi-linear regression analysis was undertaken to investigate the effects of each constituent on the prism properties. The constituents included are: i) unit strength, f'_{block} , ii) mortar strength, f'_{mortar} , iii) geometrical shape, $A_{faceshell}$, and iv) unit density, ρ .

5.1.1 Background

The t-test procedure previously discussed in Chapter 4 was used to verify if the prism strength and stiffness results provide a good statistical representation of the prism properties. Multi-linear regression analysis was then used to determine the regression model which describes the effects of each constituent property on the compressive strength of each prism type.

Multi-linear regression analysis consists of a number of multiples equal to: $n (r + 1)$, expressed as $x_{i1}, x_{i2}, \dots, x_{ir}, y_i$, where r is the number of variables and n is the number of observations. The x values are assumed to be known without error (validated by t-tests) and the y values are the random variables. The regression equation is first treated as linear, where the mean distribution of y is given by Equation 5.1a (Lapin, 1997).

$$y = \beta_0 + \beta_1 x_1 + \beta_2 x_2 + \dots + \beta_r x_r \quad (5.1a)$$

Where $\beta_0, \beta_1, \beta_2, \dots, \beta_r$ are the variable coefficients, and x_1, x_2, \dots, x_r are the variable predictors

The method of least squares is applied to obtain estimates for the coefficients (β through β_r). This minimizes the sum of the squares of the vertical distances from the observations (y_i) to the plane. For example, a multiple regression analysis with $r = 2$ (two predictors: for example block strength and mortar strength) produces a mean distribution of y with three coefficients (β_0, β_1 , and β_2) and two predictors (x_1 and x_2) as shown by Equation 5.1b. Using the method of least squares, Equation 5.1b has a sum of the squares equal to Equation 5.2 (Lapin, 1997)

$$y = \beta_0 + \beta_1 x_1 + \beta_2 x_2 \quad (5.1b)$$

$$\sum_{i=1}^n [y_i - (\beta_0 + \beta_1 x_{i1} + \beta_2 x_{i2})]^2 \quad (5.2)$$

Equation 5.2 minimizes to the normal equations 5.3, 5.4, and 5.5 (Lapin, 1997).

$$\sum y = n\beta_0 + \beta_1 \sum x_1 + \beta_2 \sum x_2 \quad (5.3)$$

$$\sum x_1 y = \beta_0 \sum x_1 + \beta_1 \sum x_1^2 + \beta_2 \sum x_1 x_2 \quad (5.4)$$

$$\sum x_2 y = \beta_0 \sum x_2 + \beta_1 \sum x_1 x_2 + \beta_2 \sum x_2^2 \quad (5.5)$$

In the above equations,

$\sum y$ is the sum of the responses

$\sum x_1$ is the sum set 1 (in this example set 1 is block strength)

$\sum x_2$ is the sum of set 2 (in this example set 2 is mortar strength)

$\sum x_1 x_2$ is the sum of the products of sets 1 and 2

$\sum x_1^2$ is the sum of the squares of set 1

$\sum x_2^2$ is the sum of the squares of set 2

$\sum x_1 y$ is the sum of the products of set 1 and all the responses

$\sum x_2 y$ is the sum of the products of set 2 and all the responses

β_0 , β_1 , and β_2 are constants

Using these equations, the variable coefficients (β_0 , β_1 , and β_2) can be determined, resulting in the regression equation (Equation 5.1a).

The residual values (e) for each variable are taken as the difference between the model values (\hat{y}) calculated from the regression equation (Equation 5.1a), and the measured or experimental values (y). An overestimated model value results in a positive residual, while a negative residual value results in an underestimated one. When the sum of the squared residual values is minimized the model is considered to have a good fit to the measured data.

The adequacy of the model is also investigated by determining the coefficient of determination, R^2 . This quantity indicates the amount of variability explained by the regression equation. It is based on the ratio of the regression sum of squares, SS_R , to the total corrected sum of squares, SS_T , as shown in Equation 5.6 (Montgomery et al., 2003).

Since the total corrected sum of squares, SS_T , is equal to the sum of the regression sum of squares, SS_R , and the error sum of squares, SS_E , as in Equation 5.7 (Montgomery et al., 2003), the coefficient of determination, R^2 , can also be described as a function of the total corrected sum of squares, SS_T , and the error sum of squares, SS_E , which can be easier to calculate than the regression sum of squares, SS_R , shown as Equation 5.8 (Montgomery et al., 2003). A well fit model is said to have a coefficient of determination, R^2 , which is close to unity.

$$R^2 = \frac{SS_R}{SS_T} \quad (5.6)$$

$$SS_T = SS_R + SS_E \quad (5.7)$$

$$R^2 = 1 - \frac{SS_E}{SS_T} \quad (5.8)$$

Where R^2 is the coefficient of determination, SS_R is the sum of squares of the residuals, SS_T is the total sum of squares, and SS_E is the sum of squares of the errors.

Variance analysis of the model is used to determine the model quality, significance, and its ability to explain the variability in predicted values, \hat{y} . Residual plots and lack of fit tests provide an indication of the fit of the model. Using the F-probability distribution (α commonly taken as 0.05), the variance significance is determined through hypothesis tests. The two hypotheses for the regression model are: (i) H_0 , where it is assumed that all coefficients are equal to zero, and (ii) H_1 , where at least one coefficient is not equal to zero, as shown in Equations 5.9 and 5.10 (Montgomery et al., 2003).

$$H_0: \beta_1 = \beta_2 = \dots = \beta_r = 0 \quad (5.9)$$

$$H_1: \beta_i \neq 0 \quad (5.10)$$

If the calculated value F_o is greater than the critical value, $F_{v_1, v_2; \alpha}$, H_0 is rejected, indicating the form of the model has at least one significant (non-zero) coefficient. When determining the critical t-value, v_1 is the number of parameters and v_2 is the number of observations less the number of parameters. The critical value ($F_{v_1, v_2; \alpha}$) can be found from tables in any standard test book (Johnson, 2005).

The statistical significance of each parameter on the regression equation was taken as the percentage where the confidence interval for the respective coefficient does not include the zero value.

5.1.2 Outline of Investigation

For the purpose of this study, two sets of multi linear regression analyses and variance analyses were conducted using Minitab 15 Statistical Software (Minitab Inc., 2008). The first model included all five prism sets: standard (S), lintel (L), knock-out (K), standard plus lintel (SL), and standard plus knock-out (SK). The second model included the three prism sets which were made of only one type of block (S, L, and K). The purpose of having these two sets of data was to compare the effect of combining two different types of blocks in a prism on its strength as opposed to a prism comprised of only one type of block.

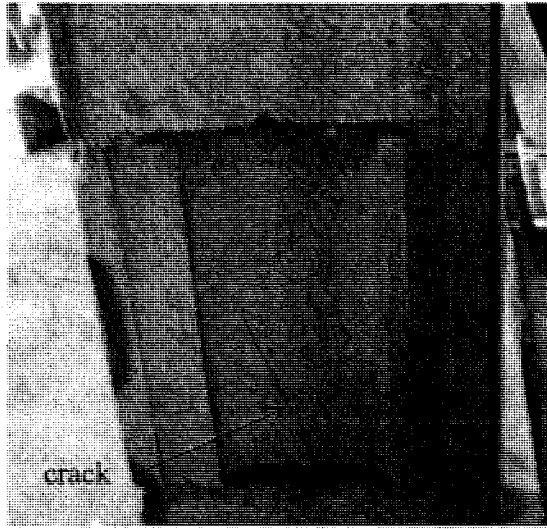
5.2 EXPERIMENTAL TEST RESULTS

The following sections discuss the results obtained from the prism compressive tests. Prism failure modes were observed visually for each prism type while the compressive strength and modulus of elasticity were determined from the test data.

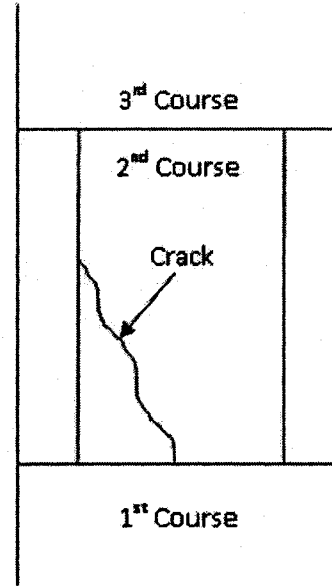
5.2.1 Failure Modes

Formation and growth of cracks was observed while the prism specimen was being loaded in compression. Cracks began to form at high stress points and provided a sense of how the specimen was going to fail. Failure for all prisms was sudden and brittle. The initiation and growth of cracks occurred quickly and failure occurred soon after. Thus, it was difficult to photograph the cracks.

The standard prism specimens (S) tended to have preliminary cracks in the webs of the blocks in the second and third courses as shown in Figure 5.1. At failure, the prisms separated through the centre of the webs splitting the blocks in two halves (lengthwise through the webs). This is shown in Figure 5.2. The units in the first and fourth courses were separated at 45 degree angles from the inner face shell to the outer face shell. This type of failure indicates that compressive forces were present in the face shells of the blocks (the only place where the prism was continuous throughout the height). As a result, tension occurred in the webs of the block resulting in initiation and progression of cracks. Failure occurred shortly after the prisms began to crack. The face shells of the central blocks were detached and exploded out in opposite directions at failure.



(a)



(b)

Figure 5.1: Standard prism crack pattern a) photo b) sketch (Duncan, 2008)



Figure 5.2 Web failure of standard prism

The prisms made of only lintel blocks (Type L) failed in a similar manner as the standard prisms (Type S). Cracks occurred in the “U-bend” of the second and third courses (Figure 5.3), with sudden failure happened soon after. The splitting direction of the block segments in the lintel (L) prisms was the same as the direction in the standard (S) prisms. The face shells of the units were split through the length of the unit at a 45° angle.

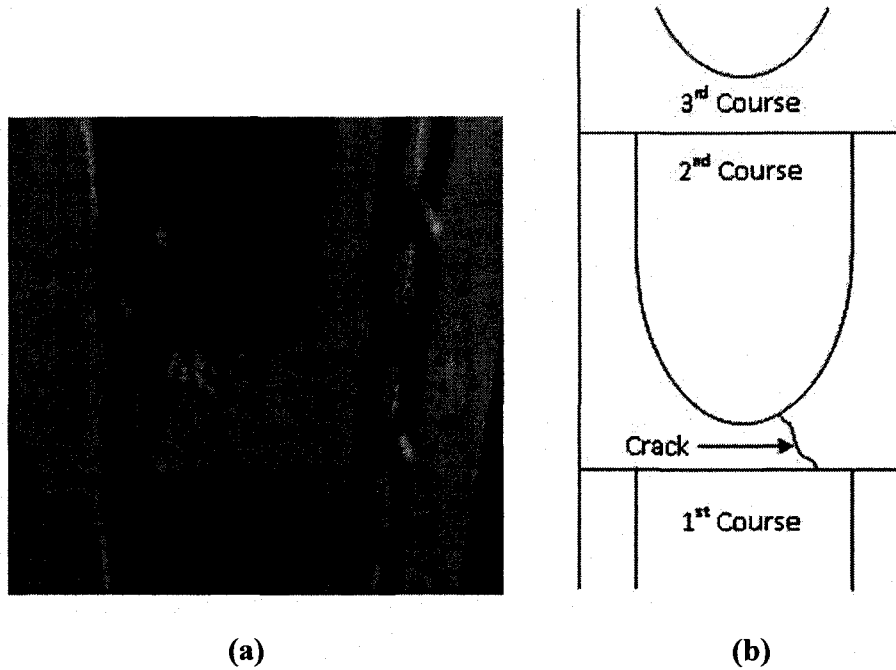


Figure 5.3 Lintel prism crack pattern a) photo b) sketch (Duncan, 2008)

The knock-out block prisms (Type K) failed in a similar way as the prisms made of standard block. However, cracks in the Type K prisms typically appeared near the cut out sections of the webs instead of the centres. The cracks occurred at the same location for both full units and half units, even though the external webs were not present in the half units of the second course from the bottom (Figure 5.4). At failure, webs were completely separated from the face shells.

The prisms which comprised of both standard units and lintel units (Type SL), as well as the prisms made of both standard units and knock-out units (Type SK) developed a combination of several crack patterns. For the standard units cracks developed in the same fashion as was for the S-prisms. The crack patterns in the lintel and knock-out units were

the same as what was observed in their respective prisms (Type L and Type K, respectively).

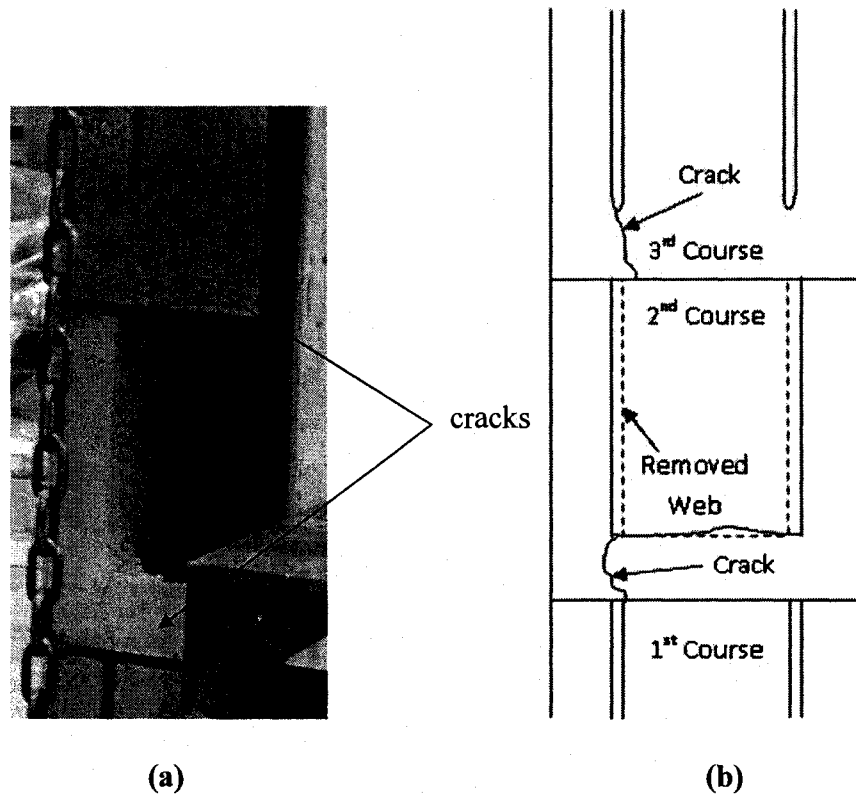


Figure 5.4: Knock-out prism crack pattern a) photo b) sketch

5.2.2 Compressive Strength

The load applied to the prisms was continuously acquired using a data acquisition system. The maximum load applied prior to failure was taken as the ultimate load capacity of the prism ($P_{ultimate}$). The face shell area ($A_{faceshell}$) was taken as the loading (compressive) area since face shell mortar bedding was used in prism construction. Thus, the ultimate compressive strength (f'_m) was calculated using Equation 5.11.

$$f'_m = \frac{P_{ultimate}}{A_{faceshell}} \quad (5.11)$$

The results of the compressive strengths of all five prism types (average \pm standard deviation) are summarized in Table 5.1 with one standard deviation (Table A1 in Appendix A shows all of the values for $A_{faceshell}$, $P_{ultimate}$, and f'_m). Using the one-sample t-test, all results were found to be accurate with a confidence interval of 95% ($\alpha = 0.05$). The results indicate that the S prism set and L prism set have a lower strength as compared to the other three prism sets (K, SL, and SK). The L prism set exhibited the lowest compressive strength, while the highest prism compressive strength was obtained from the K and SK prism sets which showed the same strength. The compressive strength of the S prism set was 16% lower than that of the K and SK prism sets and the L prism set is 27% lower than that of SL prism set. The one sample t-test was used to verify an accurate representation of the compressive strength and modulus of elasticity for each prism type.

Table 5.1 Geometrical prism results

Prism Type	Compressive Strength (MPa)	Modulus of Elasticity (GPa)			
		Measured	CSA	ACI	UBC
Standard (S)	22.9 \pm 2.2	18.2 \pm 2.8	19.5	20.6	17.2
Lintel (L)	20.1 \pm 1.1	16.4 \pm 1.4	17.1	18.1	15.1
Knock-out (K)	26.6 \pm 3.1	17.7 \pm 1.6	20.0	23.9	20.0
Standard plus Lintel (SL)	25.6 \pm 1.4	21.4 \pm 2.7	20.0	23.0	19.2
Standard plus Knock-out (SK)	26.6 \pm 2.8	22.0 \pm 3.2	20.0	23.9	20.0

Using the two sample t-test, the K, SL, and SK prisms exhibited the same statistical compressive strength. The compressive strength of the S prisms was found to be statistically higher than that of the L prisms. However, both exhibited lower compressive strengths than the K, SL, and SK prisms. The difference in compressive strength between the S, L, and SL prisms may be due to the increase in mortar bedded area between the second and third courses of the SL prisms. This increased bond area in the SL prisms, which is illustrated in Figure 5.5, was not measurable and thus, not accounted for in the calculation of the loaded area ($A_{faceshell}$). The increase in bonded area is caused by the larger mortar connection between the flanged face shells of the standard unit at the top of the second course and the full bottom of the lintel unit in the third course.

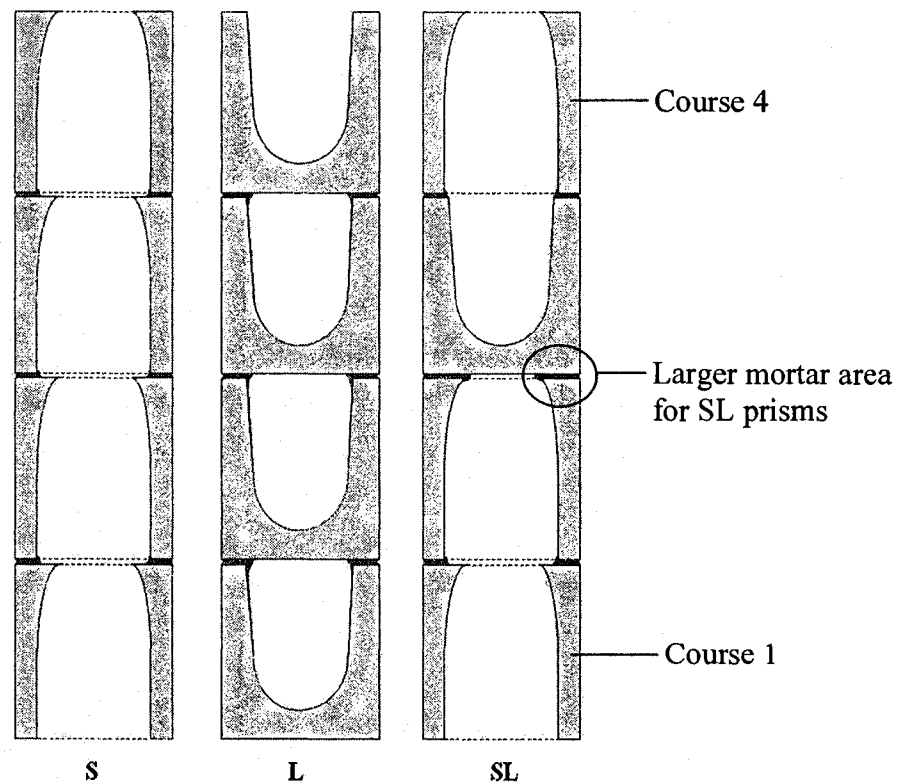


Figure 5.5 Cross section through the core of S, L, and SL prisms

The compressive strength minus one standard deviation of each prism type was also compared to the compressive strength values in Table 4 from CSA S304.1-04 (2004d) and Table 2 from ACI 530.1-05 (2005). In each case, the prism strengths met the values recommended in the Canadian and American standards (CSA S304.1-04, 2004d and ACI 530.1-05, 2005). The tables previously discussed in section 2.6.

5.2.3 Stress-Strain Characteristics

A study to determine the elastic modulus of hollow concrete masonry by Colville and Wolde-Tinsae (1993) suggested that the elastic modulus (E_m) must be taken as the chord modulus between 0.05 and 0.33 of the average prism compressive strength (f'_m). E_m is essentially constant up to $0.5f'_m$ (CSA S304.1-04, 2004d). They recommended that the elastic modulus of hollow concrete masonry can be taken as $666f'_m$, irrespective of unit type and mortar strength (Colville and Wolde-Tinsae, 1993).

The deformation of the prisms in this study was very small and not visible by naked eyes. Four linear potentiometers (LPs) were used for measuring the deformation. The modulus of elasticity was calculated between 5% to 33% of the ultimate strength (f'_m) on the stress-strain curve. A gauge length of 610 mm (as shown in Chapter 3 Figure 3.26) was used for measuring the deformation and strain. The strains were calculated using the deformation data. A typical plot for stress-strain diagram obtained from prism type S is shown in Figure 5.6. Typical similar plots for the other prism types are shown in Figures C1 through C5 in Appendix C. The typical location for each LP is shown in Figure 5.7.

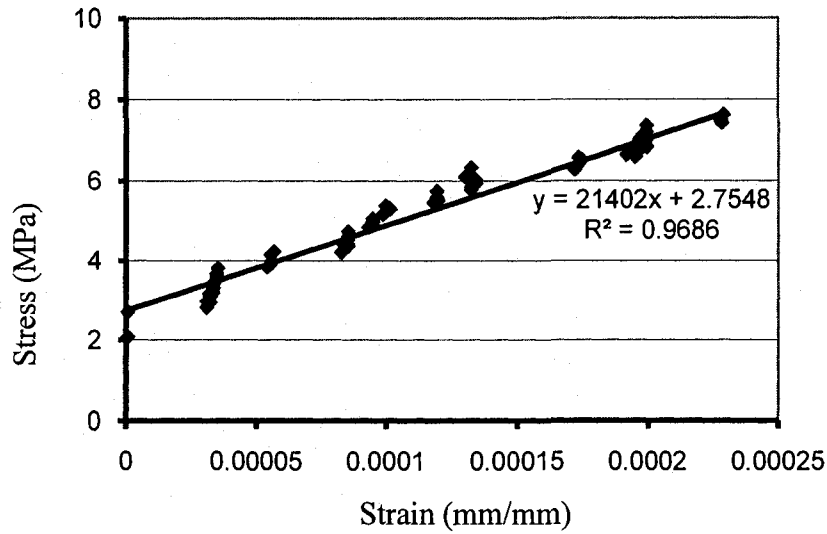


Figure 5.6: Stress versus strain relationship

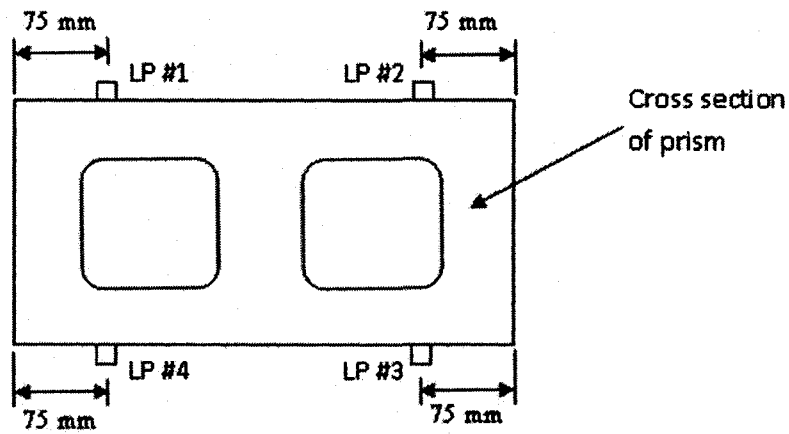


Figure 5.7 Schematic of the LPs locations

The modulus of elasticity, E_m , of the prism specimens was taken as the ratio of stress to strain and determined from Equation 5.12 from 5% to 33% of the ultimate prism strength.

$$E_m = \frac{\sigma}{\epsilon} \tag{5.12}$$

As shown in Table 5.1, the modulus of elasticity of all the prisms was similar for all except Type L. The S, L, K, SL, and SK prisms exhibited mean elastic moduli of 18.2, 16.4, 17.7, 21.4, and 22.0 GPa, with one standard deviations of 2.8, 1.4, 1.6, 2.7, and 3.2, respectively.

Canadian standard CSA S304.1-04 (2004d), the American standard ACI 530.1-05 (2005), and the Uniform Building Code (1997) relate the elastic modulus of concrete masonry assemblage, E_m , to the compressive strength of masonry, f'_m . Equations 5.13, 5.14, and 5.15 are the relationship recommended by CSA S304.1-04 (2004d), ACI 530.1-05 (2005), and UBC (1997), respectively

$$E_m = 850f'_m \geq 20 \text{ GPa} \quad (5.13)$$

$$E_m = 900f'_m \quad (5.14)$$

$$E_m = 750f'_m \quad (5.15)$$

CSA S304.1-04 (2004d) limits maximum value E_m to 20 GPa. However, in this study a majority of the prism specimens showed elastic moduli higher than 20 GPa. Table 5.1 shows a comparison between the predicted values and measured values of the modulus. Results indicate that the relationship recommended by the UBC (1997) yields the best results in general when compared to the values obtained in this study. ACI 530.1-05 (2005) recommendations overestimate the E_m value for all prism types. CSA S304.1-04 (2004d) also overestimates E_m in general except for types SL and SK.

5.3 MULTI-LINEAR REGRESSION ANALYSIS

Two regression analyses were undertaken to determine the effect of unit geometrical shape on prism strength by combining different unit types when constructing the prism specimens. The first multi-linear regression analysis, labeled Model 1, included all of the five prism types (S, L, K, SL, and SK), while the second, labeled Model 2, took into account the prisms constructed of only one type of unit (S, L, and K).

Using Minitab 15 Statistical Software (Minitab Inc., 2008), the regression equations for Model 1 and Model 2 were determined. Prism compressive strength, f'_m , was taken as the response, while the predictors (x_1, x_2, \dots etc.) comprised of unit strength (f'_{block}) mortar strength (f'_{mortar}) face shell area ($A_{faceshell}$) and unit density (ρ). Powers of unit strength and mortar strength, namely $f'_{block}{}^2$, $f'_{mortar}{}^2$, and $f'_{mortar}{}^3$ were initially not included. The residual plots for f'_{block} and f'_{mortar} were quadratic and thus, higher order terms were included to obtain linear residual plots and an optimum coefficient of determination, R^2 . The statistic significance of each predictor was determined based on the confidence interval at which there is no possibility for its coefficient to have a zero value. The variance of each model was determined using the F-probability distribution for $\alpha = 0.05$ and it was verified that the null hypothesis described in section 5.1.1 was rejected, indicating that at least one parameter is not equal to zero.

5.3.1 Regression Model 1

Regression analysis of the test data was carried out to examine the influence of mixing different type of units on the overall strength of the prism. Equation (5.16) was found to

provide a best fit when the data from all five prism specimen sets: the standard prisms (Type S), lintel prisms (Type L), knock-out prisms (Type K), standard plus lintel prisms (Type SL), and standard plus knock-out prisms (Type SK) are considered. The unit strength (f'_{block}) for the standard plus lintel prisms (Type SL) was taken as a weighted average of standard unit strength and lintel unit strength. The unit strength of the knock-out units was found to be the same as the standard units (Table 4.3). Thus, the weighted average was not required for the Type SK prisms. The weighted average of unit density (ρ) was also used for the SL and SK prisms during the analysis

$$f'_m = 131f'_{block} + 75f'_{mortar} + 0.00013A_{face\ shell} - 2f'_{block}{}^2 - 3.4f'_{mortar}{}^2 + 0.0508f'_{mortar}{}^3 - 0.076\rho - 2501 \quad (5.16)$$

Plots of the residuals (errors) for each variable are shown in Figures 5.8 through 5.15. A residual is the difference between the measured and estimated values in the regression equation. The variation in Figure 5.8 shows that there exists a possible pattern. As prism strength, f'_m , increases pattern of the residuals also increases. Higher residual variations for f'_{block} and $f'_{block}{}^2$ are seen at the higher strength values (Figure 5.9 and Figure 5.12). This may indicate that the fit of the model influenced by the block strengths. This characteristic needs to be normalized in order to effectively evaluate the effect of block geometry.

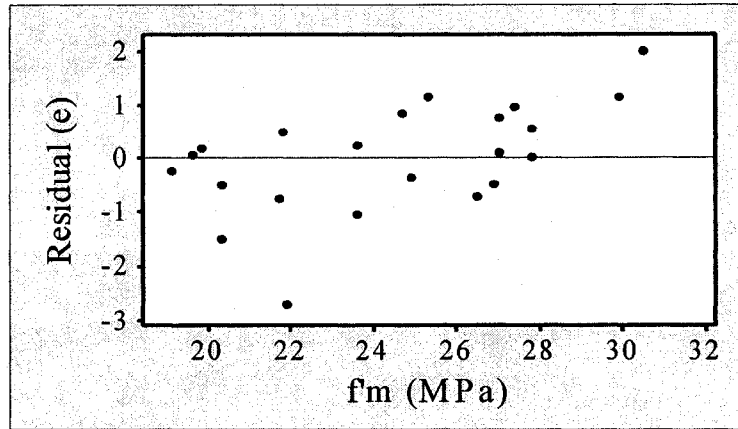


Figure 5.8 Residuals versus f'_m

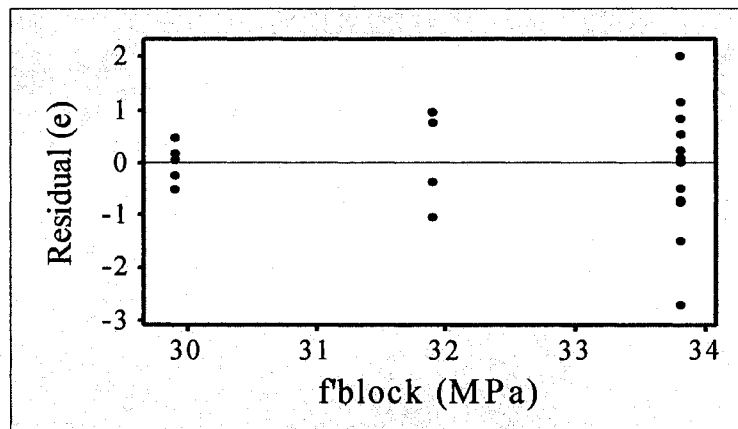


Figure 5.9 Residuals versus f'_{block}

Figures 5.10, 5.13, and 5.14, show the residuals (e) versus f'_{mortar} , $f'_{mortar}{}^2$, and $f'_{mortar}{}^3$. The results indicate a good spread with one outlier ($> \pm 2$) at a mortar strength of 24.2 MPa. This is due to the change in prism type, where four of the five mortar strengths refer to K prisms, while one refers to an SK prism with a lower compressive strength. It should be noted that five different mortar batches were used in making the prism sets associated with this model (See Table A1 in Appendix A).

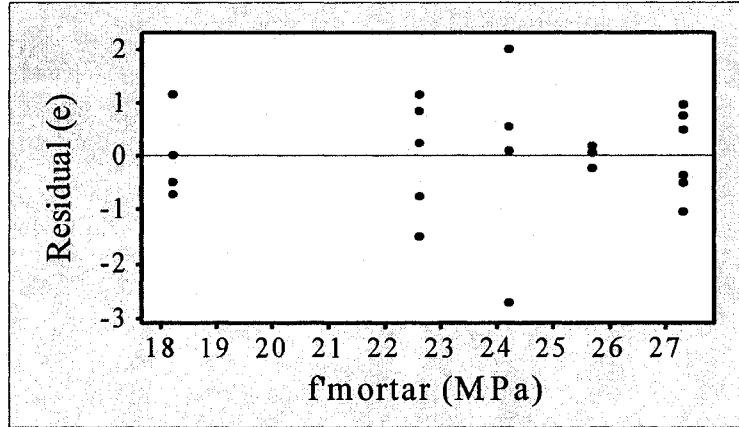


Figure 5.10 Residuals versus f_{mortar}

Three types of block units: i) standard, ii) lintel, and iii) knock-out were used in this study. Figure 5.11 displays the residual as a function of the face shell areas for all three block types. The residuals for the K prisms are positive with one negative outlier. The fit of the model might be better if this value is disregarded.

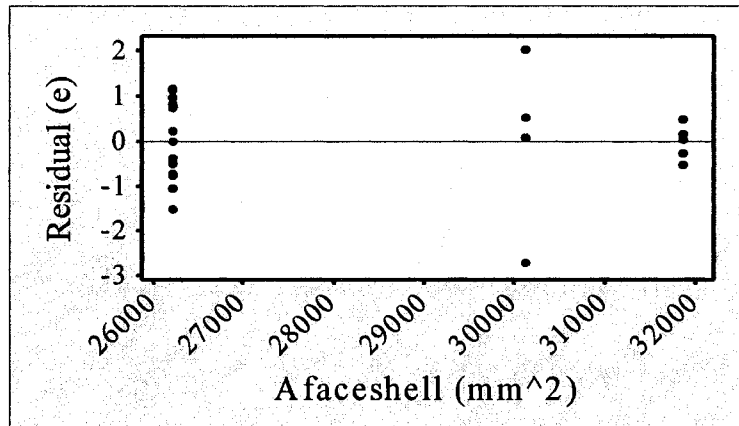


Figure 5.11 Residuals versus $A_{faceshell}$

Figure 5.15, which displays the residuals versus ρ , has a similar spread as residuals observed in for the mortar (Figures 5.10, 5.13, and 5.14); however there is an outlier for

the K prisms with a density of 2052 kg/m^3 . This is due to prism K01UM10 that has a lower compressive strength than the other four K prisms (See Table A1 in Appendix A).

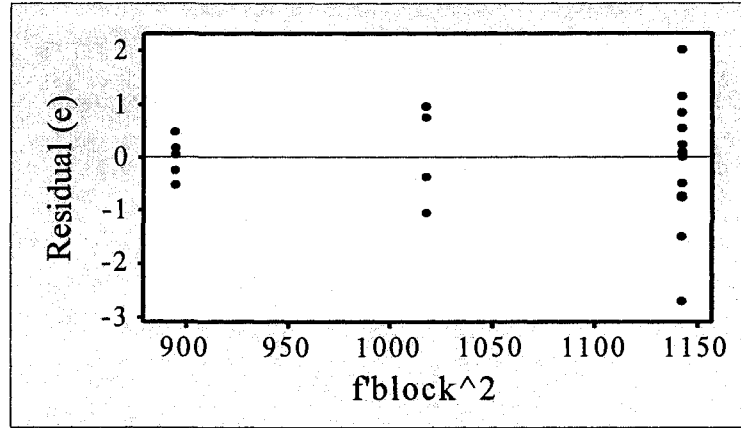


Figure 5.12 Residuals versus f_{block}^2

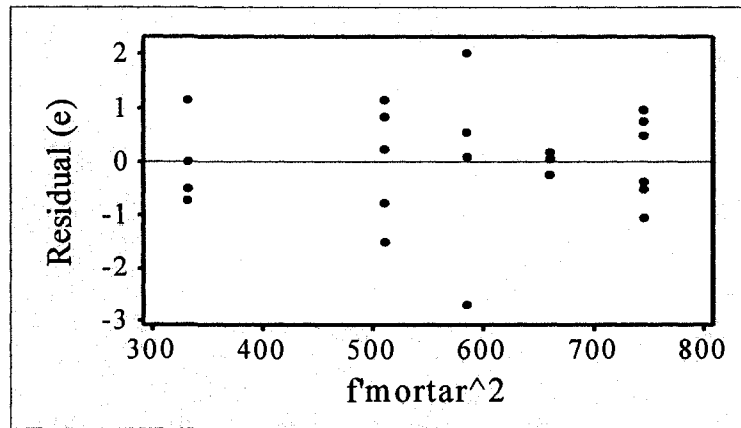


Figure 5.13 Residuals versus f_{mortar}^2

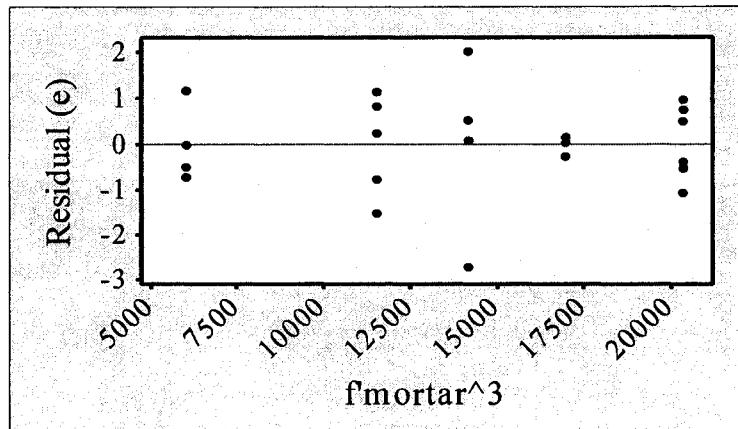


Figure 5.14 Residuals versus f_{mortar}^3

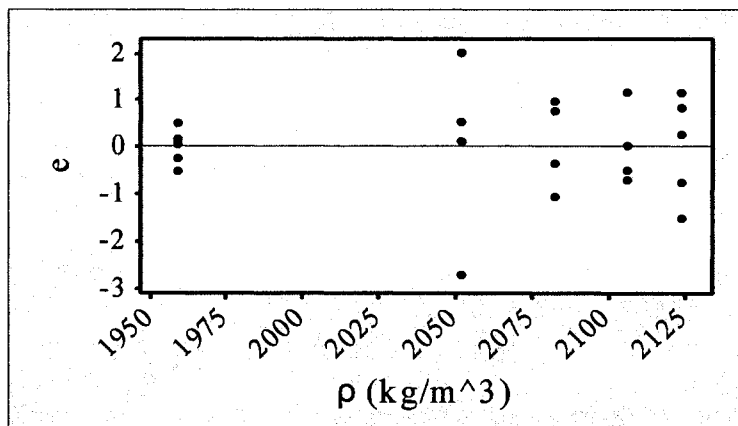


Figure 5.15 Residuals versus ρ

Figure 5.16 shows the relationship between the predicted prism compressive strength, f'_m , from the regression equation (Equation 5.16) and the measured values. This model has a coefficient of determination, R^2 , of 0.713, which suggests that 71.3% of the original variability of the measured data has been explained.

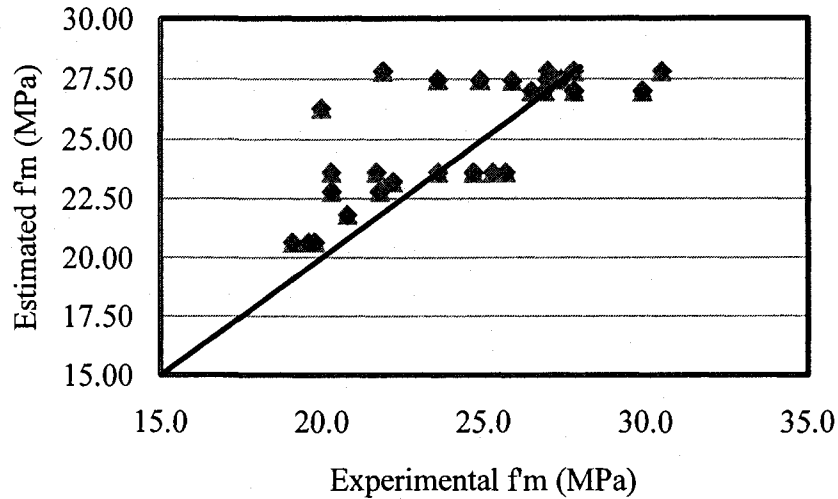


Figure 5.16 Predicted versus measured values for model 1

The analysis of variance can be seen in Table 5.2. In this table DoF stands for degrees of freedom; SS stands for sum of squares; MS stands for mean sum; and F stands for the model F-value. A critical value for $F_{v_1, v_2; \alpha}$ was determined as 2.58, which indicates that the model is significant with respect to the variables chosen where at least one parameter is not equal to zero.

Table 5.2 Analysis of variance for model 1

	DoF	SS	MS	F
Regression	7	185.081	26.44	6.02
Residual Error	17	74.562	4.391	
Total	24	259.734		

The coefficient values from Equation 5.16 with 95% confidence intervals ($\alpha = 0.05$ for t-distribution) are shown in Table 5.3. Since the confidence interval (CI) of each coefficient

includes the zero value, it shows that at this CI, it is possible that each variable could have a coefficient equal to zero, causing that variable to become obsolete in the model. The confidence level at which each predictor coefficient is statistically significant was determined by evaluating the point at which there was no possibility of the coefficient to have a zero value. Block strength (f'_{block}) was found to be statistically significant at a 92% confidence interval, while mortar strength (f'_{mortar}), face shell area ($A_{faceshell}$), and density, (ρ) were statistically significant at confidence intervals of 39%, 3%, and 26%, respectively. The squared term of block strength ($f'_{block}{}^2$) was found to be statistically significant at the same level as the linear term (92%). The squared and cubed terms of mortar strength ($f'_{mortar}{}^2$ and $f'_{mortar}{}^3$) were also found to be statistically significant near the same confidence interval as the linear term (40% and 42%, respectively).

Table 5.3 –95% confidence intervals for model 1 coefficients

Predictor	Coefficient	95% Confidence Interval	
		Low Level	Upper Level
f'_{block}	131	-14.19	276.40
f'_{mortar}	75	-229.92	379.82
$A_{faceshell}$	0.00013	-0.00677	0.00703
$f'_{block}{}^2$	-2	-4.23	0.22
$f'_{mortar}{}^2$	-3.41	-16.63	9.80
ρ	-0.076	-0.541	0.389
$f'_{mortar}{}^3$	0.0508	-0.1374	0.2390
c	-2501	-5990	995

This regression (Equation 5.16) indicates that the block strength (f'_{block}) is the primary factor in determining the prism compressive strength (f'_m) followed by the mortar strength

(f'_{mortar}) , density (ρ), and face shell area, ($A_{faceshell}$). Although face shell area was determined to be statistically significant at a very low confidence interval (3%), removing the term ($A_{faceshell}$) reduced the fit of the model (Equation 5.16). This suggests that the effect of geometrical shape on the compressive strength of the concrete masonry prisms is small. This is also suggested by the coefficient of the term (0.00013) which is very small.

A prediction for the elastic modulus of the masonry prisms, E_m , was also determined using the same linear regression method. The only predictor used in this equation was the compressive strength of the masonry prisms (f'_m). This is the method used for estimating E_m by CSA S304.1-04 (2004d), ACI 531-05 (2005), and UBC (1997). Equation 5.17 displays the relationship determined from this regression model.

$$E_m = 770f'_m \quad (5.17)$$

Figure 5.17 shows that the relationship between the predicted and measured elastic moduli (E_m) The model (Equation 5.17) is fit with a coefficient of determination (R^2) of 0.975. Table 5.4 gives the results from the analysis of variance. The critical value of $F_{v1,v2;\alpha}$ was determined as 1.38, which indicates that the model is significant with respect to the variables which were chosen, where at least one parameter is not equal to zero.

Table 5.4 Analysis of variance for E_m

	DoF	SS	MS	F
Regression	1	9583.0	9583.0	1024.52
Residual Error	26	243.2	9.4	
Total	27	9826.2		

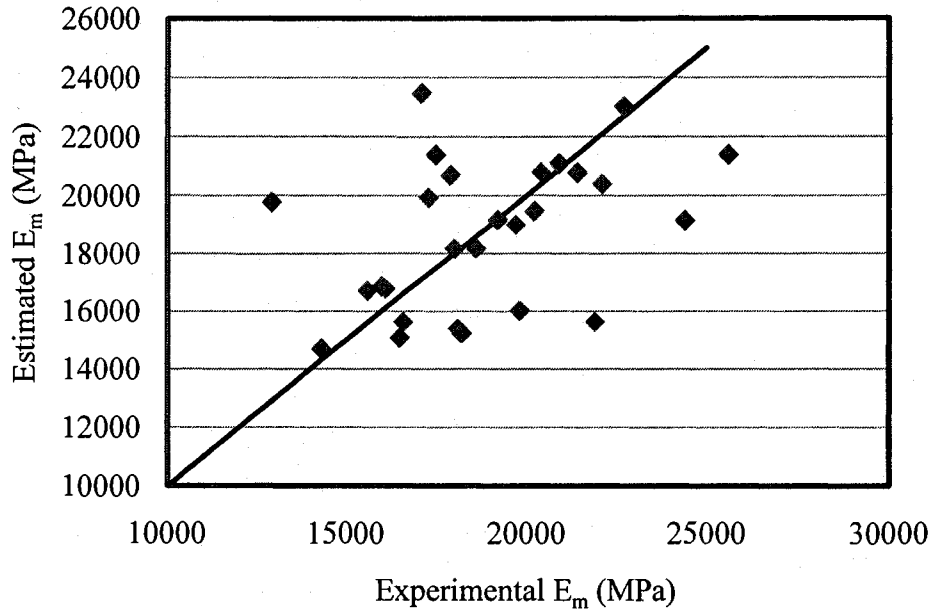


Figure 5.17 Predicted versus measured values for E_m for model 1

The only variable in this equation was prism compressive strength (f'_m) which was found to be statistically significant at a 99% confidence interval.

5.3.2 Regression Model 2

A second regression analysis was completed including the prisms constructed of one unit type only (Types S, L, and K). The same predictors were used for this regression as in Model 1. Using Minitab 15 Statistical Software (Minitab Inc., 2008), the regression equation for the three prism sets was determined. Although the same variables were used as before, squared block strength ($f'_{block}{}^2$) cubed mortar strength ($f'_{mortar}{}^3$) and unit density (ρ) were omitted. This was due to the high correlation between the variables once there were no weighted averages for the variables. Equation 5.18 shows the regression equation for Model 2.

$$f'_m = 2.45f'_{block} - 25.85f'_{mortar} + 0.00183A_{face\ shell} + 0.506f'_{mortar}{}^2 + 217.8 \quad (5.18)$$

The residual plots for each variable are shown in Figures 5.18 through 5.22. Figure 5.18 shows that as the compressive strength of the prism increases, the residuals move from a combination of negative and positive values to only positive values. This shows a tendency of the model to overestimate the prism compressive strength at higher strengths (above 26 MPa).

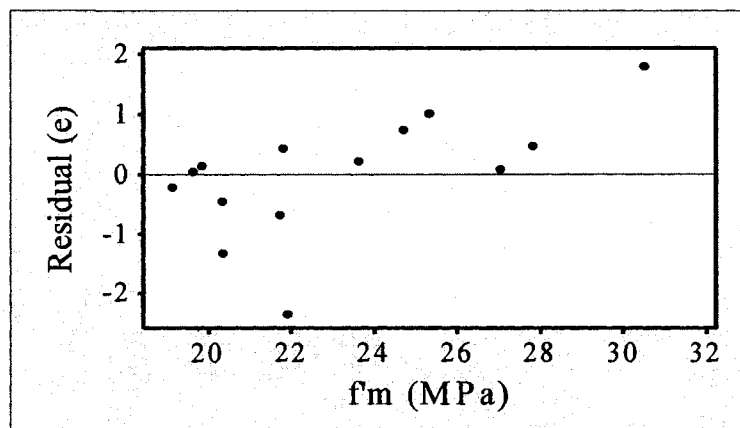


Figure 5.18 Residuals versus f'_m

The remaining plots show a linear relationship of the residuals, which is optimal. There does, however, seem to be a negative outlier from the K series; again it seems to be due to prism specimen K01UM10. This specimen also produced outliers in Model 1.

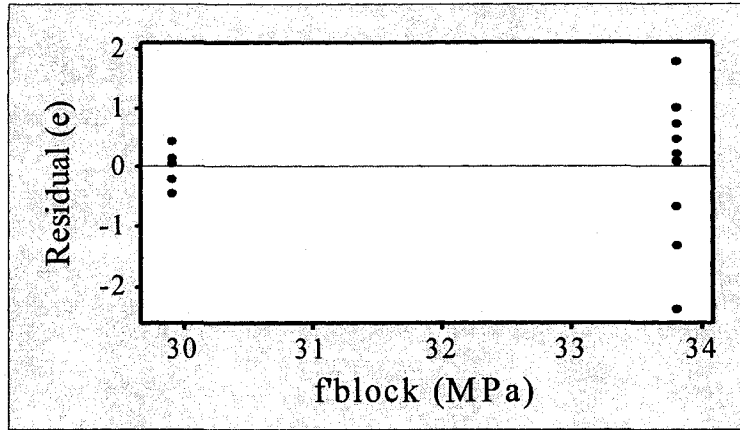


Figure 5.19 Residuals versus f_{block}

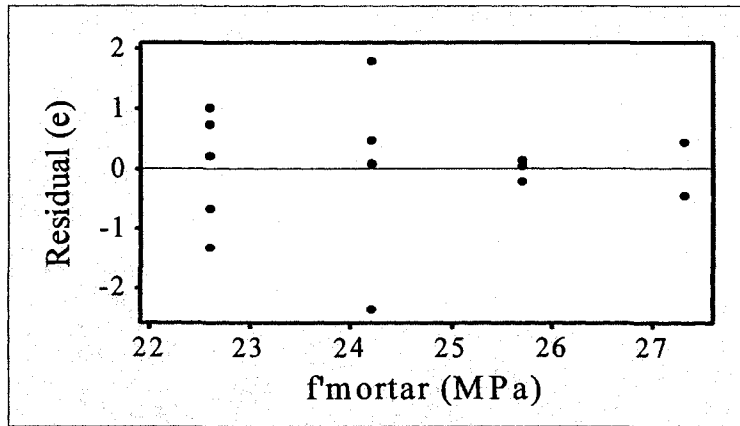


Figure 5.20 Residuals versus f_{mortar}

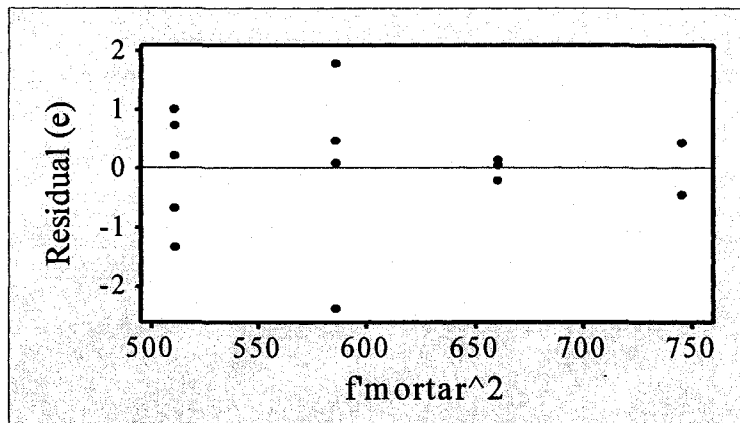


Figure 5.21 Residuals versus f_{mortar}^2

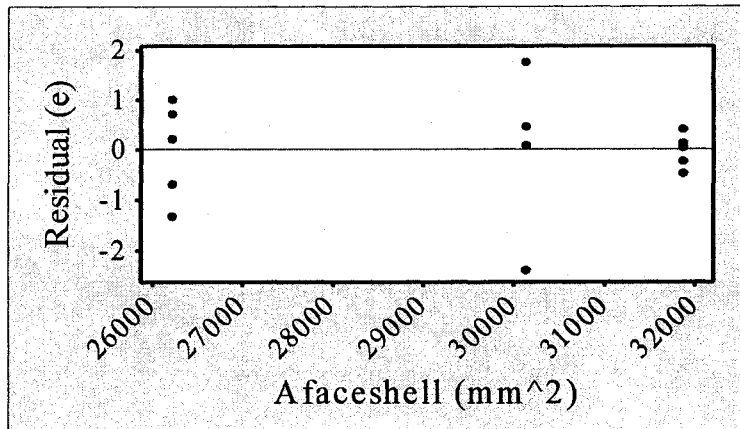


Figure 5.22 Residuals versus $A_{\text{faceshell}}$

Equation 5.18 is fit with a coefficient of determination (R^2) of 0.655, which suggests that 65.5% of the original variability has been explained. The fit of this regression equation is lower than that of Model 1 (Equation 5.16). This suggests that there is more variability among these prisms in comparison to the 5 prism sets. Table 5.5 is a representation of the analysis of variance for model 2 (Equation 5.18). The critical value of $F_{v_1v_2;\alpha}$ was determined as 3.36 (less than the F-value), which indicates this model is also significant with respect to the variables which were chosen, where at least one parameter is not equal to zero.

Table 5.5 Analysis of variance for model 2

	DoF	SS	MS	F
Regression	4	109.364	27.341	4.75
Residual Error	10	57.573	5.757	
Total	14	166.937		

The coefficient values from Equation 5.18 with 95% confidence intervals ($\alpha = 0.05$ for t-distribution) are shown in Table 5.6. For this model, block strength, f'_{block} , was statistically significant at a CI of 95%; however, this was untrue for all other variables.

Table 5.6 – 95% confidence intervals for model 2 coefficients

Variable	Coefficient	95% Confidence Interval	
		Low Level	Upper Level
f'_{block}	2.45	0.88	4.04
f'_{mortar}	-25.85	-109.83	58.13
f'_{mortar}^2	0.506	-1.113	2.125
$A_{faceshell}$	0.001832	-0.00205	0.00572
c	217.8	-729.33685	1164.83783

The same process for determining at which point each predictor is statistically significant was used as in the second model. Block strength (f'_{block}) was found to be statistically significant at a 99% confidence interval (Table 5.6). Mortar strength (f'_{mortar}) and its square (f'_{mortar}^2) were both statistically significant at 49%, which is slightly higher than those found for Model 1. Face shell area ($A_{faceshell}$) was found to be significant at a much higher level than in Model 1, at a 68% confidence interval.

Model 2 (Equation 5.18) suggests that the compressive strength of prisms comprised of one type of masonry block is primarily affected by block compressive strength. The next factor that seems to affect prism compressive strength is not mortar strength as what was found for Model 1 (Equation 5.16). The block geometry, indicated by prism compressive area is the most significant after block strength. Figure 5.23 shows the relationship between the predicted and measured prism compressive strength.

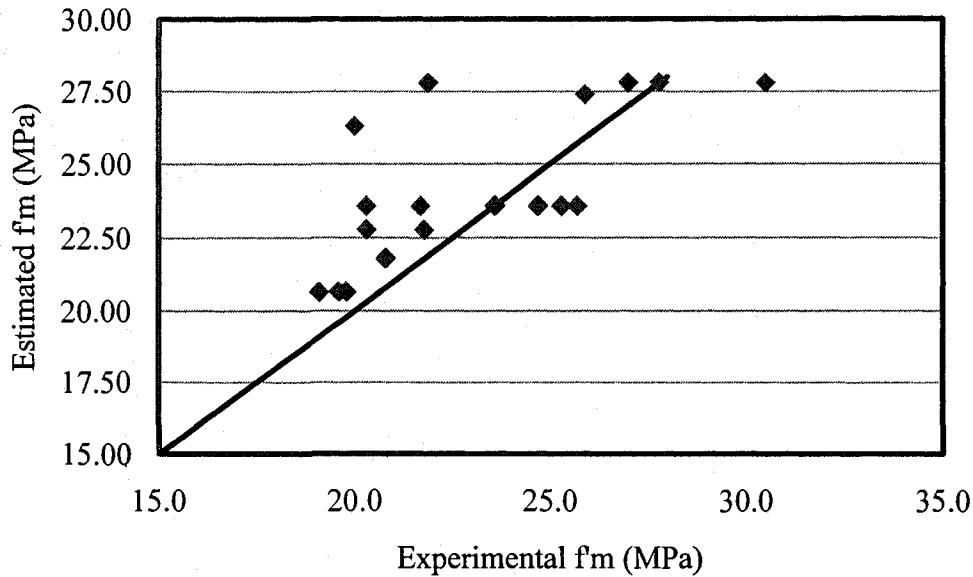


Figure 5.23 Predicted versus measured values for model 2

An estimation of the prism elastic modulus was also determined. Equation 5.19 was found to be the best fit regression equation which relates prism compressive strength to the elastic modulus of the prisms (E_m) for the three prism sets used in Equation 5.18.

$$E_m = 747 f'_m \quad (5.19)$$

Figure 5.24 shows the relationship between the predicted and measured prism elastic moduli, E_m . The model (Equation 5.19) is fit with a coefficient of determination, R^2 , of 0.968. Table 5.7 shows the variance obtained from the analysis. The critical value of $F_{v1,v2;\alpha}$ was determined as 4.38 (less than the model F-value), which indicates that the model is significant with respect to the variables which were chosen, where at least one parameter is not equal to zero.

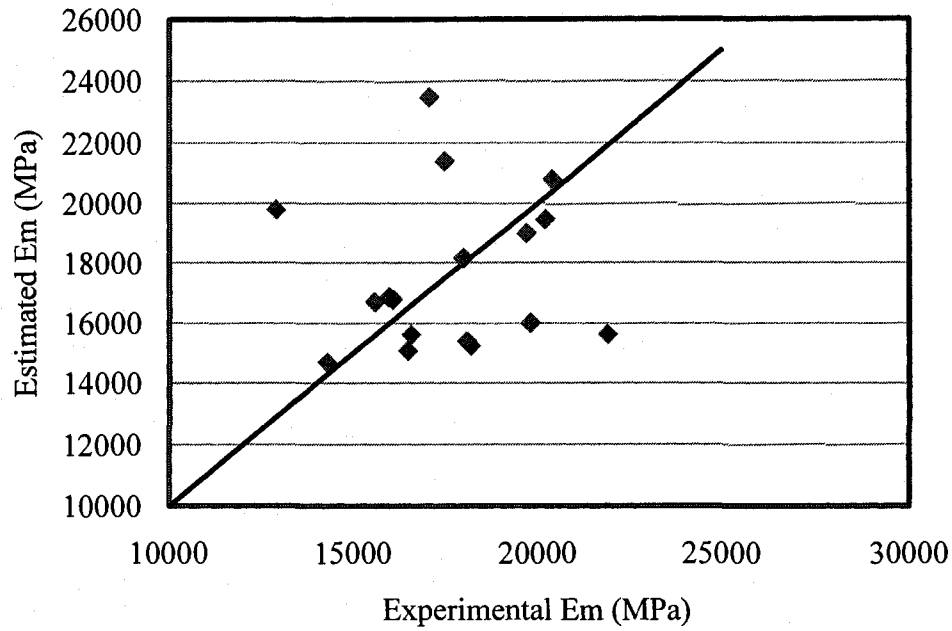


Figure 5.24 Predicted vs. measured values for E_m for model 2

Table 5.7 Analysis of variance for E_m

	DoF	SS	MS	F
Regression	1	5460.5	5460.5	511.53
Residual Error	17	181.5	10.7	
Total	18	5642.0		

The only variable in this equation was prism compressive strength which was found to be statistically significant at a 99% confidence interval.

5.4 COMPARISON OF MODELS

Both regression models (Equations 5.16 and 5.18) were found to provide a good representation of the results using variance analysis. The compressive strengths of all five

prism types met the requirements stipulated in S304.1-04 (2004) and ACI 530.1-05 (2005). Still, a comparison of the regression equations themselves and the significance of the predictors are required.

Investigating the two regression models which were completed can give a good indication of the effect of block geometry on the compressive strength of masonry prisms. Model 1 (Equation 5.16) indicates that prism compressive strength is dependent on seven predictors, however model 2 (Equation 5.18) is simpler, and is a function of only four predictors. This is mainly due to the high correlation between the omitted variables ($f'_{block}{}^2$, $f'_{mortar}{}^3$, and ρ) once the SL and SK prisms were removed. Regardless, it is found that the block strength is also statistically significant to more than 90%, whereas the statistical significance of the mortar strength is found to be less than 50%. The results of model 2 are consistent with those reported by Ramamurthy et al. (2000) where a strong correlation was reported between prism strength (f'_m) and block strength (f'_{block}) mortar strength (f'_{mortar}) and ratio of bedded web area to total web area (r). A model with a coefficient of determination higher than 0.6 was considered to be a good fit. Figure 5.25 shows a chart illustrating the measured and predicted values for each model. It can be seen that Model 1 tends to overestimate the prism compressive strength more than Model 2.

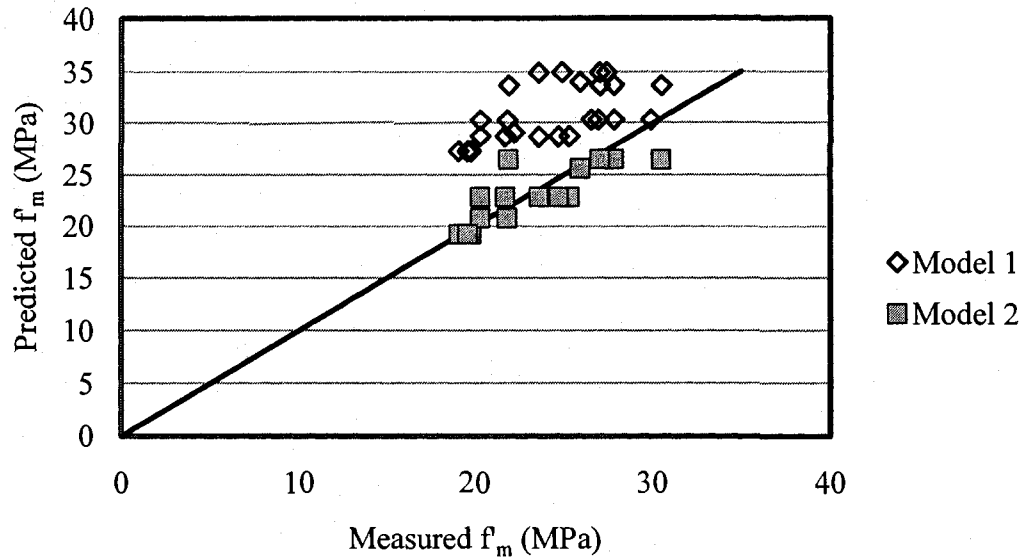


Figure 5.25 Predicted versus measured f_m values

Face shell area was included to determine the effect of block face geometry on the compressive strength of the prisms. In model 1, this parameter was found to be statistically significant at a 3% confidence interval, indicating that the compressive area of the prism did not greatly affect prism compressive strength. When the SL and SK prisms were omitted from the data sets, face shell area was found to be statistically significant at a 68% confidence interval. These results indicate that the variability of the face shell area is not statistically significant when evaluating the prism compressive strength. On the other side, if one type of block is used to construct a prism (i.e. there is no variability in the values of $A_{faceshell}$) the significance of the face shell area increases to 68%.

The regression equations (Equations 5.16 and 5.18) which relate the elastic modulus (E_m) to the compressive strength of the prisms (f_m) did not vary significantly. Using the relationship that CSA S304.1-04 (2004d) and ACI 530.1-05 (2005) suggests results in an

overestimation of the elastic modulus found through experimentation. When considering the estimated values with respect to CSA S301.4-04 (2004d) only, many of the values were over the maximum permitted value of 20,000 MPa. The correlation between the elastic modulus and masonry compressive strength that the Uniform Building Code (1997), suggests is very similar to the relationship that was determined using regression analysis. Figure 5.26 illustrates the two correlations between prism compressive strength and elastic modulus.

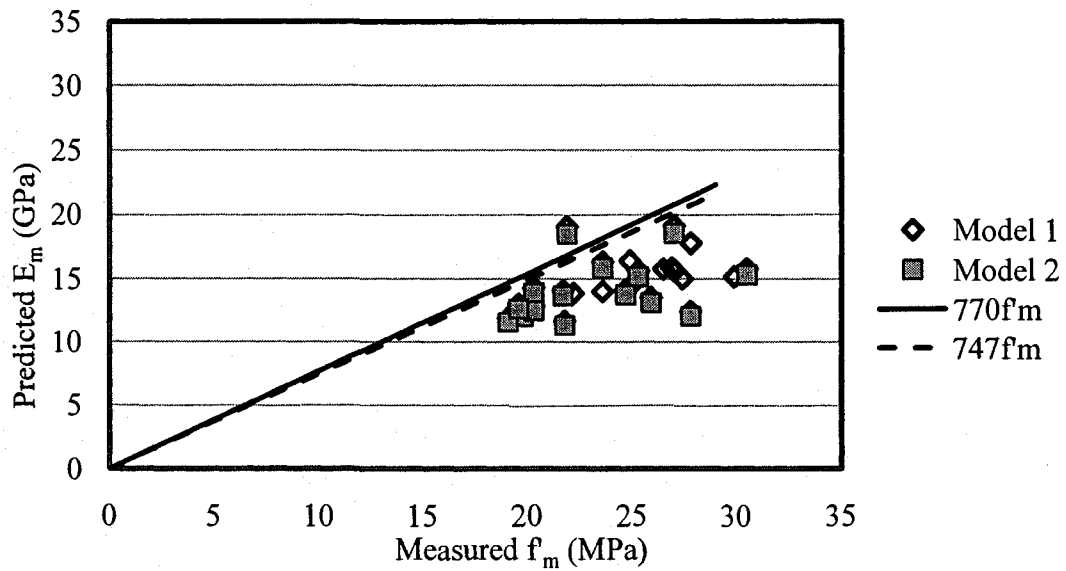


Figure 5.26 Predicted E_m versus measured f_m values

6 GROUTED PRISM RESULTS AND ANALYSIS

6.1 INTRODUCTION

The analysis of the grouted prism sets was conducted using the same method as the geometrical prism sets discussed in Chapter 5. Prism properties must be representative of the actual properties of the masonry specimens. The effect of the properties of masonry assemblage components on the prism properties must then be determined. Only standard (stretcher) units were used to construct the grouted prism specimens. Three different grout mixes were used to grout four different prism sets (one grout type was used in two sets: (i) Normal and (ii) Painted to test the effect of bond strength). The test matrix is shown in Table 3.8 of Chapter 3.

The compressive strength and stiffness results of each prism set in the grouted group were verified using the one-sample t-test. This was done to make sure that the experimental results adequately represent the actual properties of the masonry specimens. Multi-linear regression analysis was then undertaken to investigate the effects of each constituent (unit strength, mortar strength, grout strength, grout stiffness, ungrouted prism stiffness, and presence of bond) on the properties of the prism.

6.1.1 Background

The t-test procedure used to analyze the prism strength and stiffness results is the same as the one discussed in Chapter 4. Multi-linear regression analysis was then used to determine the effects of each constituent property on the compressive strength of each

prism type. The method of multi-linear regression analysis, variance analysis, and the procedure for determining the significance of each variable were discussed in section 5.1.1 of Chapter 5 and thus, not repeated in this chapter.

6.1.2 Outline of Investigation

The multi-linear regression analysis in this study was conducted using Minitab 15 Statistical Software (Minitab Inc., 2008). All four grouted prism sets, namely normal (N), strength (R), stiffness (I), and painted (P), were included in the analysis. The regression equation presented in this chapter is an extension of Model 1 (Equation 5.16) derived in Chapter 5. The point at which each predictor is statistically significant was determined using Minitab 15. It is taken as the confidence interval at which the corresponding coefficient had no possibility of being zero.

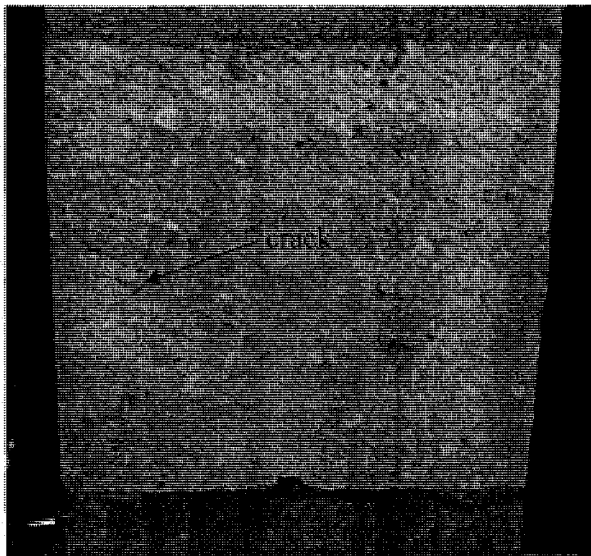
6.2 EXPERIMENTAL TEST RESULTS

The following sub-sections discuss the results obtained from the prism compressive tests. Prism failure mode was observed visually for each prism type, while the compressive strength and modulus of elasticity were determined from the data acquired from the laboratory tests.

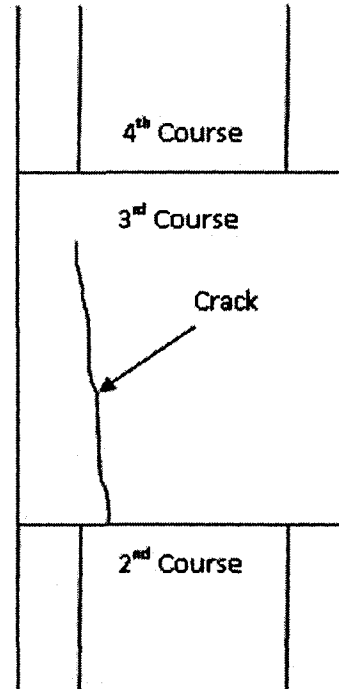
6.2.1 Failure Modes

During loading, the initiation and growth of cracks was observed for each prism specimen. Cracks appeared at high tensile stress points and provided an indication on how the specimen was going to fail. Although major cracks were not found, the half blocks in

the second course from the bottom of the prisms experienced small cracks on the webs near the face shell of the block (Figure 6.1). This type of crack formation was observed in the majority of the grouted prism specimens. After failure, pieces of the broken units were inspected to check whether or not the grout was properly bonded to the unit. A good bond between the block unit and grout material was obtained in the normal (N), strength (R), and stiffness (I) prisms. Figure 6.2 shows a typical surface for the good bonded prism specimens.



(a)



(b)

Figure 6.1: Normal prism web cracking a) photo b) sketch

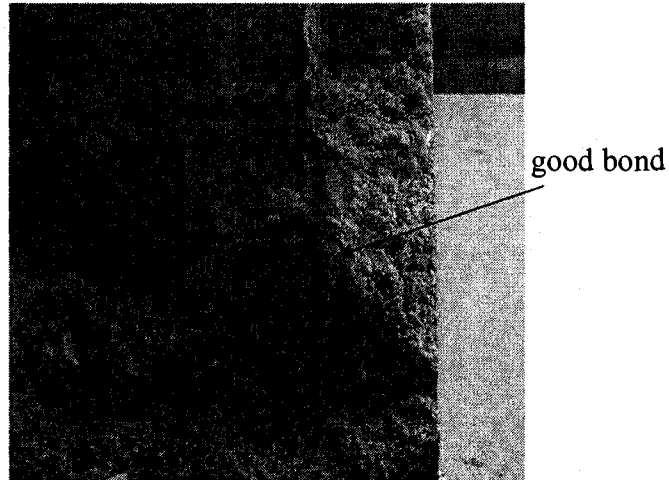


Figure 6.2: Good bond between grout and unit

The normal (N) prism specimens failed through both the face shell and grouted cores of the prism. However, localized separation also occurred sporadically between the block and grout along the face shells, as can be seen in Figure 6.3a. The strength (R) and stiffness (I) prism specimens failed in the same manner by splitting at an angle across the entire prism (Figure 6.3b). Separation between grout and unit in the strength (R) and stiffness (I) prisms was lesser than that of the normal (N) prisms. Therefore, it can be concluded that the grout used for the strength (R) and stiffness (I) prism specimens enhanced the bond.

The purpose of painting and oiling the cores of the painted prisms (P) prior to grouting was to create a film between the units and grout so that a bond does not develop. The painted (P) prisms in fact showed that no bond developed between the unit and grout and thus, complete separation between the unit and the grout occurred at failure load. Although the prism failed through both the unit and grout, the face shells of the unit completely separated from the grouted cores of the prisms as failure occurred, as shown in

Figure 6.3c. Thus, the failure mode for painted prism specimens (P) was different from that of the other grouted specimens.



(a) Normal (N) (b) Strength (R) or Stiffness (I) (c) Painted (P)

Figure 6.3: Failed grouted prisms

6.2.2 Compressive Strength

The compressive strength of the grouted prisms was determined the same way it was done for the geometrical prism sets discussed in Chapter 5. The maximum applied load prior to failure ($P_{ultimate}$) was used in calculating the ultimate strength. The loading area (A_{total}) was taken as the average length and width of the standard unit. The area of any voids caused by the misalignment of webs was disregarded. Equation 6.1 was used to determine the prism compressive strength (f'_m).

$$f'_m = \frac{P_{ultimate}}{A_{total}} \quad (6.1)$$

The compressive strength of all five prism types is given in Table 6.1. Prisms with the normal type grout (N) failed at a compressive strength of 12.8 MPa with one standard deviation of 0.6 MPa. Prism specimens with the strength (R) and stiffness (I) type grouts exhibited much higher strengths and the strengths were 17.2 MPa and 19.6 MPa with standard deviations of 1.2 MPa and 1.8 MPa, respectively. The painted prisms (P), which had the same grout mix as the normal (N) prism specimens showed a compressive strength of 13.0 MPa with a one standard deviation of 1.0 MPa. The values for ultimate load and total area are given in Table A2 in Appendix A.

Table 6.1 Grouted prism results

Prism Type	Compressive Strength (MPa)	Modulus of Elasticity (GPa)
Normal (N)	12.8 ± 0.6	11.2 ± 2.5
Strength (R)	17.2 ± 1.2	11.3 ± 1.2
Stiffness (I)	19.6 ± 1.8	12.5 ± 2.5
Painted (P)	13.0 ± 1.0	9.0 ± 1.7

Examination of the grouted prism results indicated that the deformation compatibility requirement between grout and masonry assemblage is dominant. This observation stems from that fact that prism set I yielded the highest strength value although the grout compressive strength used in prism set R was 10% higher. The effect of bonding between the grout and the block appears to be small when examining the results of prisms N and P. This could be attributed to the fact that the stiffness of the grout used for prism sets N and P was much lower than that of the ungrouted masonry. Comparing the results of prism sets R and I indicate that the compressive strength of the grout did not influence the strength of the grouted masonry prisms.

By comparing the sample means and their deviations with each other using the 2 sample t-test, any correlation between the compressive strengths of the prism types were investigated. It was determined that the N and P prism specimens had compressive strengths that were statistically the same. The R and I prism sets had higher compressive strengths than the N and P prisms; while the specimens in prism set I had statistically higher strengths than the R prisms.

The R and I prisms met the strength requirements in Table 4 of CSA S304.1-04 (2004d). The N and P prisms did not meet the minimum requirements for compressive strength (f'_m) according to CSA S304.1-04 (2004d). All four prism types also failed to meet the recommended compressive strength specified in ACI 530.1-05 (2005) even though the grout compressive strength met the requirements specified. This indicates that grout properties do have an effect on the compressive strength of concrete masonry, and must be considered for the design of masonry structures.

6.2.3 Stress-Strain Characteristics

Four linear potentiometers (LPs) over a gauge length of 610 mm were used to determine the deformation of the prism across three mortar beds (Figure 3.25). The strain was calculated using the deformation data obtained from the LPs and dividing it by the gauge length (Equation 6.2). A typical relationship between stress and strain is shown in Figure 6.4. Other similar plots are shown in Appendix B.

$$\sigma_i = \frac{P_i}{A_{total}} \quad (6.2)$$

The Modulus of Elasticity was calculated using Equation 6.3. The slope of the line between 5% and 33% of the ultimate strength was considered for calculation of E_m , as recommended by CSA A304.2-04 (2004d)

$$E = \frac{\sigma}{\epsilon} \quad (6.3)$$

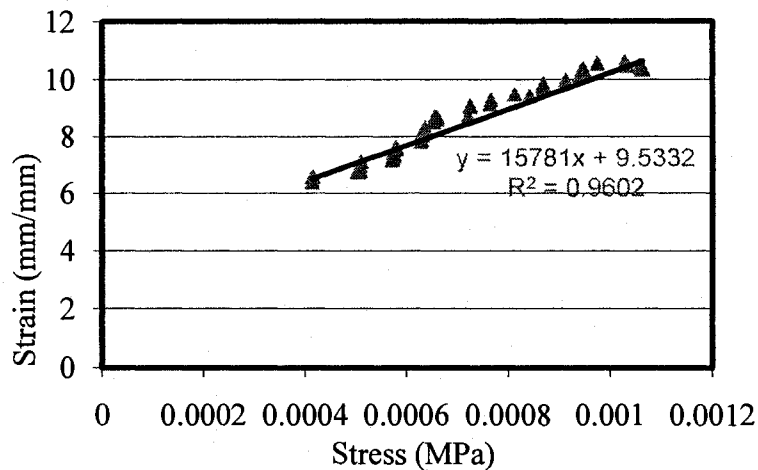


Figure 6.4 Stress versus strain for grouted prism

As shown in Table 6.1, the modulus of elasticity of the prisms was similar for types N, R, and I prism specimens. The mean elastic moduli of the S, N, R, I, and P prisms were obtained as 20.6, 11.2, 11.3, 12.5, and 9.0 GPa, with standard deviations of 2.5, 1.2, 2.5, and 1.7 GPa, respectively. These results show that the bond between the grout and the block significantly influences the stiffness of the grouted masonry prisms.

6.3 MULTI-LINEAR REGRESSION ANALYSIS

As previously stated in section 6.1.2, a regression analysis was undertaken in order to determine the effect of grout properties and unit-grout bond on the compressive strength of grouted concrete masonry prisms. Using Minitab 15 Statistical Software (Minitab Inc., 2008), the regression equation was determined. Prism compressive strength (f'_m) was taken as the response, while unit strength (f'_{block}), its square ($f'_{block}{}^2$), face shell area ($A_{faceshell}$), unit density (ρ), mortar strength (f'_{mortar}), its square and cube ($f'_{mortar}{}^2$ and $f'_{mortar}{}^3$), ratio of grout stiffness to prism stiffness (E_g/E_m), ratio of grout strength to ungrouted prism strength (f'_{grout}/f'_{mu}), ratio of grouted area to face shell area (A_g/A_f), and presence of bond (*bond*) comprised of the predictors. Prisms (Types N, R, and I) which had a good bond between the unit and grout were given a bond value of one, while the painted prisms (P), which were assumed to have no bond between unit and grout, were given a bond value of zero. The statistical significance of each predictor was determined based on the confidence interval at which there is no possibility for the corresponding coefficient to have a zero value. An analysis of variance was completed using the F-probability distribution for $\alpha = 0.05$. The null hypothesis previously discussed in section 5.1.1 was then rejected if at least one parameter coefficient is not equal to zero.

6.3.1 Regression Model

The regression model developed for the grouted prism sets was based on model 1 from Chapter 5 (Equation 5.16). Model 1 was a regression equation for prism compressive strength, f'_m (MPa), with predictors: i) unit strength, f'_{block} (MPa) ii) its square, $f'_{block}{}^2$ (MPa²), iii) face shell area, $A_{faceshell}$ (mm²), iv) unit density, ρ (kg/m³), v) mortar strength,

f'_{mortar} (MPa), vi) its square, $f'_{mortar}{}^2$ (MPa²), and vii) its cube, $f'_{mortar}{}^3$ (MPa³). Model 1 used the data from all five of the geometrical (ungROUTED) prism sets. The compressive strengths, f'_m (MPa), for the prisms in sets N, R, I, and P were calculated using Equation 5.16. The ratio of the measured values (f'_m) to predicted values using Equation 5.16 ($f'_{m(Equation\ 5.16)}$) minus a constant of 1 was taken as the response (y). The predictors then became the ratio of grout stiffness to prism stiffness, ratio of grout strength to ungrouted prism strength, ratio of grouted area to face shell area, and bond presence (0 or 1).

Isaacs (1975) used the ratio of grouted area to the net area of the prism as a variable in determining the compressive strength of grouted concrete masonry under axial loading conditions. In this study, the face shell area ($A_{faceshell}$) was considered as opposed to the net area. Hamid et al. (1978) related the ratio of grout cylinder compressive strength to prism compressive strength to the maximum depth of the prism, height of the prism, and volume of the prism. In this study, grout cylinder compressive strength (f'_{grout}) was related to the compressive strength of an ungrouted prism specimen.

Equation 6.4 illustrates the original equation for prism strength (f'_m) which was rearranged to make Equation 6.5. An intercept of one was used so that when a prism is ungrouted, the resultant equation would be equivalent to the ungrouted regression equation (Equation 5.16).

$$f'_m = f'_{m(Equation\ 5.16)} \left(1 + c_1 \frac{E_g}{E_m(S)} + c_2 \frac{A_g}{A_{faceshell}} + c_3 \frac{f'_{grout}}{f'_{m(Equation\ 5.16)}} + c_4 bond \right) \quad (6.4)$$

$$\frac{f'_m}{f'_{m(\text{Equation 5.16})}} - 1 = c_1 \frac{E_g}{E_{m(S)}} + c_2 \frac{A_g}{A_{\text{faceshell}}} + c_3 \frac{f'_{\text{grout}}}{f'_{m(\text{Equation 5.16})}} + c_4 \text{bond} \quad (6.5)$$

Where f'_m is the compressive strength of the (ungROUTED or grouted) prism, $f'_{m(\text{Equation 5.16})}$ is the predicted f'_m of the ungrouted prism using Equation 5.16, E_g is the modulus of elasticity of the grout, $E_{m(S)}$ is the modulus of elasticity of the ungrouted prism (prism set S), A_g is the area of the grout in the prism, A_f is the face shell area of the ungrouted prism, f'_{grout} is the compressive strength of the grout, and bond is the numerical value associated with the presence of bond.

Minitab 15 Statistical Software (Minitab Inc., 2008) produced the resulting linear equation (Equation 6.6) from the ratio of experimental to estimated values.

$$\frac{f'_m}{f'_{m(\text{Equation 5.16})}} - 1 = 4.02 \frac{E_g}{E_{m(S)}} - 0.469 \frac{A_g}{A_{\text{faceshell}}} - 1.47 \frac{f'_{\text{grout}}}{f'_{m(\text{Equation 5.16})}} - 0.384 \text{bond} \quad (6.6)$$

This equation indicates that as the elastic modulus of the grout (E_g) increases the strength of the grouted prism (f'_m) also increases. However, as the grouted area and grout strength increase, the compressive strength of the grouted prism will decrease.

By rearranging Equation 6.6, and substituting in Equation 5.16, the complete model equation can then be represented by Equation 6.7. The regression equation can therefore be used to predict the compressive strength of both geometric prisms (effect of block geometry) and grouted prisms (effect of properties of grout) for this study.

$$f'_m = (131f'_{block} + 75f'_{mortar} + 0.00013A_{face\ shell} - 2f'_{block}{}^2 - 3.4f'_{mortar}{}^2 + 0.0508f'_{mortar}{}^3 - 0.076\rho - 2501*(1+4.02EgEm(S) - 0.469AgA_{faceshell} - 1.47fg_{grout}'f_m(Equation\ 5.16)' - 0.384bond) \quad (6.7)$$

Figures 6.5 through 6.8 show the residual plots for the new variables associated with the model (Equation 6.7). All four residual plots have a linear spread, which indicates a normal distribution for the variable. The residual plot (Figure 6.6) for the ratio of grouted area to face shell area (A_g/A_f) indicates that the ratio is a constant value. It therefore cannot be concluded if Equation 6.7 can be used accurately for other area ratios in the estimation of prism strength.

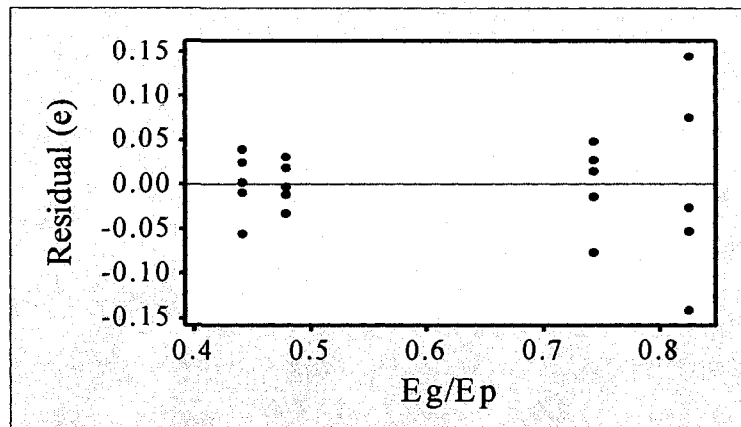


Figure 6.5 Residuals versus E_g/E_m

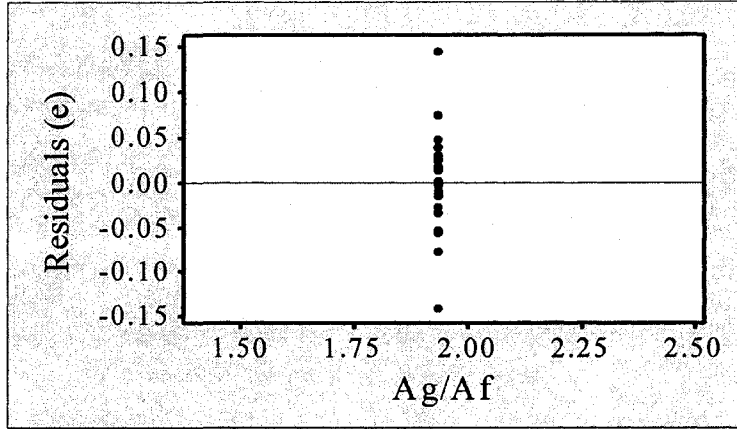


Figure 6.6 Residuals versus A_g/A_f

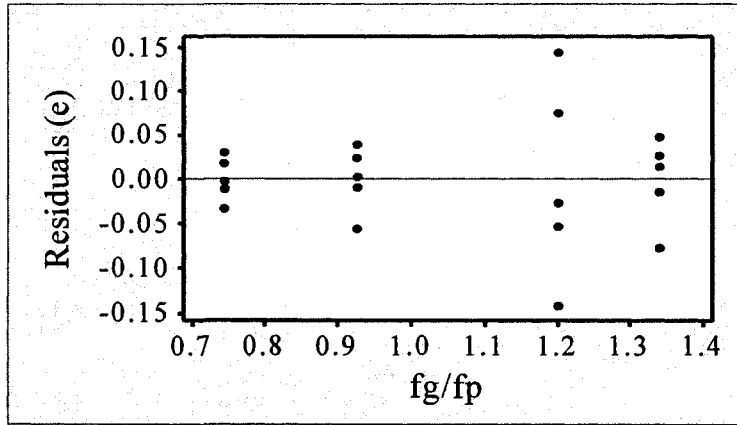


Figure 6.7 Residuals versus f_{grout}/f_{mu}

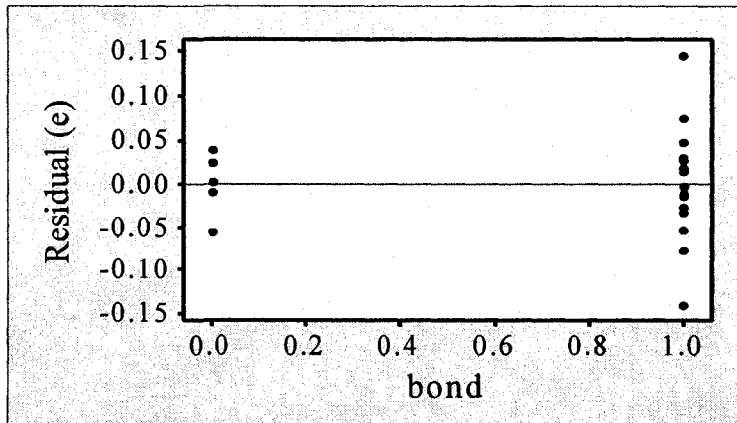


Figure 6.8 Residuals versus bond

This regression model (Equation 6.7) has a good fit since it has a coefficient of determination (R^2) of 0.979. This high value indicates that 97.9% of the original variability has been explained. Table 6.2 is the summary of the analysis of variance conducted on the model. The critical value of $F_{v_1, v_2, \alpha}$ for the regression is 3.01 which is less than the F-value from the analysis (184.96). This indicates that the model is significant with respect to the variables chosen, where at least one parameter is not equal to zero. Figure 6.9 shows the relationship between the measured prism strength and the predicted prism strength using Equation 6.7.

Table 6.2 Analysis of variance for grouted regression model

	DoF	SS	MS	F
Regression	4	3.09751	0.77438	184.96
Residual Error	16	0.06699	0.00419	
Total	20	3.16450		

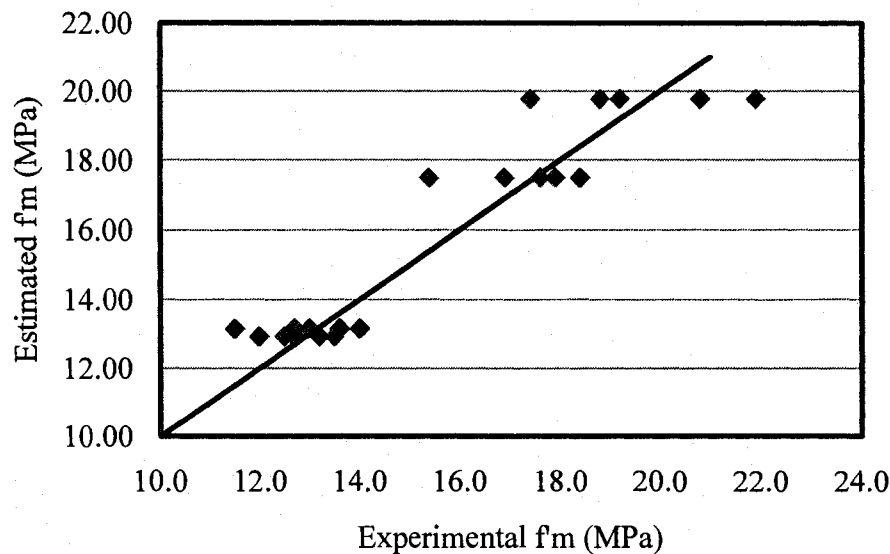


Figure 6.9 Predicted versus measured values for f'_m

The coefficient values for Equation 6.6 are shown in Table 6.3 with 95% confidence intervals, where $\alpha = 0.05$ for the t-distribution. Since non confidence interval include the zero value, it can be deduced that each variable is statistically significant at the 95% confidence interval. This indicates that with 95% confidence none of the variables have the possibility of having a coefficient equal to zero. Further investigation showed that each variable was significant at a confidence interval of 99%.

Table 6.3 95% confidence intervals for coefficients

Variable	Coefficient	95% Confidence Interval	
		Low Level	Upper Level
E_g/E_m	4.02	3.47	4.56
A_g/A_f	-0.469	-0.544	-0.395
f'_{grout}/f'_{mu}	-1.47	-1.79	-1.16
bond	-0.384	-0.496	-0.271

The influence of having no bond could not be adequately evaluated because the grout compressive strength (f'_{grout}) and the elastic modulus of the grout (E_g) were much less than those of the ungrouted prism. This indicates that grout strength has no contribution to the compressive strength of grouted prisms.

6.3.2 Elastic Modulus Estimation

Predicting the elastic modulus of grouted concrete masonry prisms (E_m) using CSA S304.1-04 (2004) and ACI 530.1-05 (2005) result in an overestimation of 80% and 95% of the experimental values, respectively (Table 6.4). In no case did the regression equation estimate the elastic modulus, E_m , to be greater than the maximum (20,000 MPa) permitted in CSA S304.1-04 (2004).

Table 6.4 Grouted prism modulus of elasticity

Prism Type	Compressive Strength (MPa)	Modulus of Elasticity (GPa)		
		Measured	CSA	ACI
Normal (N)	12.8 ± 0.6	11.2 ± 2.5	19.5	11.5
Strength (R)	17.2 ± 1.2	11.3 ± 1.2	14.6	15.5
Stiffness (I)	19.6 ± 1.8	12.5 ± 2.5	16.7	17.6
Painted (P)	13.0 ± 1.0	9.0 ± 1.7	11.1	11.7

Linear regression analysis was also used to obtain an estimation of grouted prism modulus, E_m , in terms of prism compressive strength, f'_m (Equation 6.8)

$$E_m = 689f'_m \quad (6.8)$$

This regression model has a good fit with a coefficient of determination (R^2) of 0.956. This high value indicates that 95.6% of the original variability has been explained. Table 6.5 is the summary of the analysis of variance conducted on the model. The critical value of $F_{v_1, v_2, \alpha}$ for the regression is 4.38, which is less than the F-value (416.67) for the regression. This indicates that the model is significant with respect to the variables chosen, where at least one parameter is not equal to zero.

Table 6.5 Analysis of variance for grouted E_m

	DoF	SS	MS	F
Regression	1	2413.5	2413.5	416.67
Residual Error	19	110.1	5.8	
Total	20	2523.6		

Figure 6.10 shows the relationship between the measured prism elastic modulus and the predicted prism elastic modulus using Equation 6.8.

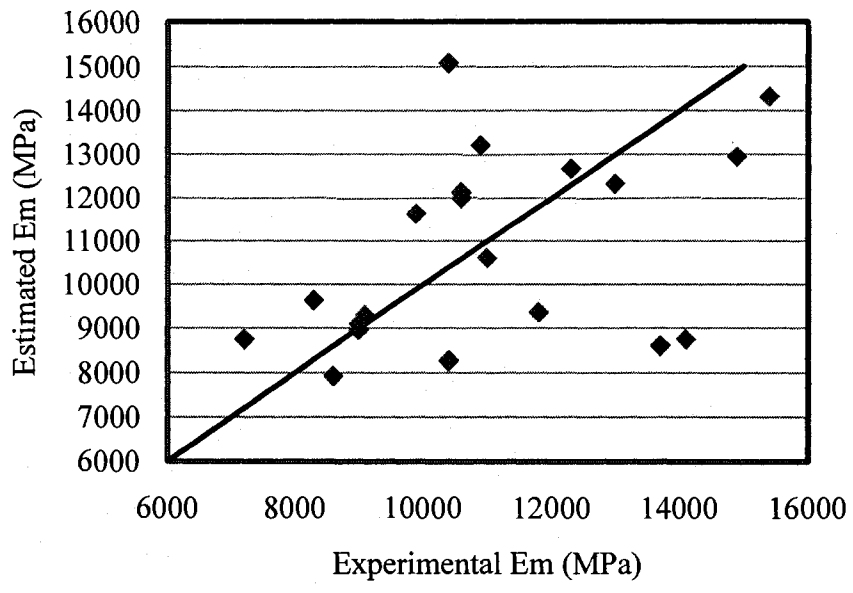


Figure 6.10 Predicted versus measured for E_m

7. SUMMARY, CONCLUSIONS AND RECOMMENDATIONS

7.1. SUMMARY

An experimental program was developed to determine the effect of concrete block face shell geometry and grout properties on the compressive strength of concrete masonry prisms. The t-test shows that the experimental results for the units, mortar, and grout were found to provide an accurate representation of the material properties. The compressive strength (f'_{block}) of the standard, lintel, and knock-out blocks were determined to be 33.8 MPa, 29.9 MPa, and 33.8 MPa, respectively, with standard deviations of 1.3, 2.2, and 2.3. Block density (ρ) was found to be 2134 kg/m³, 1959 kg/m³, and 2052 kg/m³ with standard deviations of 10.1, 9.9, and 10.7. The face shell area ($A_{faceshell}$) was taken as 26215 mm², 31858 mm², and 30117 mm², for the standard, lintel, and knock-out blocks, respectively. The mortar used in construction was found to have a compressive strength (f'_{mortar}) of 22.1 MPa, with a standard deviation of 3.5. The compressive strength and modulus of elasticity for each prism type constructed from the three block types was determined. The standard (S) prisms had a compressive strength of 22.9 MPa with a standard deviation of 2.2, while the lintel (L) and knock-out (K) prisms had compressive strengths of 20.1 MPa and 26.6 MPa, respectively with standard deviations of 1.1 and 3.1, respectively. The prisms constructed with standard units and a lintel unit (SL) had a compressive strength of 25.6 MPa with a standard deviation of 1.4. The standard plus knock-out prism set (SK) was found to have a compressive strength of 26.6 MPa with a standard deviation of 2.8. The modulus of elasticity of the S, L, K, SL, and SK prisms were 18.2 GPa, 16.4 GPa,

17.7 GPa, 21.4 GPa, and 22.0 GPa with standard deviations of 2.8, 1.4, 1.6, 2.7, and 3.2, respectively.

Each grout type was tested to determine its compressive strength (f'_{grout}) and elastic modulus (E_g). The normal type grout which was used in two prism sets (N and P) had compressive strengths of 17.0 MPa and 21.2 MPa with standard deviations of 2.0 and 3.0, and elastic moduli of 8.7 GPa and 8.0 GPa with standard deviations of 2.3 and 1.1. The strength (R) and stiffness (I) sets had grouts of compressive strengths 30.7 MPa and 27.5 MPa, and elastic moduli of 13.5 GPa and 15.0 GPa, with standard deviations of 2.5, 3.1, 2.6, and 2.2, respectively.

The results from all nine prism sets were found to provide an accurate representation of their compressive strength (f'_m) and elastic modulus (E_m). Of the geometrical set, the prisms constructed solely of standard units (S) showed a higher compressive strength and standard deviation (22.9 MPa and 2.2) than the prisms constructed of lintel units (L) only (20.1 MPa and 1.1). However, both of these prism sets had lower compressive strengths than the knock-out (K), standard plus lintel (SL), and standard plus knock-out (SK) prisms, which produced compressive strengths of 27.6 MPa, 25.6 MPa, and 26.6 MPa, with standard deviations of 3.1, 1.4, and 2.8, respectively. These three sets were found to have the same compressive strength statistically. The elastic moduli for the S, L, K, SL, and SK prisms were found to be 18.2 GPa, 16.4 GPa, 17.7 GPa, 21.4 GPa, and 22.0 GPa, with standard deviations of 2.8, 1.4, 1.6, 2.7, and 3.2, respectively.

Two multi-linear regression analyses were completed on the geometrical prism sets. The first (Model 1) included all five prism sets and produced regression equation 5.16 which had a coefficient of determination (R^2) of 0.713.

$$f'_m = 131f'_{block} + 75f'_{mortar} + 0.00013A_{face\ shell} - 2f'_{block}{}^2 - 3.4f'_{mortar}{}^2 + 0.0508f'_{mortar}{}^3 - 0.076\rho - 2501 \quad (5.16)$$

Block strength was found to be the most significant factor affecting prism compressive strength, followed by mortar strength, density, and face shell area. Using these prism sets, the elastic modulus was estimated as a factor of prism compressive strength (Equation 5.17) which had a coefficient of determination of 0.975.

$$E_m = 770f'_m \quad (5.17)$$

The second multi-linear regression analysis (Model 2) only included the data sets from the prisms comprised of one type of unit, namely the S, L, and K prisms. Equation 5.18 is the regression equation determined which had a coefficient of determination of 0.658.

$$f'_m = 2.45f'_{block} - 25.85f'_{mortar} + 0.00183A_{face\ shell} + 0.506f'_{mortar}{}^2 + 217.8 \quad (5.18)$$

Block strength remained the most significant factor affection prism strength. However, face shell area became much more significant than in Model 1. Mortar strength was the

least influence, however still significant. The elastic modulus was again estimated using these three prism sets (Equation 5.19) and produced a coefficient of variation of 0.968.

$$E_m = 747f'_m \quad (5.19)$$

The normal grouted (N) and the painted or no bond (P) prism specimen produced statistically the same compressive strengths, at 12.8 MPa and 13.0 MPa, with standard deviations of 0.6 and 1.0, respectively. The prisms grouted with the strength (R) and stiffness (I) grouts were found to have higher compressive strengths than the N and P prisms statistically, at 17.2 MPa and 19.6 MPa, with standard deviations of 1.2 and 1.8, respectively. The stiffness prisms had statistically higher compressive strengths than the strength prisms. The corresponding elastic moduli for the N, R, I, and P prisms were 11.2 GPa, 11.3 GPa, 12.5 GPa, and 9.0 GPa with standard deviations of 2.5, 1.2, 2.5, and 1.7, respectively.

The regression analysis for the grouted specimens was based on the regression equation for all five geometrical prism sets (Equation 5.16). For this model, the strength of the grouted specimen was taken as the ungrouted equation multiplied by the ratios of grout properties to prism properties plus a constant of 1. If grout was excluded from the prism, the equation then became the same as the original ungrouted (Equation 5.16). The resulting regression equation (Equation 6.7) had a coefficient of determination of 0.979 with all new factors being statistically significant.

$$f'_m = (131f'_{block} + 75f'_{mortar} + 0.00013A_{face\ shell} - 2f'_{block}{}^2 - 3.4f'_{mortar}{}^2 + 0.0508f'_{mortar}{}^3 - 0.076\rho - 2501*(1 + 4.02EgE m(S) - 0.469AgA_{faceshell} - 1.47fgROUT'fm(Equation 5.16)) - 0.384bond) \quad (6.7)$$

The elastic modulus for the grouted prisms was estimated as a function of prism strength and is shown in equation 6.8, which had a coefficient of variation of 0.956.

$$E_m = 689f'_m \quad (6.8)$$

7.2. CONCLUSIONS

The following conclusions can be drawn based on the experimental results and statistical analyses:

- The compressive strength of prisms is not statistically influenced by the face shell area of the non-standard unit but rather by its compressive strength when included in the prism.
- Prism compressive strength appears to be statistically affected by unit face shell area and not by the variability of the unit face shell.
- Block strength is the most significant factor when determining prism compressive strength.
- Mortar strength affects to a lesser degree the prism compressive strength.

- Deformation compatibility between grout and masonry is most critical to the strength of grouted prisms.
- Bond between the grout and block is found to influence the stiffness of the grouted masonry but not the strength.

7.3. RECOMMENDATIONS

The following recommendations are suggested for future research which may assist in further investigating the effect of unit geometry, grout properties, and unit-grout bond on the compressive strength of concrete masonry.

- Testing more types of non-standard units commonly used, such as A-block, H-block, etc.
- Testing of walls constructed in similar ways of the prisms for validating conclusions derived from this study.
- Include the effect of unit tensile strength on prism compressive strength
- Utilization of grouts with a greater variance in properties.
- Further investigation into the effect of bonding, for example, good bond, poor bond, and no bond with grouts which have similar properties to the prism.

REFERENCES

1. Ameny, P.; Loov, R.E.; Shrive, N.G. (1983) Prediction of Elastic Behaviour of Masonry, *International Journal of Masonry Construction*, v3, n1, p. 1-9.
2. American Concrete Institute, Structural Engineering Institute of the American Society of Civil Engineers, The Masonry Society (2005) *Specification for Masonry Structures (ACI 530.1-05/ASCE 6-05/TMS 602-05)*, Masonry Standards Joint Committee, Farmington Hills, Michigan, USA.
3. American Society for Testing and Materials International (2007) *Standard Specification for Grout for Masonry*. Philadelphia: ASTM Publishing Services, (C 476-07).
4. American Society for Testing and Materials International (2005) *Standard Test Methods for Sampling and Testing Concrete Masonry Units and Related Units*. Philadelphia: ASTM Publishing Services, (C 140-05a).
5. American Society for Testing and Materials International (2001) *Standard Test Methods for Sampling and Testing Concrete Masonry Units and Related Units*. Philadelphia: ASTM Publishing Services, (C 140-01).
6. Canadian Standards Association (2004a) *A165 Series-04 CSA Standards on Concrete Masonry Units*, Canadian Standards Association, Mississauga, Ontario.
7. Canadian Standards Association (2004b) *A179-04 Mortar and Grout for Unit Masonry*, Canadian Standards Association, Mississauga, Ontario.
8. Canadian Standards Association (2004c) *A23-04 Methods of Test and Standard Practices for Concrete*, Canadian Standards Association, Mississauga, Ontario.
9. Canadian Standards Association (2004d) *S304.1-04 Design of Masonry Structures*, Canadian Standards Association, Mississauga, Ontario.
10. Colville, J. and Wolde-Tinsae, A.M. (1990) Compressive Strength of Hollow Concrete Masonry. *5th North American Masonry Conference*, 3-6 June 1990 University of Illinois at Urbana-Champaign, Illinois, USA. p. 663-672.

11. Drysdale, R.G.; Hamid, A.A. (1982) Influence of the Characteristics of the Units on the Strength of Block Masonry, *Proceedings of the Second North American Masonry Conference*, University of Maryland, College Park, MD, August 1982, Paper No. 2.
12. Duncan, L.J.; Das, S.; Chidiac, S.E. (2008) Strength of Concrete Masonry Prisms Composed of Various Units, *2nd Canadian Conference on Effective Design of Structures*, 20–23 May 2008, Hamilton, Ontario, Canada.
13. Farny, J.A.; Melander, J.M.; Greenwald, J.H. (2005) Mortar Quality Assurance: A Review of North American Practices, *10th Canadian Masonry Symposium*, 8-12 June 2005 Banff, Alberta, Canada. p. 19-30.
14. Ganzerli, S.; Rosslow, J.; Young, T.; Krebs, K.; Mujumdar, V. (2003) Compression Strength Testing for Nonstandard Concrete Masonry Units. *Ninth North American Masonry Conference*, 1-4 June 2003 Clemson, South Carolina, USA, p. 60-70.
15. Hamid, A. A. and Drysdale, R. G. (1979) Suggested Failure Criteria for Grouted Concrete Masonry Under Axial Compression, *ACI Journal*, October 1979, p 1047-1061.
16. Hedstrom, Edwin G. and Hogan, Mark B. (1990) The Properties of Masonry Grout in Concrete Masonry, *Masonry: Components to Assemblages*, *ASTM STP 1063*, 47-62.
17. International Code Council (1997) *Uniform Building Code*, International Code Council, <http://www.iccsafe.org/dyn/prod/4012S06.html>
18. Isaacs, H. (1975) The Ultimate Compressive Strength of Grouted Hollow Concrete Block Masonry, *Journal: Constructional Review*, v 48, n 2, 36-47.
19. Johnson, R. A. (2005), *Statistics: Principles and Methods*, John Wiley & Sons Inc., New York, NY.
20. Khalifa, M.A. and Magzoub, A.E. (1994) Compressive Strength of Masonry Prisms, *Proceedings of the Structures Congress, Structures Congress XII*, p 1100-1105.
21. Lapin, Lawrence L., (1997) *Modern Engineering Statistics*, Duxbury Press, Pacific Grove, CA

22. Long, L.; Hamid, A.A.; Drysdale, R.G. (2005) Small Scale Modeling of Concrete Masonry Using ½-Scale Units: A Preliminary Study, *Proceedings, Tenth Canadian Masonry Symposium*,
23. Maurenbrecher, A.H.P. (1985) Axial Compression Tests on Masonry Walls and Prisms, *Proceedings of the Third North American Masonry Conference*, p. 19.1 – 19.14.
24. Maurenbrecher, A.H.P. (1980) Effect of Test Procedures on Compressive Strength of Masonry Prisms, *Proceedings, Second Canadian Masonry Symposium*, p. 119-132.
25. Maurenbrecher, A.H.P. (1978) Use of the Prism Test to Determine Compressive Strength of Masonry, *Proceedings of the North American Masonry Conference*, p. 91-2 – 91-13.
26. Minitab Inc. (2008) *Minitab 15 Statistical Software*, Minitab Inc., www.minitab.com.
27. Montgomery, Douglas C. and Runger, George C. (2003) *Applied statistics and probability for engineers 3rd ed.*, John Wiley & Sons, Inc., New York, NY.
28. O’Leary, Jeffrey S. (1996) Improved Method for Testing Grout Used as Masonry Cell Fill, *Masonry: Esthetics, Engineering and Economy, ASTM STP 1246*, p. 73-87.
29. Ramamurthy, K.; Sathish, V.; Ambalavanan, R. (2000) Compressive Strength Prediction of Hollow Concrete Block Masonry Prisms, *ACI Structural Journal*, January-February 2000, p. 61-67.
30. Self, M.W. (1975) Structural Properties of Load-Bearing Concrete Masonry, *Masonry: Past and Present, ASTM STP 589*, p. 233-254
31. Thomas, Robert D. and Mujumdar, Vilas (2003) Determining Concrete Masonry Unit Compressive Strength Using Coupon Testing, *Masonry: Opportunities in the 21st Century, ASTM STP 1432*, p. 138-152.
32. Wong, Hong E. and Drysdale, Robert G. (1985) Compression Characteristics of Concrete Block Masonry Prisms, *Masonry: Research, Application, and Problems, ASTM STP 871*, p. 167-177.

APPENDIX A

Table A1 Geometrical prism matrix test data

Type	Name	Test Day	Mortar Batch(es)	$A_{\text{faceshell}}$ (mm)	P_{ultimate} (kN)	f_m (MPa)	E_m (GPa)
Standard	S05UM5p6	Dec 1 2006	5, 6	26215	569	21.7	18.3
	S06UM5p6	Dec 1 2006	5, 6	26215	532	20.3	18.6
	S08UM5p6	Dec 5 2006	5, 6	26215	619	23.6	21.2
	S09UM5p6	Dec 5 2006	5, 6	26215	663	25.3	20.3
	S10UM5p6	Dec 5 2006	5, 6	26215	648	24.7	18.4
Lintel	L01UM9	Dec 14 2006	9	31858	631	19.8	16.1
	L02UM9	Dec 14 2006	9	31858	608	19.1	15.5
	L03UM8	Dec 19 2006	8	31858	695	21.8	15.2
	L04UM8	Dec 19 2006	8	31858	647	20.3	16.7
	L05UM9	Dec 20 2006	9	31858	624	19.6	16.9
Knock-Out	K01UM10	Nov 10 2006	10	30117	660	21.9	24.8
	K02UM10	Nov 13 2006	10	30117	919	30.5	20.5
	K03UM10	Nov 22 2006	10	30117	837	27.8	16.2
	K04UM10	Dec 1 2006	10	30117	813	27.0	24.8
	K05UM9	Dec 1 2006	9	30117	780	25.9	11.0
Standard plus Lintel	SL02UM8	Dec 13 2006	8	26215	619	23.6	18.2
	SL03UM8	Dec 13 2006	8	26215	653	24.9	18.7
	SL04UM8	Dec 13 2006	8	26215	718	27.4	19.5
	SL05UM8	Dec 14 2006	8	26215	653	24.9	21.3
	SL06UM8	Dec 14 2006	8	26215	708	27.0	20.3
Standard plus Knock-Out	SK01UM10	Nov 7 2006	10	26215	582	22.2	18.0
	SK02UM7	Dec 12 2006	7	26215	695	26.5	20.5
	SK03UM7	Dec 12 2006	7	26215	784	29.9	19.7
	SK04UM7	Dec 12 2006	7	26215	729	27.8	23.1
	SK05UM7	Dec 13 2006	7	26215	705	26.9	20.6

Table A2 Grouted prism matrix

Type	Name	Test Day	Mortar Batch	f'_{grout} (MPa)	E_g (GPa)	A_{total} (mm)	$P_{ultimate}$ (kN)	f'_m (MPa)	E_m (GPa)
Normal	N01G1p2	Jun 7 2007	1, 2	17.0	8.7	76864	961	12.5	13.7
	N02G1p2	Jun 7 2007	1, 2	17.0	8.7	76864	1038	13.5	9.1
	N03G1p2	Jun 11 2007	1, 2	17.0	8.7	76864	1015	13.2	9.0
	N04G1p2	Jun 11 2007	1, 2	17.0	8.7	76864	922	12.0	10.4
	N05G1p2	Jun 11 2007	1, 2	17.0	8.7	76864	976	12.7	14.1
Strength	R01GM3	Jun 20 2007	3	30.7	13.5	76864	1184	15.4	11.0
	R02GM3	Jun 20 2007	3	30.7	13.5	76864	1376	17.9	13.0
	R03GM3	Jun 20 2007	3	30.7	13.5	76864	1414	18.4	12.3
	R04GM3	Jun 20 2007	3	30.7	13.5	76864	1353	17.6	10.6
	R05GM3	Jun 21 2007	3	30.7	13.5	76864	1299	16.9	9.9
Stiffness	I01GM4	Jun 21 2007	4	27.5	15.0	76864	1599	20.8	15.4
	I02GM4	Jun 21 2007	4	27.5	15.0	76864	1476	19.2	10.9
	I03GM4	Jun 25 2007	4	27.5	15.0	76864	1445	18.8	14.9
	I04GM4	Jun 25 2007	4	27.5	15.0	76864	1337	17.4	10.6
	I05GM5	Jun 25 2007	5	27.5	15.0	76864	1683	21.9	10.4
Painted	P01GM11	Jul 5 2007	11	21.2	8.0	76864	976	12.7	7.2
	P02GM11	Jul 5 2007	11	21.2	8.0	76864	1045	13.6	11.8
	P03GM11	Jul 5 2007	11	21.2	8.0	76864	999	13.0	9.0
	P04GM11	Jul 6 2007	11	21.2	8.0	76864	1076	14.0	8.3
	P05GM11	Jul 6 2007	11	21.2	8	76864	884	11.5	8.6

Table A3 Standard unit properties

Unit	A_{net} (mm ²)	$P_{ultimate}$ (kN)	f'_{block} (MPa)	Width (mm)	Height (mm)	Length (mm)	$t_{faceshell}$ (mm)	t_{web} (mm)	Density (kg/m ³)	IRA (kg/m ² /min)
1	39729	1420	35.9	194	192	396	33.25	26.15	2109	0.529
2	39361	1330	33.6	194	194	395	33.04	26.25	2126	0.686
3	39591	1280	32.3	194	193	397	33.22	26.16	2122	0.505
4	39906	1330	33.6	194	192	396	33.08	26.57	2126	0.501
5	39381	1340	33.8	195	194	395	32.99	26.11	2137	0.584

Table A4 Lintel unit properties

Unit	A_{net} (mm ²)	$P_{ultimate}$ (kN)	f'_{block} (MPa)	Width (mm)	Height (mm)	Length (mm)	$t_{faceshell}$ (mm)	Density (kg/m ³)	IRA (kg/m ² /min)
1	31869	980	30.76	192	192	395	40.34	1952	1.851
2	31758	1030	32.33	192	193	395	40.2	1973	1.669
3	31741	920	28.88	192	191	394	40.28	1952	3.403
4	32173	980	30.76	193	194	397	40.52	1965	1.834
5	31751	850	26.68	193	194	396	40.09	1951	2.551

Table A5 Knock-out unit properties

Unit	A _{net} (mm ²)	P _{ultimate} (kN)	f _{block} (MPa)	W (mm)	H (mm)	L (mm)	t _{faceshell} (mm)	t _{web} (mm)	Density (kg/m ³)	IRA (kg/m ² /min)
1	44750	1540	34.3	194	192	397	39.16	35.83	2056	1.408
2	44880	1620	36.1	194	192	397	39.16	35.77	2049	1.604
3	44932	1615	36.0	194	191	397	39.16	35.78	2063	1.424
4	45183	1404	31.3	194	191	397	39.15	35.59	2057	1.350
5	44865	1424	31.7	195	192	396	39.17	35.73	2035	2.296

Table A6 Grout 7 day results

Core	Length (mm)	Diameter (mm)	Ultimate Strength (MPa)	Modulus of Elasticity (MPa)
N1	92.15	43.84	11.79	17652
N2	83.69	43.99	10.24	10424
N3	92.72	43.79		
N4	91.74	43.9	14.25	2807
N5	91.08	43.88	7.50	16038
Average	90.28	43.88	10.95	11730.20
COV (%)	4.13	0.17	25.84	57.18
R2	91.83	44.04	31.10	13901
R3	90.53	43.98	34.70	20028
R4	90.77	43.97	29.59	15935
R5	90.71	44.07	27.70	
Average	90.96	44.02	30.77	16621.33
COV (%)	0.65	0.11	9.63	18.77
I1	93.11	43.93	28.61	13601
I2	89.17	44.02	22.51	7320
I3	90.59	43.92	23.20	11747
I4	86.5	43.87	26.78	17009
Average	89.84	43.94	25.27	12419.15
COV (%)	3.07	0.14	11.51	32.52
P1	91.24	44.02	18.27	5422.10
P2	88.80	43.91	21.59	6248.00
P3	88.61	43.99	19.32	8398.10
P4	91.76	43.91	21.74	4793.20
P5	89.18	43.91	18.07	4223.00
Average	89.92	43.95	19.80	5816.88
COV (%)	1.64	0.12	8.95	27.98

Table A7 Grout test day results

Core	Length (mm)	Diameter (mm)	Ultimate Strength (MPa)	Modulus of Elasticity (MPa)
N1	92.15	43.84	11.79	17652
N2	83.69	43.99	10.24	10424
N3	92.72	43.79		
N4	91.74	43.9	14.25	2807
N5	91.08	43.88	7.50	16038
Average	90.28	43.88	10.95	11730.20
COV (%)	4.13	0.17	25.84	57.18
R2	91.83	44.04	31.10	13901
R3	90.53	43.98	34.70	20028
R4	90.77	43.97	29.59	15935
R5	90.71	44.07	27.70	
Average	90.96	44.02	30.77	16621.33
COV (%)	0.65	0.11	9.63	18.77
I1	93.11	43.93	28.61	13601
I2	89.17	44.02	22.51	7320
I3	90.59	43.92	23.20	11747
I4	86.5	43.87	26.78	17009
Average	89.84	43.94	25.27	12419.15
COV (%)	3.07	0.14	11.51	32.52
P1	91.24	44.02	18.27	5422.10
P2	88.80	43.91	21.59	6248.00
P3	88.61	43.99	19.32	8398.10
P4	91.76	43.91	21.74	4793.20
P5	89.18	43.91	18.07	4223.00
Average	89.92	43.95	19.80	5816.88
COV (%)	1.64	0.12	8.95	27.98

Table A8 Mortar Mix Proportions

Material	Weight (lb)
Portland Type 10	17
Masonry Sand	62.8
Hydrated Lime	3.5
Water	15

APPENDIX B

Table B1 Block t-tests

Property	Block 1	Block 2	CI (%)	DF (n)	$t_{\alpha/2}$	t	Comparable
Strength	Standard	Knockout	95	6	2.447	0.01	Y
	Standard	Lintel	95	6	2.447	3.52	N
	Knockout	Lintel	95	7	2.365	2.82	N
IRA	Standard	Knockout	95	4	2.776	5.91	N
	Standard	Lintel	95	4	2.776	5.23	N
	Knockout	Lintel	95	6	2.447	1.76	Y
Density	Standard	Knockout	95	7	2.365	10.94	N
	Standard	Lintel	95	7	2.365	26.17	N
	Knockout	Lintel	95	7	2.365	14.3	N

Table B2 Mortar t-tests

Batch A	Batch B	DF	t	$t_{\alpha/2}$	$t < t_{\alpha}$	Batch A	Batch B	DF	t	$t_{\alpha/2}$	$t < t_{\alpha/2}$
1	2	2	-0.06	2.920	Y	4	6	2	-6.75	2.920	N
1	3	3	0.24	2.353	Y	4	7	2	-4.66	2.920	N
1	4	3	6.94	2.353	N	4	8	3	-9.36	2.353	N
1	5	3	1.43	2.353	Y	4	9	2	-15.74	2.920	N
1	6	3	-1.54	2.353	Y	4	10	3	-12.37	2.353	N
1	7	2	5.08	2.920	N	4	11	3	-6.61	2.353	N
1	8	3	-3.63	2.353	N	5	6	3	-2.61	2.353	N
1	9	2	-4.02	2.920	N	5	7	2	2.59	2.920	Y
1	10	2	-2.15	2.920	Y	5	8	3	-4.67	2.353	N
1	11	2	2.63	2.920	Y	5	9	2	-5.42	2.920	N
2	3	2	0.18	2.920	Y	5	10	2	-3.69	2.920	N
2	4	2	3.66	2.920	N	5	11	2	0.59	2.920	Y
2	5	2	0.90	2.920	Y	6	7	2	5.17	2.920	N
2	6	3	-0.97	2.353	Y	6	8	3	-1.66	2.353	Y
2	7	2	2.30	2.920	Y	6	9	2	-0.90	2.920	Y
2	8	3	-2.28	2.353	Y	6	10	2	0.27	2.920	Y
2	9	2	-1.76	2.920	Y	6	11	2	3.57	2.920	N
2	10	2	-0.95	2.920	Y	7	8	2	-8.05	2.920	N
2	11	2	1.30	2.920	Y	7	9	2	-27.03	2.920	N
3	4	3	8.56	2.353	N	7	10	2	-15.10	2.920	N
3	5	3	1.45	2.353	Y	7	11	2	-4.79	2.920	N
3	6	2	-1.88	2.920	Y	8	9	2	1.42	2.920	Y
3	7	2	7.54	2.920	N	8	10	2	2.62	2.920	Y
3	8	2	-4.26	2.920	N	8	11	2	6.19	2.920	N
3	9	2	-6.41	2.920	N	9	10	3	3.20	2.353	N
3	10	3	-3.38	2.353	N	9	11	3	12.91	2.353	N
3	11	3	3.37	2.353	N	10	11	3	8.02	2.353	N
4	5	3	-4.80	2.353	N						

Table B3 Grout t-tests

Grout 1	Grout 2	CI (%)	DF (n)	$t_{\alpha/2}$	t	$t < t_{\alpha/2}$
Normal 7d	Normal td	95	4	2.776	3.33	N
Strength 7d	Strength td	95	5	2.571	0.79	Y
Stiffness 7d	Stiffness td	95	6	2.447	1.1	Y
Painted 7d	Painted td	95	6	2.447	0.9	Y
Normal td	Strength td	95	4	2.776	4.54	N
Normal td	Stiffness td	95	5	2.571	5.78	N
Normal td	Painted td	95	5	2.571	2.36	Y
Strength td	Stiffness td	95	5	2.571	0.42	Y
Strength td	Painted td	95	4	2.776	2.83	N
Stiffness td	Painted td	95	7	2.365	3.29	N

Table B4 Geometrical prism t-tests

Property	Prism 1	Prism 2	CI (%)	DF (n)	$t_{\alpha/2}$	t	$t < t_{\alpha/2}$
Strength	Standard	SK	95	7	1.895	3.65	N
	Standard	SL	95	8	1.86	1.78	Y
	Standard	Knockout	95	6	1.943	1.86	Y
	Standard	Lintel	95	7	1.895	3.47	N
	SK	SL	95	6	1.943	2.13	N
	SK	Knockout	95	5	2.015	0.72	Y
	SK	Lintel	95	5	2.015	8.62	N
	SL	Knockout	95	5	2.015	0.67	Y
	SL	Lintel	95	6	1.943	6.4	N
	Knockout	Lintel	95	4	2.132	4.4	N
Modulus of Elasticity	Standard	SK	95	5	2.015	1.42	Y
	Standard	SL	95	7	1.895	0.1	Y
	Standard	Knockout	95	4	2.132	0.08	Y
	Standard	Lintel	95	6	1.943	5.68	N
	SK	SL	95	5	2.015	1.49	Y
	SK	Knockout	95	4	2.132	0.55	Y
	SK	Lintel	95	4	2.132	6.07	N
	SL	Knockout	95	4	2.132	0.05	Y
	SL	Lintel	95	6	1.943	5.45	N
	Knockout	Lintel	95	4	2.132	1.27	Y

Table B5 Grouted prism t-tests

Property	Prism 1	Prism 2	CI (%)	DF (n)	$t_{\alpha/2}$	t	$t < t_{\alpha/2}$
Strength	Normal	Strength	95	8	1.86	8.75	N
	Normal	Stiffness	95	4	2.132	8.29	N
	Normal	Painted	95	6	1.943	0.36	Y
	Strength	Stiffness	95	6	1.943	2.75	N
	Strength	Painted	95	8	1.86	6.96	N
	Stiffness	Painted	95	6	1.943	7.47	N
Modulus of Elasticity	Normal	Strength	95	5	2.015	0.02	Y
	Normal	Stiffness	95	7	1.895	0.75	Y
	Normal	Painted	95	7	1.895	1.69	Y
	Strength	Stiffness	95	5	2.015	0.96	Y
	Strength	Painted	95	6	1.943	2.57	N
	Stiffness	Painted	95	7	1.895	2.56	N

APPENDIX C

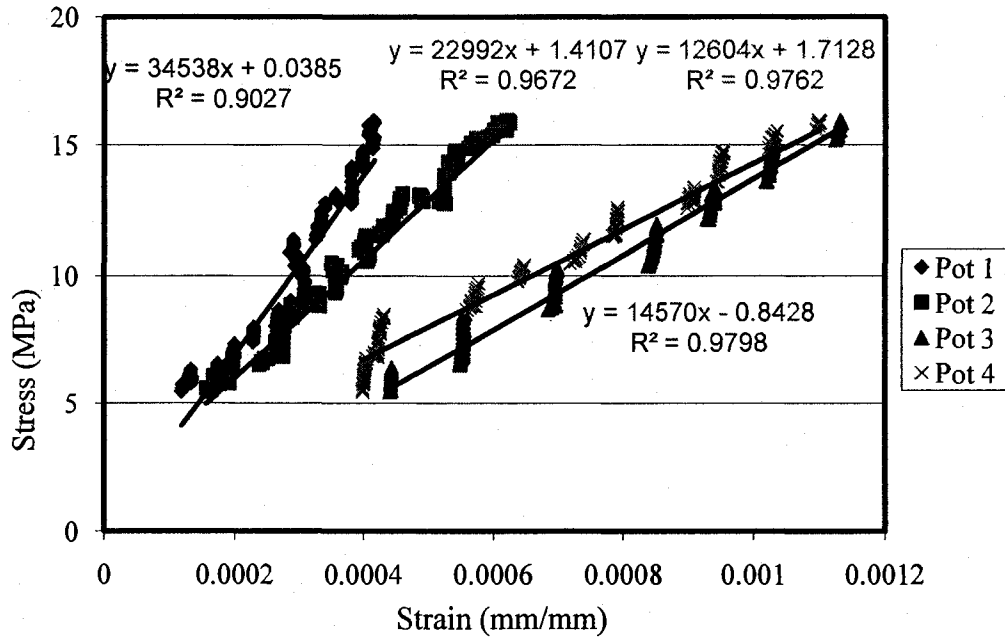


Figure C1 Stress versus strain for S type prism

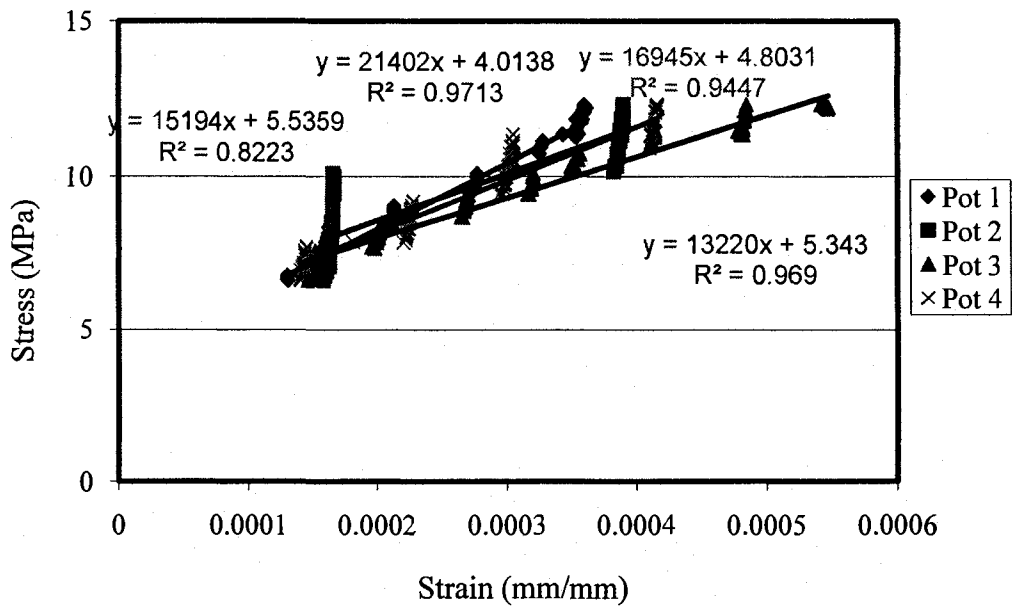


Figure C2 Stress versus strain for L type prism

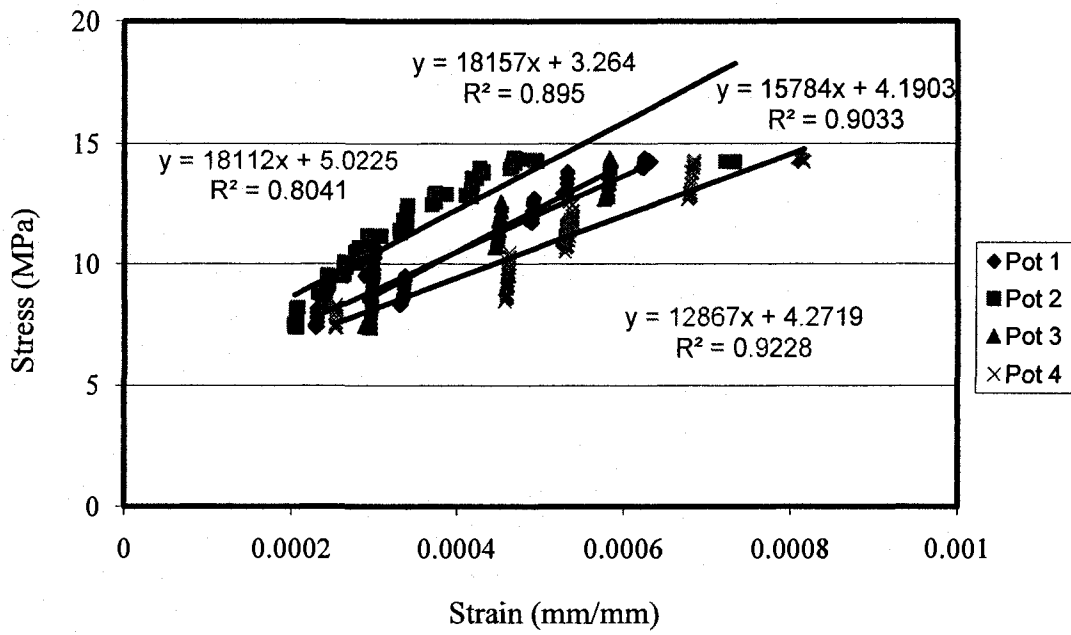


Figure C3 Stress versus strain for K type prism

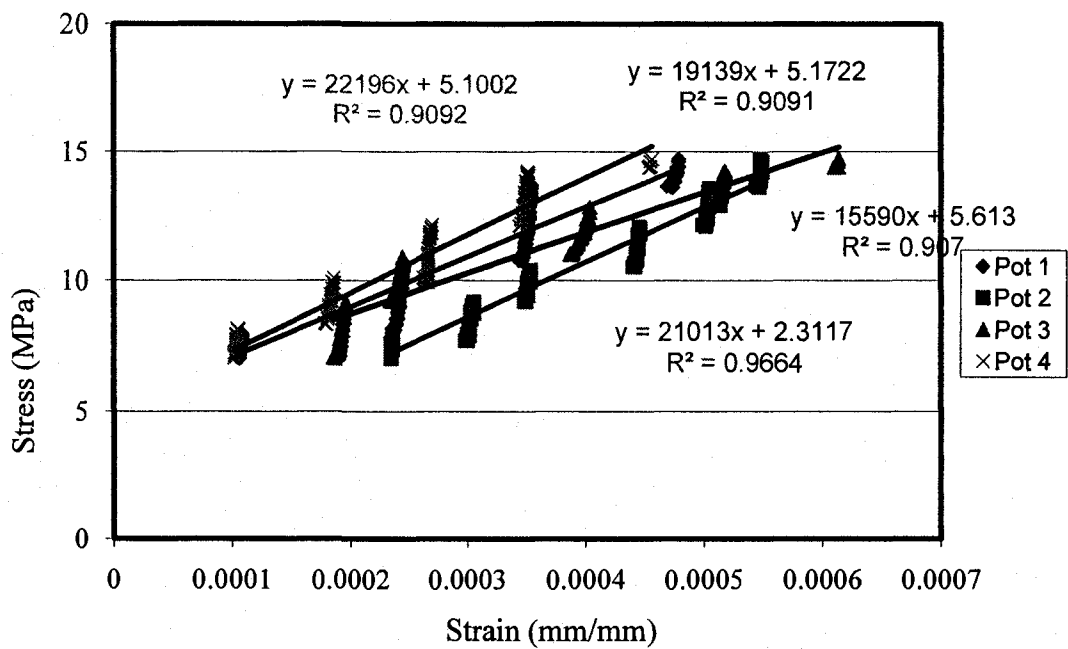


Figure C4 Stress versus strain for SL type prism

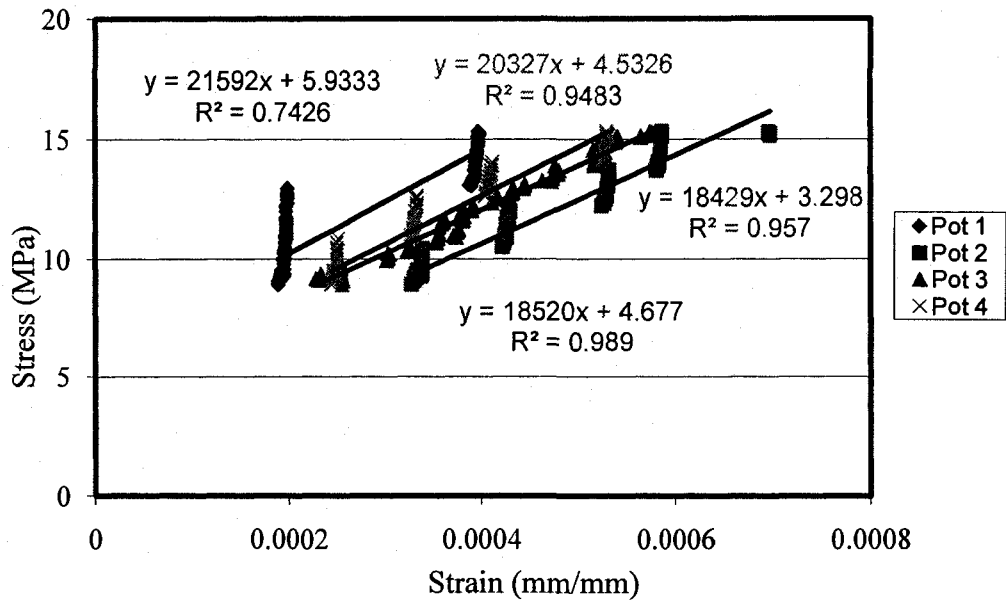


Figure C5 Stress versus strain for SK type prism

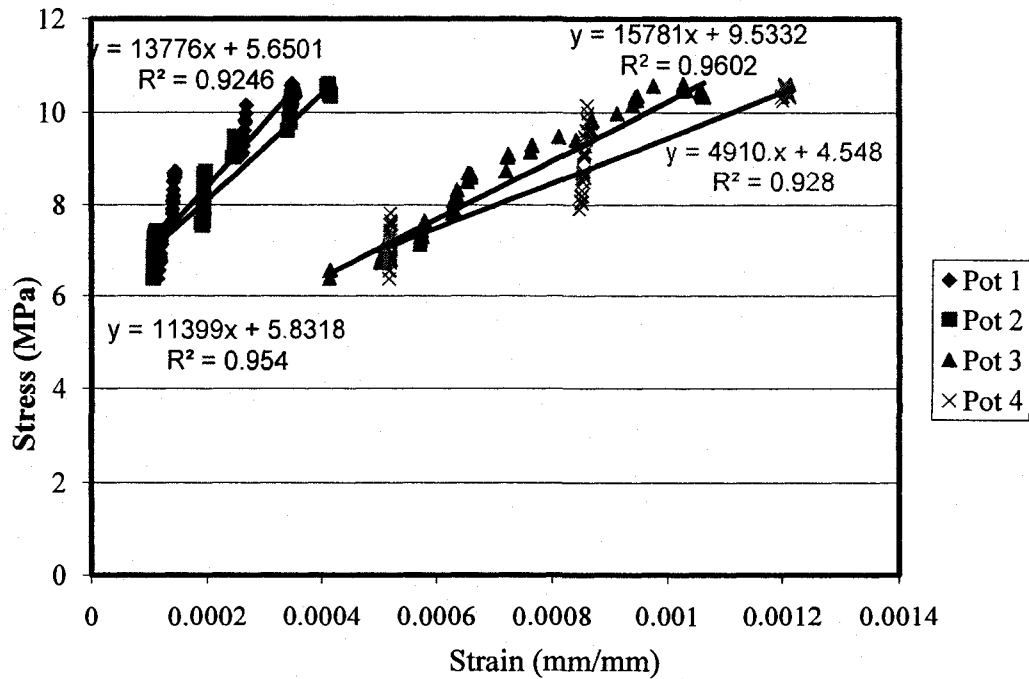


Figure C6 Stress versus strain for N type prism

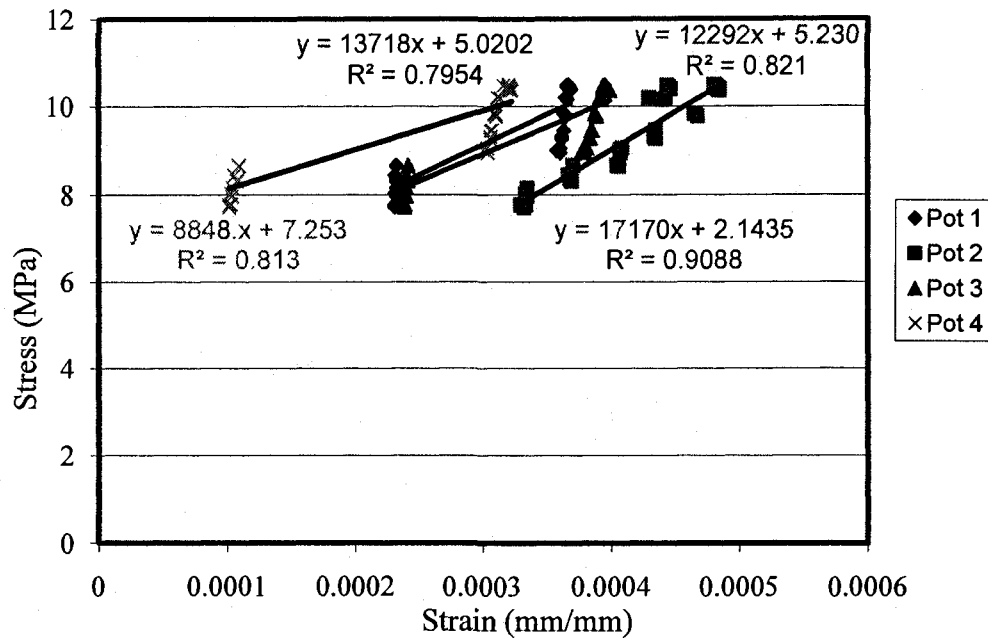


Figure C7 Stress versus strain for R and I type prisms

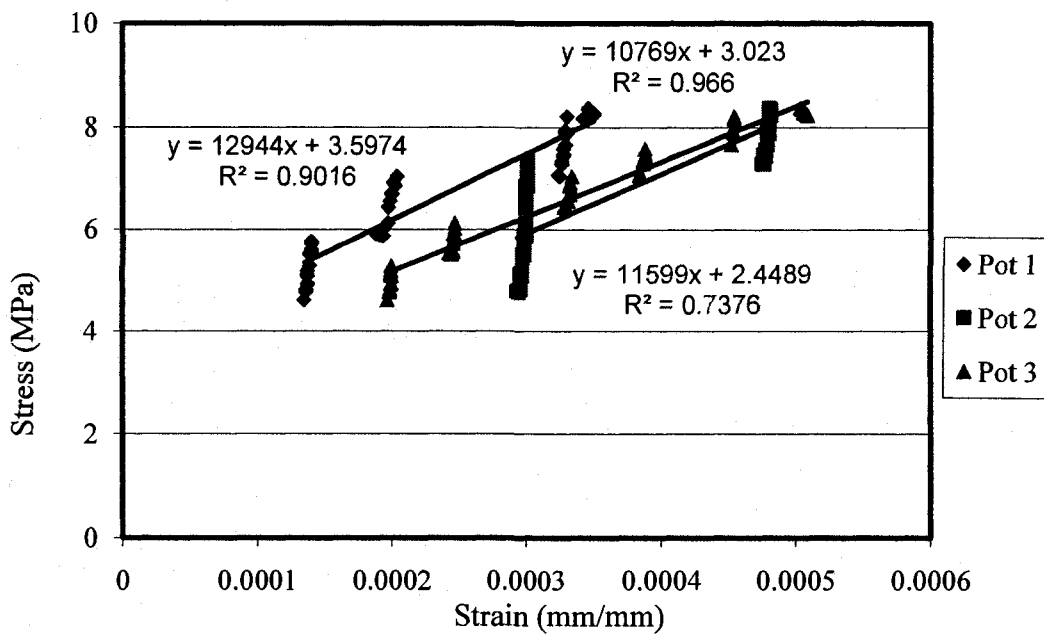


Figure C9 Stress versus strain for P type prism

VITA AUCTORIS

NAME:

Laura J. Duncan

PLACE OF BIRTH:

Windsor, Ontario

EDUCATION

Laura Secord Secondary School, St.
Catharines

1996-2001

University of Windsor, Windsor, Ontario

2001-2005 B.A.Sc.

University of Windsor, Windsor, Ontario

2005-2008 M.A.Sc.